

AD _____
(Leave blank)

Award Number: W81XWH-07-1-0619

TITLE: Genetic and Environmental Pathways in Type 1 Diabetes Complications

PRINCIPAL INVESTIGATOR: Massimo Trucco, M.D.

CONTRACTING ORGANIZATION: Children's Hospital of Pittsburgh
Pittsburgh, PA 15213

REPORT DATE: September 2008

TYPE OF REPORT: Annual

PREPARED FOR: U.S. Army Medical Research and Materiel Command
Fort Detrick, Maryland 21702-5012

DISTRIBUTION STATEMENT: (Check one)

Approved for public release; distribution unlimited

Distribution limited to U.S. Government agencies only;
report contains proprietary information

The views, opinions and/or findings contained in this report are those of the author(s) and should not be construed as an official Department of the Army position, policy or decision unless so designated by other documentation.

REPORT DOCUMENTATION PAGE

Form Approved
OMB No. 0704-0188

Public reporting burden for this collection of information is estimated to average 1 hour per response, including the time for reviewing instructions, searching existing data sources, gathering and maintaining the data needed, and completing and reviewing this collection of information. Send comments regarding this burden estimate or any other aspect of this collection of information, including suggestions for reducing this burden to Department of Defense, Washington Headquarters Services, Directorate for Information Operations and Reports (0704-0188), 1215 Jefferson Davis Highway, Suite 1204, Arlington, VA 22202-4302. Respondents should be aware that notwithstanding any other provision of law, no person shall be subject to any penalty for failing to comply with a collection of information if it does not display a currently valid OMB control number.
PLEASE DO NOT RETURN YOUR FORM TO THE ABOVE ADDRESS.

1. REPORT DATE (DD-MM-YYYY) 26-09-2008		2. REPORT TYPE Annual		3. DATES COVERED (From - To) 27 Aug 2007-26 Aug 2008	
4. TITLE AND SUBTITLE Genetic and Environmental Pathways in Type 1 Diabetes Complications				5a. CONTRACT NUMBER	
				5b. GRANT NUMBER W81XWH-07-1-0619	
				5c. PROGRAM ELEMENT NUMBER	
6. AUTHOR(S) Massimo Trucco, M.D. Email: mnt@pitt.edu				5d. PROJECT NUMBER	
				5e. TASK NUMBER	
				5f. WORK UNIT NUMBER	
7. PERFORMING ORGANIZATION NAME(S) AND ADDRESS(ES) Children's Hospital of Pittsburgh of UPMC Health System 3705 Fifth Avenue at DeSoto Street Pittsburgh, PA 15213				8. PERFORMING ORGANIZATION REPORT NUMBER	
9. SPONSORING / MONITORING AGENCY NAME(S) AND ADDRESS(ES) U.S. Army Medical Research and Materiel Command Fort Detrick, MD 21702-5012				10. SPONSOR/MONITOR'S ACRONYM(S)	
				11. SPONSOR/MONITOR'S REPORT NUMBER(S)	
12. DISTRIBUTION / AVAILABILITY STATEMENT Approved for public release; distribution unlimited.					
13. SUPPLEMENTARY NOTES					
14. ABSTRACT Genetic factors contribute to risk for developing nephropathy in patients with Type 1 Diabetes (T1D). Cigarette smoking is deleterious to kidney function and is a risk factor for Diabetic-Nephropathy (DN) as well as End Stage Renal Disease (ESRD) in patients with T1D. The proposed study investigates how environmental exposure(s) (e.g., smoking) and genetic variants interact to amplify risk for T1DN and substantially increase incidence of ESRD. The specific aims are: 1) Identify genetic variants conferring risk to T1DN by performing a staged follow-up of our initial Genome-Wide Association Scan (GWAS) results; 2) Ensure that SNPs identified by Aim 1 affect risk of T1DN, as opposed to risk for T1D; 3) Identify genetic variants that interact with smoking status in conferring risk for T1DN; 4) Confirm results obtained during Aims 1-3 using an independent cohort of case and control participants. The relevance of the study to public health is that 16 million people in the US have diabetes with 800,000 new cases diagnosed each year. Diabetic complications threatening vision, kidney, and nerve function affect most diabetic patients. Improved prediction of risk for developing diabetes and diabetic complications among active duty members of the military, their families and retired military personnel will potentially allow focused preventative treatment of at-risk individuals, providing significant healthcare savings and improved patient well being.					
15. SUBJECT TERMS End Stage Renal Disease; Genetic Association; Genome Scanning; Nephropathy; Type 1 Diabetes					
16. SECURITY CLASSIFICATION OF: a. REPORT U		17. LIMITATION OF ABSTRACT UU	18. NUMBER OF PAGES 95	19a. NAME OF RESPONSIBLE PERSON USAMRMC	
b. ABSTRACT U		19b. TELEPHONE NUMBER (include area code)			
Standard Form 298 (Rev. 8-98) Prescribed by ANSI Std. Z39.18					

Children's Hospital of Pittsburgh
W81XWH-07-1-0619
Annual Report (08/27/2006 – 08/26/2008)
Table of Contents

Introduction	4
Body.....	4
First Quarter.....	4
Second Quarter.....	8
Third Quarter.....	13
Fourth Quarter	18
Key Research Accomplishments.....	20
Conclusions.....	22
 Appendix	 24

Appendix 1: T1D GWAS p-values

Appendix 2: Wellcome Trust Information

ASHI Quarterly 31:50-52, 2007.

Methods Mol Biol 373:25-38, 2007.

Pediatr Diabetes 8:307-322, 2007

Am J Hum Genet 82:453-463, 2008.

INTRODUCTION:

Type 1 Diabetes (T1D) is associated with increased risk of T1D-Nephropathy (T1DN) and is usually accompanied by other diabetic-related complications such as retinopathy, neuropathy, blood pressure elevation, and high risk of cardiovascular morbidity and mortality. Sixteen million people in the US have diabetes with 800,000 new cases diagnosed each year. Diabetic complications affect most diabetic patients. Diabetes occurs in men, women, children and the elderly. African, Hispanic, Native and Asian Americans are particularly susceptible to its most severe complications. An estimated 20% to 40% of T1D patients will develop diabetic nephropathy, clinically first evidenced by microalbuminuria, during their lifetime. If untreated nearly all T1D patients experiencing microalbuminuria will progress to overt nephropathy, evidenced by macroalbuminuria, and culminating in T1D-End Stage Renal Disease (T1D-ESRD). Improved prediction of risk for developing diabetes and diabetic complications among active duty members of the military, their families and retired military personnel will potentially allow focused preventative treatment of at-risk individuals, providing significant healthcare savings and improved patient well being.

BODY:

Our first quarterly scientific progress report (08/27/07 – 11/30/07) detailed the following steps forward in reaching the aims of our study.

The proposed study will investigate how environmental exposure(s) and genetic variants interact to amplify risk for Type 1 Diabetic (T1D) nephropathy (T1DN) and substantially increase incidence of end-stage renal disease (T1D-ESRD). The work that will be performed during the proposed 2 year study will exploit the results of our previously funded application to the DOD entitled "*New Advanced Technology to Improve Prediction of Type 1 Diabetes and Its Complications*", the aims of which are nearing completion. The previous project produced 3 principal results: 1) Transmission/Disequilibrium Testing (TDT) analysis using a cohort of 92 case family trios for the association of 121 candidate genes with T1DN, identifying significant association between T1DN and 4 of the loci tested; 2) Recruitment of an independent cohort of 2,881 participants, consisting of 1,174 case/control singletons and 569 case/control family trios; and 3) a genome-wide association scan (GWAS) of 197 singleton cases and 197 controls all of whom were non-smokers.

The currently proposed work follows up on the significant genetic signals identified during our previous project.

To accomplish our aims we originally proposed the following tasks:

Task 1. Using our available cohort of 257 T1DN (case) family trios perform an additional series of GWAS using the 500,000 SNP typing microarray in order to confirm the strongest genetic signals associated with diabetic kidney disease.

Task 2. Recruit an additional 200 participants with T1DN who have never smoked cigarettes in order to increase the total number of singleton case participants to greater than 280.

Task 3. Design customized microarrays in order to examine the significant genetic markers using an independent cohort of singleton cases and controls matched for exposure to cigarette smoking. The available cohort for this stage of the project is: Non-Smokers, 86 case and 201 control; Smokers, 295 case and 198 control.

Task 4. Perform SNP genotyping of the most significant genetic markers using an available control cohort consisting of 312 family trios matched for exposure to cigarette smoking: Non-Smokers, 216; Smokers, 96.

Task 5. In order to complete the analysis of the genetic and environmental exposure data for association with T1DN we will compare the genetic marker frequency (i.e., SNPs, Copy Number Variation, Haplotype, Gene-Gene, and Gene-Environment interactions) with occurrence of the disease.

This quarterly report provides a perfect opportunity to present an update of our progress regarding the T1D genome-wide scan (GWAS). The technical and statistical solutions successfully used to confirm the genetic regions most associated T1D will then be used to investigate T1DN associations. A cohort of 422 T1D and 2,144 non-T1D participants were used to investigate whether it would be possible to identify novel SNPs for association with the phenotype (Table 1). The T1D participants

were recruited from the Children's Hospital of Pittsburgh (N=28) and obtained from the GoKinD study (N=394). Non-T1D participants were provided by the KORA and POPGEN studies and were received as computer files of genotype information. All participants, whether collected in Pittsburgh or provided by KORA/POPGEN, were genotyped using the Affymetrix 500K GeneChip. This is the same SNP typing array that was used by the Wellcome Trust Case Control Consortium (WTCCC). We are in the process of applying for access to the WTCCC dataset and anticipate having a positive reply before February 2008.

Table 1. Characteristics of Case and Control Participants.

	Case Participants		Control Participants	
	<u>CHP</u>	<u>GoKinD</u>	<u>KORA</u>	<u>POPGEN</u>
<i>Demographic Characteristics:</i>				
Number of Singletons	28	394	1644	500
European American (%)	100%	100%	---	---
German Resident (%)	---	---	100%	100%
Male Gender (%)	50%	46.7%	49.5%	51.8%
<i>History of Diabetes:</i>				
Type 1 Diabetes (%)	100%	100%	---	---
Mean Age at T1D Diagnosis (yr)	12.7(7.9)	12.2(7.1)	---	---

Values in parentheses indicate standard deviation from the mean.

As expected, we observed a large signal corresponding to the HLA region that exceeded genome-wide significance (Figure 1). Other notable signals were observed but fell short of the Bonferroni correction for the threshold of significance (p-value less than 4×10^{-7}). Suggestive signals observed for several previously identified T1D loci are summarized in Table 2. For example, the *PHTF1/PTPN22* loci ($p=1 \times 10^{-5}$), *CTLA4* ($p=3 \times 10^{-4}$), and *IL2RA* ($p=1 \times 10^{-3}$) are commonly considered as confirmed susceptibility loci associated with T1D. Other suggested T1D susceptibility loci (e.g., *ITPR3*, *NOD2*, and *PDX1*) were also identified by the GWAS. In contrast, the confirmed loci *CD25*, *IFIH1*, and *INS* were not readily observed as nearby SNPs did not exceed a p-value of 0.001. This was possibly the result of the Affymetrix GeneChip not including a sufficient number of SNPs in linkage disequilibrium with the implicated alleles.

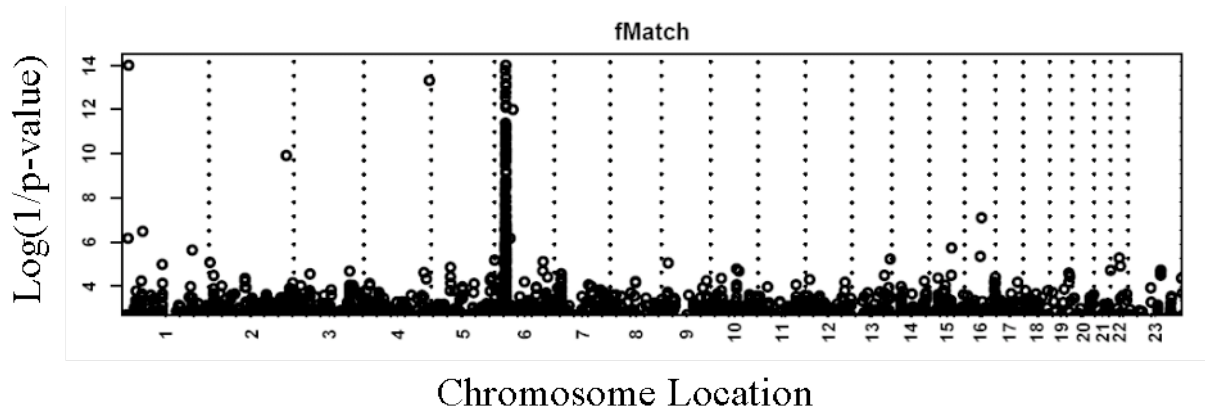


Figure 1. Summary of the GWAS data obtained for T1D. The x-axis is chromosome and location while the y-axis is the -Log of the p-value. As expected the HLA region on chromosome 6p attained genome-wide significance. All other p-values exceeding 1×10^{-7} have been removed from consideration due to poor quality genotyping data. The complete list of GWAS data is included in the Appendix.

Table 2. Confirmed and suggested T1D loci identified during the T1D GWAS.

<u>Chr</u>	<u>Locus</u>	<u>Location</u>	<u>dbSNP_ID</u>	<u>Dominant</u>	<u>Additive</u>	<u>Recessive</u>
1	PHTF1	114,045,700	rs1230649	1.2E-02	7.2E-04	1.0E-01
1	PHTF1	114,105,331	rs6679677	3.3E-05	1.0E-05	4.4E-02
1	PTPN22	114,216,891	rs2488457	3.8E-03	7.1E-04	1.2E-01
2	CTLA4	204,428,384	rs11571292	2.5E-02	4.0E-03	2.6E-04
2	CTLA4	204,449,111	rs231726	7.3E-03	3.4E-04	5.2E-04
2	CTLA4	204,449,411	rs1427676	6.5E-03	4.5E-04	6.0E-04
6	ITPR3	33,650,501	rs9296095	2.2E-04	3.1E-03	1.0E-02
6	ITPR3	33,682,987	rs444697	2.5E-04	3.9E-05	5.1E-04
10	IL2RA	6,132,099	rs10905669	6.2E-02	1.0E-03	3.9E-02
13	PDX1	27,374,640	rs9554196	6.5E-04	1.8E-02	9.5E-03
13	PDX1	27,377,980	rs9319399	3.8E-04	1.6E-02	7.5E-03
13	PDX1	27,378,356	rs9551419	7.4E-04	2.2E-02	9.5E-03
16	NOD2	49,281,588	rs9933594	9.1E-04	1.3E-02	6.3E-03

Table 3 lists select data obtained from the GWAS. Of the loci identified, there were 12 that are currently listed by T1DBase (<http://t1dbase.org>) as candidates for T1D. Moreover, there are a number of novel loci that may be interesting to evaluate during a staged investigation of the phenotype. For example, the GWAS identified loci involved in insulin signaling (*CRK* and *IRS2*), cytokine signaling (*IL6ST*, *IRF4*, *TRAF3/p1*) and potassium ion transport (*KCNH7* and *KCNQ1*). Moreover, the GWAS identified a subunit of mitochondrial complex 1 (*NDUFA10*) and the apoptosis regulatory factor *FKSG2* that may influence superoxide production and subsequent susceptibility to programmed cell death.

Table 3. Select loci observed during the T1D GWAS.

<u>Chr</u>	<u>Locus</u>	<u>Location</u>	<u>dbSNP_ID</u>	<u>Dominant</u>	<u>Additive</u>	<u>Recessive</u>
<i>T1DBase Candidate Loci:</i>						
1	IL12RB2	67,612,161	rs3828069	5.7E-03	9.3E-03	9.8E-04
1	PHTF1/PTPN22	114,105,331	rs6679677	3.3E-05	1.0E-05	4.4E-02
2	CTLA4	204,428,384	rs11571292	2.5E-02	4.0E-03	2.6E-04
3	SENP7	102,504,337	rs16843699	8.5E-04	7.5E-04	6.8E-02
6	ITPR3	33,682,987	rs444697	2.5E-04	3.9E-05	5.1E-04
10	IL2RA	6,132,099	rs10905669	6.2E-02	1.0E-03	3.9E-02
11	LRP5	67,813,346	rs11606508	2.2E-03	3.1E-03	9.4E-04
12	CD4	6,775,811	rs1075836	6.0E-02	2.7E-04	5.9E-02
12	TRAFD1	111,002,025	rs1980364	9.6E-04	9.4E-03	5.3E-04
12	PTPN11	111,462,160	rs10850053	6.7E-04	9.2E-03	5.5E-04
13	PDX1	27,377,980	rs9319399	3.8E-04	1.6E-02	7.5E-03
16	NOD2	49,281,588	rs9933594	9.1E-04	1.3E-02	6.3E-03
<i>Novel T1D Candidate Loci:</i>						
2	KCNH7	163,442,376	rs10203602	1.1E-03	2.4E-04	3.7E-03
2	TRAF3IP1	238,928,000	rs821804	1.7E-05	7.1E-05	4.4E-05
2	NDUFA10	240,555,969	rs4854067	1.6E-03	2.5E-02	1.2E-04
5	IL6ST	55,388,527	rs10042443	2.2E-04	1.4E-05	1.4E-04
6	IRF4	374,457	rs950286	5.2E-05	6.7E-06	4.8E-03
8	FKSG2	36,899,367	rs1010669	6.3E-02	1.6E-02	3.9E-05
8	EYA1	72,362,997	rs4738123	5.0E-03	6.2E-05	8.7E-04
9	IL6RL1	91,744,788	rs7864499	2.0E-04	5.1E-04	2.6E-03
11	KCNQ1	2,781,804	rs163166	4.4E-05	1.7E-02	3.3E-03
13	IRS2	109,307,346	rs1041637	1.6E-03	6.0E-06	1.8E-04
15	SEMA6D	45,680,428	rs16959754	8.7E-06	9.1E-05	6.3E-06
17	CRK	1,278,556	rs8070640	2.7E-05	9.4E-04	5.7E-05

The complete list of SNPs implicated during the GWAS has been included in the Appendix. That file contains the chromosome location of each SNP as well as the p-value associated with the 3 major modes of inheritance (i.e., additive, dominant, and recessive). The Appendix also summarizes the quality control analysis for those SNPs with p-values less than 0.0001 and indicates which SNPs overlap T1D candidate loci that have been listed by T1DBase. This is the principal file that is being used to determine which signals obtained during the GWAS for T1D should be studied during Stage 2 analysis of the T1D results.

There are expected to be 14,047 participants available for the T1D project (Table 4). Our repository is anticipated to contain a modest number of T1D family trios (N=719), T1D singletons (N=4,246), and non-T1D control singletons (N=7,644). Table 4 summarizes the available cohorts and details the source of each participant, and whether material is provided as DNA or as a computer file of previously determined genotypes. When genotypes are provided they were obtained using the same Affymetrix 500K GeneChip that was used during our GWAS for T1D.

Table 4. Summary of cohort available and anticipated for T1D analysis.

Source	Family Trios	Case and Control Singletons		
	T1D Family Trios	Case	Control	Comment
EMIL	150	300	2500	DNA available
GoKinD	569	1746		DNA available
KORA			1644	GeneChip data available
POPGEN			500	GeneChip data available
Pittsburgh		200		DNA available
WTCCC		2000	3000	GeneChip data available

At this stage of the project we need to prioritize the SNPs identified during the GWAS and then evaluate suggestive SNPs using the T1D family trios. The University of Pittsburgh Genomics Core Laboratory has recently acquired the Sequenom SNP typing platform. The Sequenom system provides sufficient throughput and genotyping accuracy for projects such as ours. The fee for using this system has not yet been finalized but is anticipated to be about 10 cents per SNP. This is about one-fifth the fee associated with genotyping using TaqMan methodology. It is anticipated that when working with T1D family trios we will genotype 2,157 participants (N=3x719) for about 45 SNPs at a cost of roughly \$9,700. Choosing the 45 SNPs to genotype is the aim that needs to be completed in the near future.

The next phase of analysis will have 2 goals. The first being to measure the p-values for confirmed and suggested T1D loci and the second being to test whether the signals associated with novel T1D loci are reproducible.

12. Statement of Plans and Milestones for the Next Quarter

There are 2 goals (Goal 1 and 2) that we anticipate completing and 1 goal (Goal 3) that will be initiated during the next research period.

Goal 1. Increase the number of participants. **Milestone 1A.** Apply to the WTCCC for access to the T1D and control cohorts. **Milestone 1B.** Continue to recruit T1D case trios and singletons from Pittsburgh.

Our application to the WTCCC for access to their cohort of T1D (N=2,000) and non-T1D control (N=3,000) singletons has been finalized. The project title is "Detection of Susceptibility Loci in Multifactorial Disease". The principal aim is to combine our original GWAS results with the GWAS performed by WTCCC followed by statistical genetic analysis. It is anticipated that the outcome will be an analysis with increased power to detect true signals for association with T1D risk. We will also continue to recruit T1D participants through our collaboration with the University of Pittsburgh Transplantation Institute. Samples collected from Pittsburgh will

be used to increase the size of our DNA repository enabling increased power of the genetic study to detect true association signals.

Goal 2. Determine high priority SNPs to study. **Milestone 2A.** Identify confirmed and/or suggestive T1D risk loci using our original GWAS. **Milestone 2B.** Identify novel loci to evaluate for T1D risk.

Data obtained during our original GWAS will be compared with the list of confirmed and suggested T1D risk loci in order to identify where the different datasets overlap. Moreover, novel SNPs identified during the original GWAS will be compiled based upon the following criteria: i) SNPs with p-values less than 0.0001; ii) SNPs with p-values less than 0.001 occurring within 50,000bp of a known locus; and iii) Clusters of 3 or more SNPs with p-values less than 0.001 occurring within 50,000bp of one another. The priority SNPs will be used to compile a list that will direct subsequent laboratory analyses.

Goal 3. Initiate genotyping of priority SNPs. **Milestone 3A.** Use the cohort of T1D family trios to evaluate confirmed SNPs for T1D risk. **Milestone 3B.** Use the cohort of T1D family trios to evaluate novel SNPs for T1D risk.

Our DNA repository includes a collection of T1D family trios (N=719) that can be used to evaluate the SNPs identified during Goal 2. SNPs will be chosen from the list of confirmed and suggestive T1D risk as well as from the list of novel genetic variants. The genotype of each SNP will be determined among the various participants and the results will be evaluated by transmission disequilibrium testing to determine association with T1D.

[In our second quarterly scientific progress report \(12/01/07 – 02/29/08, we presented the following data:](#)

Type 1 Diabetes Genome-Wide Association Study Update:

The previous quarterly report summarized our progress regarding the genome-wide association (GWA) scan for Type 1 Diabetes (T1D) susceptibility alleles. We have reported the genotype results from a cohort of 422 T1D (case) and 2,144 non-T1D (control) participants using 322,347 SNPs. The anthropometric properties of the case and control cohort has been described in the previously quarterly report but is reproduced below for convenience.

Table 1. Characteristics of Case and Control Participants.

	Case Participants		Control Participants	
	<u>CHP</u>	<u>GoKinD</u>	<u>KORA</u>	<u>POPGEN</u>
<i>Demographic Characteristics:</i>				
Number of Singletons	28	394	1644	500
European American (%)	100%	100%	----	----
German Resident (%)	----	----	100%	100%
Male Gender (%)	50%	46.7%	49.5%	51.8%
<i>History of Diabetes:</i>				
Type 1 Diabetes (%)	100%	100%	----	----
Mean Age at T1D Diagnosis (yr)	12.7(7.9)	12.2(7.1)	----	----

Values in parentheses indicate standard deviation from the mean.

As outlined in the following sections, the research goals for the first quarter of 2008 were 3-fold: 1) Increase the number of participants; 2) Determine high priority SNPs to study; and 3) Initiate genotyping of high priority SNPs. Our progress for each goal is addressed below.

Goal 1. Increase the number of participants. **Milestone 1A.** Apply to the Wellcome Trust Case Control Consortium (WTCCC) for access to the T1D and control cohorts. **Milestone 1B.** Continue to recruit T1D case trios and singletons from Pittsburgh.

In Milestone 1A we proposed to increase the number of participants in our GWA study by applying to the WTCCC for access to their GWA dataset. The WTCC dataset contains SNP genotypes collected from 2,000 T1D and 3,000 non-T1D participants. The WTCCC and our group used identical Affymetrix manufactured genotyping arrays to evaluate risk for T1D. Therefore, SNPs evaluated by the WTCCC and Pittsburgh GWA studies are essentially the same. As a result, the dataset collected at Pittsburgh and by the WTCCC can be combined in order to increase the overall size of the study thus replicating the study while simultaneously improving the power of the study to identify T1D susceptibility alleles. Once the application for data sharing is approved by the WTCCC committee that evaluates requests, our analysis of the WTCCC dataset can begin immediately. The application is complete, pending final signatures from the University of Pittsburgh Office of Grants and Research, and we anticipate submission to the WTCCC will occur during the upcoming research quarter. A copy of the application is attached as an Appendix to this quarterly report.

In Milestone 1B, we proposed to continue recruitment of T1D case trios and singletons from the University of Pittsburgh Medical Center (UPMC). Recruitment of new participants is one of the primary focuses of the project and patients will be recruited continuously during the project's lifetime. The new participants recruited during Goal 1 will be used to confirm the genetic signals identified from the cohort described in Table 1 that was used during our previously completed GWA. We can follow the health of these patients at multiple times during the project since our IRB approved protocol allows us to contact formerly recruited human subjects for the purpose of updating their health information and, when appropriate, collecting a second vial of blood. Table 2 summarizes the current collection of T1D participants recruited in Pittsburgh.

Table 2. Characteristics of Singleton and Family Trios Participants Recruited at Pittsburgh.

	Pittsburgh Cohorts		GoKinD Cohort
	<u>Singletons</u>	<u>Family Trios</u>	<u>Family Trios</u>
<i>Demographic Characteristics:</i>			
Number of Participants	46	26	569
European American (%)	100	100	100
<i>History of Diabetes:</i>			
Type 1 Diabetes (%)	100	100	100
Mean Age at T1D Diagnosis (yr)	14(7)	14(7)	11(6)

Values in parentheses indicate standard deviation from the mean. Pittsburgh samples were recruited at the University of Pittsburgh Medical Center. GoKinD participants were recruited by the Genetics of Kidneys in Diabetes Study.

Goal 2. Determine high priority SNPs to study. **Milestone 2A.** Identify confirmed and/or suggestive T1D risk loci using our original GWA study. **Milestone 2B.** Identify novel loci to evaluate for T1D risk.

We have completed Milestones 2A by evaluating our T1D GWA data against a list of known and suspected T1D risk loci. The identities of the T1D risk loci were obtained from T1Dbase (<http://t1dbase.org>) a world-wide-web accessible database of T1D genetic risk information. The genomic location of these confirmed T1D susceptibility loci were compared with the location of SNPs that during the previously completed GWA associated with p-values exceeding 0.001. The analysis identified 12 strongly associated SNPs occurring within 50Kb of T1D candidate loci. SNPs occurring near confirmed T1D loci are summarized in the Table 3.

Table 3. Summary of GWA Results for SNPs located within 50Kb of confirmed T1D Susceptibility Loci.

<u>Chr</u>	<u>dbSNP ID</u>	<u>Location</u>	<u>Locus</u>	<u>Official Full Name</u>
1	Rs6679677	114,105,331	PHTF1	Putative homeodomain transcription factor 1
2	Rs231726	204,449,111	CTLA4	Cytotoxic T-lymphocyte-associated protein 4
2	Rs1427676	204,449,411	CTLA4	Cytotoxic T-lymphocyte-associated protein 4
7	Rs10232298	127,006,653	PAX4	Paired box 4

10	Rs10905668	6,132,061	IL2RA	Interleukin 2 receptor, alpha
10	Rs10905669	6,132,099	IL2RA	Interleukin 2 receptor, alpha
10	Rs7074372	6,228,597	IL2RA	Interleukin 2 receptor, alpha
12	Rs11171739	54,756,892	ERBB3	v-erb-b2 erythroblastic leukemia viral oncogene homolog 3 (avian)
13	Rs3812863	27,443,268	PDX1	Pancreatic and duodenal homeobox 1
16	Rs9746695	11,115,395	CLEC16A	C-type lectin domain family 16, member A
16	Rs11640295	11,298,229	CLEC16A	C-type lectin domain family 16, member A
20	Rs2425756	44,223,669	CD40	CD40 molecule, TNF receptor superfamily member 5

Signals from the HLA region on chromosome 6 are excluded from the information presented in the table.

Milestone 2B has also been completed during the last quarterly research period. The GWA scan was evaluated to identify SNPs that implicated novel genetic loci for further investigation. As summarized in Table 4 there were 24 loci identified by SNPs that had p-values exceeding the 10th percentile of all association signals garnered during the previously completed GWA. For several loci, such as, KCNH7, STXBP5, and RXFP2 there were clusters of 5 or more SNPs covering genomic regions from 64Kb and up to 247Kb. These loci, as well as others with strong evidence for association are included in Table 4.

Table 4. Summary of GWA Results for SNPs located within 50Kb of Novel Loci.

Chr	dbSNP_ID	Location	Locus	Official Full Name
1	rs10858046	114,875,303	AMPD1	Adenosine monophosphate deaminase 1 (isoform M)
1	rs6689415	114,908,992	AMPD1	Adenosine monophosphate deaminase 1 (isoform M)
1	rs2268697	115,029,016	AMPD1	Adenosine monophosphate deaminase 1 (isoform M)
1	rs6427093	165,823,621	CREG1	Cellular repressor of E1A-stimulated genes 1
1	rs2094028	194,417,119	KCNT2	Potassium channel, subfamily T, member 2
1	rs16839682	194,497,622	KCNT2	Potassium channel, subfamily T, member 2
2	rs12470503	163,405,297	KCNH7	Potassium voltage-gated channel, subfamily H (eag-related), member 7
2	rs1001911	163,421,846	KCNH7	Potassium voltage-gated channel, subfamily H (eag-related), member 7
2	rs1492990	163,422,123	KCNH7	Potassium voltage-gated channel, subfamily H (eag-related), member 7
2	rs10203602	163,442,376	KCNH7	Potassium voltage-gated channel, subfamily H (eag-related), member 7
2	rs1364562	163,449,972	KCNH7	Potassium voltage-gated channel, subfamily H (eag-related), member 7
2	rs307869	163,469,837	KCNH7	Potassium voltage-gated channel, subfamily H (eag-related), member 7
2	rs2028201	201,011,255	KCTD18	Potassium channel tetramerisation domain containing 18
2	rs821804	238,928,000	TRAF3IP1	TNF receptor-associated factor 3 interacting protein 1
2	rs523437	239,063,548	TRAF3IP1	TNF receptor-associated factor 3 interacting protein 1
2	rs580209	239,065,169	TRAF3IP1	TNF receptor-associated factor 3 interacting protein 1
5	rs10042443	55,388,527	IL6ST	Interleukin 6 signal transducer (gp130, oncostatin M receptor)
6	rs950286	374,457	IRF4	Interferon regulatory factor 4
6	rs4959880	387,206	IRF4	Interferon regulatory factor 4
6	rs13214605	394,483	IRF4	Interferon regulatory factor 4
6	rs2498587	118,133,432	GOPC	Golgi associated PDZ and coiled-coil motif containing
6	rs9322085	147,354,835	STXBP5	Syntaxin binding protein 5 (tomasyn)
6	rs7765767	147,366,631	STXBP5	Syntaxin binding protein 5 (tomasyn)
6	rs1529017	147,392,995	STXBP5	Syntaxin binding protein 5 (tomasyn)
6	rs6919814	147,412,758	STXBP5	Syntaxin binding protein 5 (tomasyn)
6	rs6920096	147,412,791	STXBP5	Syntaxin binding protein 5 (tomasyn)
6	rs1881660	147,420,052	STXBP5	Syntaxin binding protein 5 (tomasyn)
6	rs6930740	147,438,438	STXBP5	Syntaxin binding protein 5 (tomasyn)
6	rs6920901	147,470,991	STXBP5	Syntaxin binding protein 5 (tomasyn)

7	rs1294610	7,332,182	C1GALT1	Core 1 synthase, glycoprotein-N-acetylgalactosamine 3-beta-galactosyltransferase, 1
7	rs1294651	7,381,742	C1GALT1	Core 1 synthase, glycoprotein-N-acetylgalactosamine 3-beta-galactosyltransferase, 1
7	rs1404829	144,255,618	TPK1	Thiamin pyrophosphokinase 1
9	rs2808784	115,961,345	COL27A1	Collagen, type XXVII, alpha 1
9	rs2567724	115,961,754	COL27A1	Collagen, type XXVII, alpha 1
9	rs10982093	115,976,726	COL27A1	Collagen, type XXVII, alpha 1
10	rs2803590	88,362,973	BMPR1A	Bone morphogenetic protein receptor, type 1A
10	rs2803568	88,426,595	BMPR1A	Bone morphogenetic protein receptor, type 1A
11	rs574434	100,384,527	PGR	Progesterone receptor
12	rs7305099	845,537	WNK1	WNK lysine deficient protein kinase 1
12	rs12828016	868,626	WNK1	WNK lysine deficient protein kinase 1
13	rs7328020	30,310,128	ALOX5AP	Arachidonate 5-lipoxygenase-activating protein
13	rs4941903	31,140,471	RXFP2	Relaxin/insulin-like family peptide receptor 2
13	rs7336382	31,146,759	RXFP2	Relaxin/insulin-like family peptide receptor 2
13	rs3950017	31,151,027	RXFP2	Relaxin/insulin-like family peptide receptor 2
13	rs641696	31,376,444	RXFP2	Relaxin/insulin-like family peptide receptor 2
13	rs203415	31,387,796	RXFP2	Relaxin/insulin-like family peptide receptor 2
13	rs1041637	109,307,346	IRS2	Insulin receptor substrate 2
14	rs1873274	62,287,052	KCNH5	Potassium voltage-gated channel, subfamily H (eag-related), member 5
15	rs4779798	27,197,881	APBA2	Amyloid beta (A4) precursor protein-binding, family A, member 2 (X11-like)
15	rs2676083	31,397,903	RYR3	Ryanodine receptor 3
15	rs2596181	31,438,457	RYR3	Ryanodine receptor 3
18	rs9959583	20,993,778	ZNF521	Zinc finger protein 521
18	rs8085678	20,998,828	ZNF521	Zinc finger protein 521
18	rs1971613	21,589,323	ZNF521	Zinc finger protein 521
19	rs687136	45,366,831	AKT2	v-akt murine thymoma viral oncogene homolog 2
19	rs687155	45,366,846	AKT2	v-akt murine thymoma viral oncogene homolog 2

Signals from the HLA region on chromosome 6 are excluded from the information presented in the table.

Goal 3. Initiate genotyping of priority SNPs. **Milestone 3A.** Use the cohort of T1D family trios to evaluate confirmed SNPs for T1D risk. **Milestone 3B.** Use the cohort of T1D family trios to evaluate novel SNPs for T1D risk.

As outlined in Goal 3 Milestones 3A and 3B we have begun the process of evaluating SNPs selected from those shown in Tables 3 and 4 in order to evaluate interesting SNPs near confirmed T1D loci (Milestone 3A) and SNPs occurring near interesting genes (Milestone 3B) for risk of T1D. The 17 SNPs listed in Table 5 indicate those that have been selected for this step. At this stage of the process we have acquired the necessary reagents for PCR amplification and iPlex (Sequenom, Inc. San Diego, CA) style genotyping of DNA samples. The DNA samples are taken from our repository of affected (T1D) family trios. The data will be evaluated initially by TDT analysis.

Table 5. SNPs selected for iPlex Based Genotyping.

Chr	dbSNP ID	Location	Locus	Official Full Name
1	rs10858046	114,875,303	AMPD1	Adenosine monophosphate deaminase 1 (isoform M)
1	rs10917913	162,343,920	MGST3	Microsomal glutathione S-transferase 3
1	rs7555369	162,344,746	MGST3	Microsomal glutathione S-transferase 3
1	rs16839682	194,497,622	KCNT2	Potassium channel, subfamily T, member 2
2	rs12470503	163,405,297	KCNH7	Potassium voltage-gated channel, subfamily H (eag-related), member 7

2	rs1001911	163,421,846	KCNH7	Potassium voltage-gated channel, subfamily H (eag-related), member 7
2	rs1492990	163,422,123	KCNH7	Potassium voltage-gated channel, subfamily H (eag-related), member 7
2	rs10203602	163,442,376	KCNH7	Potassium voltage-gated channel, subfamily H (eag-related), member 7
2	rs1364562	163,449,972	KCNH7	Potassium voltage-gated channel, subfamily H (eag-related), member 7
5	rs10042443	55,388,527	IL6ST	Interleukin 6 signal transducer (gp130, oncostatin M receptor)
6	rs13214605	394,483	IRF4	Interferon regulatory factor 4
6	rs7765767	147,366,631	STXBP5	Syntaxin binding protein 5 (tomasyn)
9	rs7864499	91,744,788	IL6RL1	Interleukin 6 receptor-like 1
9	rs10982093	115,976,726	COL27A1	Collagen, type XXVII, alpha 1
12	rs12828016	868,626	WNK1	WNK lysine deficient protein kinase 1
18	rs9959583	20,993,778	ZNF521	Zinc finger protein 521
18	rs8085678	20,998,828	ZNF521	Zinc finger protein 521

12. Statement of Plans and Milestones for the Next Quarter

There are 3 goals that will be the focus of our work during the next research quarter.

Goal 1. Continue to recruit new T1D affected singletons and family trios. **Milestone 1A.** File application for access to the Wellcome Trust Case Control Consortium for access to the T1D (N=2,000) and control (N=3,000) cohorts. **Milestone 1B.** Continue to recruit T1D case trios and singletons from Pittsburgh.

Critical to the success of the project to identify novel loci associated with T1D is the inclusion of as many T1D affected family trios and singletons as possible. To accomplish this goal we will, throughout the lifespan of the project, continue to identify genetic datasets that are available for incorporation into our research (Milestone 1A) and recruit new participants from resources available through our association with UPMC (Milestone 1B). We anticipate that these milestones, or very similar milestones, will be the first goal of every research quarterly report.

Goal 2. Genotype select SNPs using T1D affected family trios. **Milestone 2A.** Using iPlex genotyping methodology genotype SNPs (N=12) occurring near confirmed T1D susceptibility loci (listed in Table 3) in T1D affected family trios (N=595) to measure association at truly positive SNPs. **Milestone 2B.** Beginning with the SNPs (N=17) listed in Table 5 of this quarterly report, genotype available T1D (N=595) affected family trios using iPlex methodology (Sequenom, Inc., San Diego, CA).

We will accomplish Goal 2 by formatting DNA samples from 595 T1D affected family trios (comprised of DNA from father, mother, and affected offspring) into 384-well trays. Sequenom iPlex methodology will be used to genotype the SNPs listed in Tables 3 and 5 for confirmed and novel T1D susceptibility loci, respectively. The iPlex methodology is a mass spectrometer based approach to DNA genotyping and the method is available at the University of Pittsburgh Genomics Core Laboratory. In the event that select SNPs need to be confirmed by an alternative strategy, we will employ TaqMan genotyping methodology that is available in the PI's laboratory.

Goal 3. Analyze the genotyping results garnered during Goal 2 in order to determine which SNPs replicate signal for association with T1D when analyzed in affected family trios. **Milestone 3A.** Evaluate genotyping data from Goal 2 for quality based upon SNP missingness occurring less than 5% of the time, sample missingness occurring less than 5% of the time, and consistency with known family pedigrees. **Milestone 3B.** Perform transmission equilibrium test (TDT) analysis of high quality genotyping data garnered in Goal 2 in order to identify SNPs that replicated in the GWA and TDT analyses.

The Goal 3 will be accomplished using the experimental data garnered during completion of Goal 2. Data will be initially characterized for quality by determined which, if any, samples or SNP genotyping assays result in failure frequency exceeding 5% of the total number of assays performed. Quality control will also include a test for family pedigree consistent with the pattern of Mendelian inheritance between parents and offspring. Datasets that are consistent with parental genotypes and quality control threshold for missingness will be used to determine by TDT analysis p-values associated with T1D susceptibility.

In our third quarterly scientific progress report (03/01/08 – 05/31/08) we then reported the following findings:

Type 1 Diabetes Genome-Wide Association Study Update:

As outlined in the following sections, the research goals for the second quarter of 2008 were 3-fold: 1) continue to recruit new T1D affected singletons and family trios; 2) genotype select SNPs using T1D affected family trios; and 3) analyze the genotyping results in order to determine which SNPs replicate signal for association with T1D. Our progress for each goal is addressed below.

Goal 1. Continue to recruit new T1D affected singletons and family trios. **Milestone 1A.** File application for access to the Wellcome Trust Case Control Consortium for access to the T1D (N=2,000) and control (N=3,000) cohorts. **Milestone 1B.** Continue to recruit T1D case trios and singletons from Pittsburgh.

The overall goal of the project is to identify novel genetic loci that impact risk of developing T1D. Critical to the success of the research is the inclusion of as many T1D affected singletons and family trios as possible. To accomplish this goal we will throughout the lifespan of the project identify publicly available genetic datasets (Milestone 1A) and recruit new participants (Milestone 1B) that can be incorporated into our study. Milestone 1A has recently been completed. On June 9, 2008 we submitted our application to the Wellcome Trust Case Control Consortium (WTCCC) that, if approved, will allow access to the WTCCC cohort of 2,000 T1D and 3,000 non-T1D singletons. This collection of case and control samples has been genotyped previously using the same methodology that was used during the genome-wide association scan (GWAS) performed in our laboratory. An important outcome of this is that it allows the preexisting WTCCC and Pittsburgh datasets to be combined in order to provide a powerful resource to test association statistics between genetic loci and T1D risk. We anticipate that during the next research quarter we will be notified as to whether our application to the WTCCC has been approved. If this is the case we will immediately begin to compare genetic association signals observed in our data with that observed by the WTCCC.

The second milestone of Goal 1 was to continue to recruit T1D case trios and singletons from Pittsburgh. The updated table for recruited T1D singletons and family trios is illustrated below (Table 1). In addition to participants recruited at Pittsburgh, we have arranged for DNA samples from participants recruited at Ulm, Germany (N=440). The German cohort consists of T1D (N=190) and non-T1D (N=250) singletons. The non-T1D samples add significantly to our study in that they represent a new collection of control samples to which the genetics of T1D case samples can be compared. The N=2,238 samples listed in Table 1 are available as DNA and are now contained within the Pittsburgh repository.

Table 1. T1D Singleton (N=1,988), non-T1D Singletons (N=250), and Family Trio (N=595) Characteristics.

	Pittsburgh Cohort		GoKinD Cohort		German Cohort	
	Singleton (T1D)	Trio (T1D)	Singleton (T1D)	Trio (T1D)	Singleton (T1D)	Singleton (non-T1D)
<i>Demographic Characteristics:</i>						
Number of Participants	55	26	1743	569	190	250
Caucasian (%)	100	100	100	100	100	100
Type 1 Diabetes (%)	100	100	100	100	100	0

Pittsburgh samples were recruited at the University of Pittsburgh Medical Center. GoKinD participants were recruited by the Genetics of Kidneys in Diabetes Study. The German cohort was recruited from Ulm, Germany as part of the EMIL cohort study.

Goal 2. Genotype select SNPs using T1D affected family trios. **Milestone 2A.** Using iPlex genotyping methodology genotype SNPs occurring near confirmed T1D susceptibility loci in T1D affected family trios (N=569) in order to measure association at truly positive SNPs. **Milestone 2B.** Beginning with the novel and clustered SNPs listed in Table 2 of this quarterly report, genotype available T1D (N=569) affected family trios using iPlex methodology.

Genetic loci were identified using results obtained from the T1D GWAS and are listed in Table 2. Loci have been sorted by whether they represent unique signals for T1D risk (i.e., Cluster of Greater Than 6 SNPs and Novel T1D Candidates) or have been identified previously by genetic analysis of preexisting T1D cohorts (i.e., T1DBase Candidate). Among the loci recognized as unique signals were genes encoding the insulin signaling proteins AKT2 and IRS2. Although no previously published genetic screens have associated genetic polymorphisms of these loci with T1D risk, gene knockout and knockdown studies performed in mice have indicated that insulin signaling through IRS2 is critical for pancreatic beta cell survival, and activity of the IRS2/AKT2 dependent insulin signaling pathway has been suggested to play a role in T1D onset. During the next research period, the loci listed in Table 2 will continue to form the basis for choosing which SNPs to test by iPlex genotyping technology.

Goal 3. Analyze genotyping results garnered during Goal 2 in order to determine which SNPs replicate signal for association with T1D when analyzed in affected family trios. **Milestone 3A.** Evaluate genotyping data from Goal 2 for quality based upon SNP missingness occurring less than 5% of the time, sample missingness occurring less than 5% of the time, and consistency with known family pedigrees. **Milestone 3B.** Perform transmission equilibrium test (TDT) analysis of high quality genotyping data garnered in Goal 2 in order to identify SNPs that replicated in the GWA and TDT analyses.

In order to complete the milestones of Goal 3 we have used iPlex genotyping methodology to evaluate a subset of the loci identified during analysis of the T1D GWAS (Table 3). The iPlex methodology is a mass spectrometer based approach to DNA genotyping. The method is available at the University of Pittsburgh Genomics Core Laboratory. The iPlex generated genotyping results have been obtained for 10 loci (Table 3) on DNA samples from 569 T1D affected family trios. As our work into elucidating the genetics of T1D susceptibility progresses we will continue to evaluate genetic loci for association with the T1D phenotype.

Using the criteria stated in Milestones 3A and 3B of Goal 3 we evaluated potential risk loci for genetic association with T1D. The first set of genotyping data has been characterized for quality of the genotyping results. Quality control analyses showed that the first 15 SNPs tested exhibited greater than 95% success for providing genotype data and that greater than 95% of the DNA samples provided genotyping data for each SNP (data not shown). Quality control testing also included the requirement that family pedigrees were consistent with the pattern of Mendelian inheritance of genetic markers between parents and offspring. It was observed that all T1D family trios passed the pedigree test. High quality genotyping results were also examined for accuracy and reproducibility by comparing genotypes determined using TaqMan and iPlex (Table 4). Quality control analysis of the iPlex data indicated that genotyping results were highly reproducible when compared with the identical samples genotyped using TaqMan assays. Taken together, these analyses indicate that SNP typing assays, DNA samples, and the iPlex methodology were of sufficient quality to accomplish the goal of association testing for all interesting genetic markers.

Summarized in Table 5 are the results for genetic association testing of 15 SNPs with the T1D phenotype. The assay used T1D affected family trios (N=569) and was evaluated using the Transmission Disequilibrium Test (TDT). The results indicate that this first set of SNPs did not replicate the results observed during the T1D GWAS of case and control singletons. A likely cause of this discrepancy is that the GWAS data was confounded by population stratification of T1D (case) and non-T1D (control) participants, a common occurrence in case and control analyses. The TDT test is notable for controlling errors that correlate with population stratification. In fact, the overall study design for our research project anticipated this possibility when we chose to follow up on the results of the case and control T1D GWAS with replication using T1D affected family trios and TDT analysis. TDT analysis of additional loci (Table 6) will occur during the next

research period and will confirm whether these other signals, observed as significant during the T1D GWAS, were due to population stratification or reflect true positive signals for genetic association.

Table 2. High value loci identified by genome-wide association scan for T1D.

<u>Locus</u>	<u>Classification</u>	<u>Locus</u>	<u>Classification</u>
ADNP2	Cluster of > 6 SNPs	CERKL	T1DBase Candidate
CFDP1	Cluster of > 6 SNPs	CLEC16A	T1DBase Candidate
KHDRBS2	Cluster of > 6 SNPs	CNTN4	T1DBase Candidate
LOC646112	Cluster of > 6 SNPs	CTLA4	T1DBase Candidate
SEMA6D	Cluster of > 6 SNPs	CYBA	T1DBase Candidate
TWISTNB	Cluster of > 6 SNPs	DBP	T1DBase Candidate
AKT2	Novel T1D Candidate	DEPDC2	T1DBase Candidate
ALOX5AP	Novel T1D Candidate	DIAPH3	T1DBase Candidate
AMPD1	Novel T1D Candidate	ELF1	T1DBase Candidate
APBA2	Novel T1D Candidate	ERBB3	T1DBase Candidate
BMPR1A	Novel T1D Candidate	FADD	T1DBase Candidate
C1GALT1	Novel T1D Candidate	FBXL4	T1DBase Candidate
CCK	Novel T1D Candidate	IL2RA	T1DBase Candidate
COL27A1	Novel T1D Candidate	IL6	T1DBase Candidate
CREG1	Novel T1D Candidate	IRF8	T1DBase Candidate
GOPC	Novel T1D Candidate	ITPR3	T1DBase Candidate
IL6RL1	Novel T1D Candidate	LOC728091	T1DBase Candidate
IL6ST	Novel T1D Candidate	LPL	T1DBase Candidate
IRF4	Novel T1D Candidate	MAPK14	T1DBase Candidate
IRS2	Novel T1D Candidate	MED12L	T1DBase Candidate
KCNH5	Novel T1D Candidate	OPCML	T1DBase Candidate
KCNT2	Novel T1D Candidate	PALLD	T1DBase Candidate
KCTD18	Novel T1D Candidate	PAX4	T1DBase Candidate
MGST3	Novel T1D Candidate	PDX1	T1DBase Candidate
PGR	Novel T1D Candidate	PHTF1	T1DBase Candidate
RXFP2	Novel T1D Candidate	PKD1L1	T1DBase Candidate
RYR3	Novel T1D Candidate	POLR2B	T1DBase Candidate
SLC30A8	Novel T1D Candidate	SENP7	T1DBase Candidate
STXBP5	Novel T1D Candidate	SEZ6L	T1DBase Candidate
TPK1	Novel T1D Candidate	SLC7A1	T1DBase Candidate
TRAF3IP1	Novel T1D Candidate	SLCO3A1	T1DBase Candidate
WNK1	Novel T1D Candidate	SOS2	T1DBase Candidate
ZNF521	Novel T1D Candidate	SPG7	T1DBase Candidate
AIRE	T1DBase Candidate	STAT4	T1DBase Candidate
ANKRD15	T1DBase Candidate	TLR2	T1DBase Candidate
AR	T1DBase Candidate	TLR7	T1DBase Candidate
BARD1	T1DBase Candidate	TMEM23	T1DBase Candidate
C4orf31	T1DBase Candidate	TNFSF11	T1DBase Candidate
C9orf25	T1DBase Candidate	TRAFD1	T1DBase Candidate
CAT	T1DBase Candidate	ULBP3	T1DBase Candidate
CD40	T1DBase Candidate	VDR	T1DBase Candidate
CD48	T1DBase Candidate		

Table 3. Novel T1D genetic loci tested using iPlex genotyping.

<u>Locus</u>	<u>Description</u>
AMPD1	Adenosine monophosphate deaminase 1 (isoform M)
COL27A1	Collagen, type XXVII, alpha 1
IL6RL1	Interleukin 6 receptor-like 1
IL6ST	Interleukin 6 signal transducer (gp130, oncostatin M receptor)
IRF4	Interferon regulatory factor 4
KCNH7	Potassium voltage-gated channel, subfamily H (eag-related), member 7
MGST3	Microsomal glutathione S-transferase 3
STXBP5	Syntaxin binding protein 5 (tomasyn)
WNK1	WNK lysine deficient protein kinase 1
ZNF521	Zinc finger protein 521

Table 4. Quality control analysis for iPlex and TaqMan genotyping of rs8078936 and rs222747

<i>Genotype Based Typing:</i>	iPlex Genotyping			TaqMan Genotyping			Chi Square
	<u>AA</u>	<u>AB</u>	<u>BB</u>	<u>AA</u>	<u>AB</u>	<u>BB</u>	
rs8078936	394	1423	1252	391	1433	1252	0.88
rs222747	182	1170	1735	179	1151	1732	0.78
<i>Allele Based Typing:</i>	iPlex Genotyping			TaqMan Genotyping			
<u>dbSNP_ID</u>	<u>Allele A</u>	<u>Allele B</u>		<u>Allele A</u>	<u>Allele B</u>		<u>p-value</u>
rs8078936	2211	3927		2215	3937		0.98
rs222747	1534	4640		1509	4615		0.79

p-values were calculated using chi square analysis and 1 degree of freedom.

Table 5. TDT results from T1D affected family trios (N=569)

<u>dbSNP ID</u>	<u>Chr</u>	<u>Location</u>	<u>Locus</u>	Transmission Disequilibrium Test Data			
				<u>Allele 1</u>	<u>Allele 2</u>	<u>Total</u>	<u>p-value</u>
rs10858046	1	114,875,303	AMPD1	239	235	474	0.85
rs10917913	1	162,343,920	MGST3	283	264	547	0.42
rs7555369	1	162,344,746	MGST3	263	281	544	0.44
rs12470503	2	163,405,297	KCNH7	236	257	493	0.34
rs1001911	2	163,421,846	KCNH7	255	225	480	0.17
rs1492990	2	163,422,123	KCNH7	254	226	480	0.20
rs10203602	2	163,442,376	KCNH7	197	204	401	0.73
rs1364562	2	163,449,972	KCNH7	199	205	404	0.77
rs10042443	5	55,388,527	IL6ST	226	238	464	0.58
rs13214605	6	394,483	IRF4	175	183	358	0.67
rs7765767	6	147,366,631	STXBP5	248	267	515	0.40
rs7864499	9	91,744,788	IL6RL1	225	213	438	0.57
rs10982093	9	115,976,726	COL27A1	112	112	224	1.00
rs12828016	12	868,626	WNK1	238	248	486	0.65
rs8085678	18	20,998,828	ZNF521	272	265	537	0.76

Table 6. High priority SNPs for TDT analysis during the upcoming research quarter.

<u>dbSNP_ID</u>	<u>Chr</u>	<u>Location</u>	<u>Locus</u>	<u>dbSNP_ID</u>	<u>Chr</u>	<u>Location</u>	<u>Locus</u>
rs6689415	1	114,908,992	AMPD1	rs10825557	10	51,709,687	TMEM23
rs2268697	1	115,029,016	AMPD1	rs2803590	10	88,362,973	BMPR1A
rs6427093	1	165,823,621	CREG1	rs11032755	11	34,533,161	CAT
rs2094028	1	194,417,119	KCNT2	rs574434	11	100,384,527	PGR
rs1441147	2	182,220,101	CERKL	rs7305099	12	845,537	WNK1
rs2696344	2	182,241,456	CERKL	rs7484827	12	46,409,830	VDR
rs2028201	2	201,011,255	KCTD18	rs1170188	13	41,576,971	TNFSF11
rs523437	2	239,063,548	TRAF3IP1	rs1170187	13	41,577,835	TNFSF11
rs580209	2	239,065,169	TRAF3IP1	rs670676	13	41,599,739	TNFSF11
rs9877118	3	2,578,450	CNTN4	rs1041637	13	109,307,346	IRS2
rs6771904	3	152,630,421	MED12L	rs7155762	14	49,487,928	SOS2
rs7654918	4	58,045,356	POLR2B	rs7155791	14	49,487,980	SOS2
rs343173	4	121,980,468	C4orf31	rs2676083	15	31,397,903	RYR3
rs950286	6	374,457	IRF4	rs16959754	15	45,680,428	SEMA6D
rs2498587	6	118,133,432	GOPC	rs10781976	16	73,872,339	CFDP1
rs6920096	6	147,412,791	STXBP5	rs1559339	16	73,876,147	CFDP1
rs6920901	6	147,470,991	STXBP5	rs4888405	16	73,985,697	CFDP1
rs6922684	6	150,491,727	ULBP3	rs11076678	16	87,165,397	CYBA
rs4870524	6	150,820,890	ULBP3	rs7184960	16	88,489,162	SPG7
rs1294610	7	7,332,182	C1GALT1	rs1971613	18	21,589,323	ZNF521
rs1404829	7	144,255,618	TPK1	rs1064059	18	75,994,674	ADNP2
rs2380437	8	69,156,370	DEPDC2	rs3786803	19	35,655,444	LOC728091
rs7032335	9	34,572,883	C9orf25	rs687136	19	45,366,831	AKT2
rs2808784	9	115,961,345	COL27A1	rs687155	19	45,366,846	AKT2
rs2567724	9	115,961,754	COL27A1	rs281408	19	53,925,218	DBP
				rs12975781	19	53,941,510	DBP

12. Statement of Plans and Milestones for the Next Quarter

There are 3 goals that will be the focus of our work during the next research quarter.

Goal 1. Continue to recruit new T1D affected singletons and family trios. **Milestone 1A.** As a continuing goal of the project into the genetics of T1D we will pursue the recruitment of new T1D case trios and singletons from Pittsburgh. **Milestone 1B.** Continue to arrange new collaborations with researchers at other institutions (e.g., Wellcome Trust Case Control Consortium and EMIL researchers at Ulm, Germany) to gain increased access to DNA repositories and datasets useful for evaluating the genetics of T1D

Goal 2. Continue to genotype select SNPs using T1D affected family trios. **Milestone 2A.** Select loci from those listed in Table 6 for use during genotyping replication studies. **Milestone 2B.** Using the T1D affected family trios determine the genotype of each SNP chosen during Milestone 2A.

Goal 3. Analyze the genotyping results garnered during Goal 2 in order to determine which SNPs replicate signal for association with T1D when analyzed using affected family trios. **Milestone 3A.** Analyze the results from Goal 2 by Transmission Disequilibrium Testing to identify loci that reproduce the results observed during the T1D GWAS study.

In the fourth and final quarterly scientific progress report (06/01/08 - 08/26/08) of year 01, we now report on our cumulative results.

Type 1 Diabetes Genome-Wide Association Study Update:

As outlined in the following sections, the research goals for the third quarter of 2008 were 3-fold: 1) continue to recruit new Type 1 Diabetes (T1D) affected singletons and family trios; 2) continue to genotype select SNPs using T1D affected family trios; and 3) analyze the genotyping results garnered during Goal 2 in order to determine which SNPs replicate signal for association with T1D when analyzed using affected family trios. Our progress for each goal is addressed below.

Goal 1. Continue to recruit new T1D affected singletons and family trios. **Milestone 1A.** As a continuing goal of the project into the genetics of T1D we will pursue the recruitment of new T1D case trios and singletons from Pittsburgh.

Milestone 1B. Continue to arrange new collaborations with researchers at other institutions (e.g., Wellcome Trust Case Control Consortium and EMIL researchers at Ulm, Germany) to gain increased access to DNA repositories and datasets useful for evaluating the genetics of T1D.

The first and second milestones of Goal 1 were to continue to recruit T1D case trios and singletons from Pittsburgh and to actively pursue collaborations with other research centers to increase the samples available to our study. The updated table for recruited T1D singletons and family trios is illustrated below indicating that during the last research quarter an additional 3 participants were recruited in Pittsburgh (Table 1). In contrast, participants recruited at Ulm, Germany have increased substantially from N=440 reported previously to N=2,608 during the last research quarter. The German cohort now consists of T1D (N=858) and non-T1D (N=1,750) singletons. The non-T1D samples add significantly to our study in that they represent a collection of control samples to which the genetics of T1D case samples can be compared. As of the end of the present research quarter, the N=4,978 samples listed in Table 1 are available as DNA and are now contained within the Pittsburgh repository.

Milestones 1A and 1B of Goal 1 represent goals that will be pursued continuously throughout the project. For the recently completed research quarter the milestones were accomplished upon recruitment of additional participants from Pittsburgh and, more significantly, upon receipt of greater than 2,000 DNA samples from our collaborator in Germany.

Table 1. T1D Singleton (N=2,659), non-T1D Singletons (N=1,750), and T1D Family Trio (N=595) Characteristics.

	Pittsburgh Cohort	GoKinD Cohort		German Cohort	
	Singleton (T1D)	Trio (T1D)	Singleton (T1D)	Trio (T1D)	Singleton (T1D)
<i>Demographic Characteristics:</i>					
Number of Participants	58	26	1,743	569	858
Caucasian (%)	100	100	100	100	100
Type 1 Diabetes (%)	100	100	100	100	0

Pittsburgh samples were recruited at the University of Pittsburgh Medical Center. GoKinD participants were recruited by the Genetics of Kidneys in Diabetes Study. The German cohort was recruited from Ulm, Germany as part of the EMIL cohort study.

Goal 2. Continue to genotype select SNPs using T1D affected family trios. **Milestone 2A.** Select loci from those listed in Table 6 (of the previous quarterly report) for use during genotyping replication studies. **Milestone 2B.** Using the T1D affected family trios determine the genotype of each SNP chosen during Milestone 2A.

As indicated in Table 2, select SNPs were chosen for analysis using mass spectrometry based genotyping method developed by Sequenom, Inc (San Diego, CA). SNPs were chosen based upon the signal observed during the initial genome-wide association (GWA) scan for T1D that has been described in preceding quarterly reports. In total, 21 SNPs were genotyped using the Sequenom iPLEX method and high quality data was returned on 19, providing an overall return of high quality data from SNPs sent for analysis of 90%. The 2 SNPs that failed to provide genotyping data were rs16839682 (KCNT2) and rs9959583 (ZNF521) and were due to lack of signal indicating that these samples may have failed to amplify during sample preparation. Subsequent analysis of the genotyping data obtained from the 19 successfully genotyped markers indicated that family pedigree remained intact and that missing data due to failure to genotype remained below 5% (data not shown).

Successful completion of Milestones 2A and 2B for the current research quarter was achieved upon creation of the genotyping data for these SNPs (Milestone 2A) and quality control analysis for missingness and family pedigree (Milestone 2B).

Table 2. List of SNPs for analysis of association with T1D.

<u>dbSNP ID</u>	<u>Chr</u>	<u>Location</u>	<u>Candidate Locus</u>	<u>Cytogenetic Band</u>	<u>Distance (kb)¹</u>
rs10858046	1	114,875,303	<i>AMPD1</i>	1p13	141.9
rs10917913	1	162,343,920	<i>MGST3</i>	1q23	1,523.2
rs7555369	1	162,344,746	<i>MGST3</i>	1q23	1,522.3
rs12470503	2	163,405,397	<i>KCNH7</i>	2q24.2	1.9
rs1001911	2	163,421,846	<i>KCNH7</i>	2q24.2	18.4
rs1492990	2	163,422,123	<i>KCNH7</i>	2q24.2	18.6
rs10203602	2	163,442,376	<i>KCNH7</i>	2q24.2	38.9
rs1364562	2	163,449,972	<i>KCNH7</i>	2q24.2	46.5
rs10042443	5	55,388,527	<i>IL6ST</i>	5q11	62.0
rs13214605	6	394,483	<i>IRF4</i>	6p25-p23	38.3
rs7765767	6	147,366,631	<i>STXBP5</i>	6q24.3	199.9
rs7864499	9	91,744,788	<i>IL6RL1</i>	9q22.2	138.5
rs10982093	9	115,976,726	<i>COL27A1</i>	9q32	intron
rs12828016	12	868,626	<i>WNK1</i>	12p13.3	nonsynonymous
rs877610	17	3,422,240	<i>TRPV1</i>	17p13.3	nonsynonymous
rs8078936	17	3,427,145	<i>TRPV1</i>	17p13.3	intron
rs161393	17	3,436,263	<i>TRPV1</i>	17p13.3	intron
rs222747	17	3,439,949	<i>TRPV1</i>	17p13.3	nonsynonymous
rs8085678	18	20,998,828	<i>ZNF521</i>	18q11.2	intron

1. Distance between SNP and candidate locus if extragenic. If SNP is intragenic than its functional position is indicated.

Goal 3. Analyze the genotyping results garnered during Goal 2 in order to determine which SNPs replicate signal for association with T1D when analyzed using affected family trios. **Milestone 3A.** Analyze the results from Goal 2 by Transmission Disequilibrium Testing to identify loci that reproduce the results observed during the T1D GWAS study.

Transmission disequilibrium testing (TDT) of the genotype data obtained during completion of Goal 2 is the focus of the third goal for the current research quarter. The goal was completed by calculating the p-value of association correlated with the 19 SNPs listed in Table 3 in order to estimate the risk of developing T1D. The analysis was based upon genotyping data obtained from 569 family trios in which the offspring was T1D positive. Of the 19 SNPs examined signals for inheritance of one allele over the other, and thus an indication that alleles associate with T1D, varied between 50% (or essentially random) for locus *COL27A1* and 53.7% for SNP rs161393 located within the *TRPV1* locus. Analysis of the genotyping data for rs161393 indicated that out of 486 heterozygous parents there were 225 offspring inheriting allele A and 261 that inherited allele B. This corresponded to a chi square value of 2.7 and p-value of 0.1. However, the criteria of our study has been that for SNPs to be considered as exhibiting significant association with T1D the p-values must be less than 0.05. Thus, for the SNPs examined so far for association with T1D the conclusion is that they are not likely to significantly impact disease risk.

Completion of Goal 3 was accomplished by analysis of the genotyping data obtained during the recently completed research quarter. The results failed to identify novel T1D loci but the analysis did confirm that the genotyping method and laboratory procedures in place in Pittsburgh are sufficient to routinely obtain high quality genetic information from a large number of samples (N=1,707) and on a large number of genetic markers (N=19). The operational infrastructure that has been developed to accomplish the goals of the 2007 and 2008 research period will be used to investigate genetic influence of diabetes complications, while continuing to investigate candidate markers for T1D, in the upcoming research period(s).

Table 3. Transmission disequilibrium analysis of T1D affected family trios.

<u>dbSNP ID</u>	<u>Chr</u>	<u>Location</u>	<u>Locus</u>	<u>Allele 1</u>	<u>Allele 2</u>	<u>Total</u>	<u>%Trans</u>	<u>Chi Sq</u>	<u>p-value</u>
rs10858046	1	114,875,303	<i>AMPD1</i>	239	235	474	50.4	0.0	8.5E-01
rs10917913	1	162,343,920	<i>MGST3</i>	283	264	547	51.7	0.7	4.2E-01

rs7555369	1	162,344,746	<i>MGST3</i>	263	281	544	48.3	0.6	4.4E-01
rs12470503	2	163,405,397	<i>KCNH7</i>	236	257	493	47.9	0.9	3.4E-01
rs1001911	2	163,421,846	<i>KCNH7</i>	255	225	480	53.1	1.9	1.7E-01
rs1492990	2	163,422,123	<i>KCNH7</i>	254	226	480	52.9	1.6	2.0E-01
rs10203602	2	163,442,376	<i>KCNH7</i>	197	204	401	49.1	0.1	7.3E-01
rs1364562	2	163,449,972	<i>KCNH7</i>	199	205	404	49.3	0.1	7.7E-01
rs10042443	5	55,388,527	<i>IL6ST</i>	226	238	464	48.7	0.3	5.8E-01
rs13214605	6	394,483	<i>IRF4</i>	175	183	358	48.9	0.2	6.7E-01
rs7765767	6	147,366,631	<i>STXBP5</i>	248	267	515	48.2	0.7	4.0E-01
rs7864499	9	91,744,788	<i>IL6RL1</i>	225	213	438	51.4	0.3	5.7E-01
rs10982093	9	115,976,726	<i>COL27A1</i>	112	112	224	50.0	0.0	1.0E+00
rs12828016	12	868,626	<i>WNK1</i>	238	248	486	49.0	0.2	6.5E-01
rs877610	17	3,422,240	<i>TRPV1</i>	45	47	92	48.9	0.0	8.3E-01
rs8078936	17	3,427,145	<i>TRPV1</i>	227	259	486	46.7	2.1	1.5E-01
rs161393	17	3,436,263	<i>TRPV1</i>	225	261	486	46.3	2.7	1.0E-01
rs222747	17	3,439,949	<i>TRPV1</i>	197	208	405	48.6	0.3	5.8E-01
rs8085678	18	20,998,828	<i>ZNF521</i>	272	265	537	50.7	0.1	7.6E-01

Statement of Plans for the First Quarterly Report of the 2008 to 2009 research period

The goals listed below based upon Task 2 (recruit participants with T1D or T1DN) and Task 3 (genotype candidate genetic markers for association with T1DN) of the overall research project and will use our available cohort of T1DN (cases) and T1D (controls) to perform an additional series of genetic analyses based upon the GWA study that used the 500,000 SNP typing microarray previously reported. The overall goal will be to confirm the strongest genetic signals associated with diabetes complications and will focus upon T1D nephropathy (T1DN).

There are 3 goals that will be the focus of our work during the next research quarter.

Goal 1. Expand genetic analysis to include (T1DN) phenotype. **Milestone 1A.** Analyze available anthropometric data linked with T1D cohort for presence of diabetes complications. **Milestone 1B.** Determine the size of the available cohort for T1D nephropathy (T1DN) and T1D with healthy kidney function.

Goal 2. Garner genetic data to test for association of select SNPs with T1DN. **Milestone 2A.** Use the T1DN and T1D cohort identified during Goal 1 to initiate genotyping of candidate SNPs for their association with T1DN.

Goal 3. Analyze the results of genotyping obtained using the T1DN cohort. **Milestone 3A.** Using T1DN family trios calculate the p-value for association of candidate SNPs with the T1DN phenotype. **Milestone 3B.** Using T1DN and T1D singletons calculate the p-value for association of select SNPs with the T1DN phenotype.

KEY RESEARCH ACCOMPLISHMENTS:

1. Creation of a sample repository containing DNA from 3,170 T1D and 1,750 non-T1D participants
2. Establishment of laboratory methods for multiplex genotyping of 30 or more SNPs simultaneously from as many as 5,000 samples
3. Initiation of genetic studies to evaluate candidate genetic markers for association with diabetes complications
4. Analysis of genetic data to evaluate candidate genes for association with diabetes phenotypes
5. Publication of 9 manuscripts

REPORTABLE OUTCOMES:

Manuscripts (9 publications)

1. Ringquist, S., Nichol, L., Trucco, M. Transplantation Genetics. (2007) *In: Emery and Rimoin's Principles and Practice of Medical Genetics.* eds. D.L. Rimoin, M. Conner, R.E. Pyeritz, B.R. Korf, and A.E. Emery 5th Edition, Elsevier Books, Oxford.
2. Ringquist, S., Pecoraro, C., Trucco, M. (2007) Web-based program for pyrosequencing primer design. ASHI Quarterly 31:50-52.
3. Ringquist S, Pecoraro C, Lu Y, Styche A, Rudert WA, Benos PV, Trucco M. (2007) Web-based primer design software for genome-scale genotyping by pyrosequencing. *Methods Mol Biol* 373:25-38.
4. Ringquist S, Styche A, Rudert WA, Trucco M. (2007) Pyrosequencing-based strategies for improved allele typing of human leukocyte antigen loci. *Methods Mol Biol* 373:115-134.
5. Pasquali L, Bedeir A, Ringquist S, Styche A, Bhargava R, Trucco G. (2007) Quantification of CpG island methylation in progressive breast lesions from normal to invasive carcinoma. *Cancer Lett* 257:136-144.
6. Pasquali L, Trucco M, Ringquist S. (2007) Navigating pathways affecting type 1 diabetic kidney disease. *Pediatr Diabetes* 8:307-322.
7. Luca D, Ringquist S, Klei L, Lee AB, Gieger C, Wichmann HE, Schreiber S, Krawczak M, Lu Y, Styche A, Devlin B, Roeder K, Trucco M. (2008) On the use of general control samples for genome-wide association studies: genetic matching highlights causal variants. *Am J Hum Genet* 82:453-463.
8. Zhang L, Perdomo G, Kim DH, Qu S, Ringquist S, Trucco M, Dong HH. (2008) Proteomic analysis of fructose-induced fatty liver in hamsters. *Metabolism* 57:1115-1124.
9. Lu, L., Boehm, J., Nichol, L., Trucco, M., and Ringquist, S. (2008) Multiplex HLA typing by pyrosequencing. *Methods in Molecular Biology* (in press).

Abstracts

None

Presentations

None

Patents and Licenses Applied for and/or Issued

None

Degrees Obtained that are Supported by this Award

None

Development of Cell Lines, Tissue or Serum Repositories

1. Repository of DNA samples collected from T1D and T1DN patients exceeding 5,000 samples.

Informatics such as Databases and Animal Models, etc

None

Funding Applied for Based on Work Supported by this Award

None

Employment or Research Opportunities Applied for and/or Received Based on Experience/Training Supported by this Award

None

CONCLUSION:

The principal conclusions for the first year of funding are that: 1) we have been successful in recruiting and obtained via collaboration a large cohort (nearly 5,000 participants) for analysis of diabetes complications and 2) that laboratory methods are in place and have been tested for analysis of large number of samples for association between SNP and T1D related phenotypes. Our work during the first year primarily focused on increasing the cohort size and on validating laboratory methods for genetic analysis. Now that these have been accomplished we will begin to test our principle hypothesis that risk for diabetes complications is dependent upon genes and that environmental factors such as smoking will influence that risk.

The work generated thus far has resulted in 9 publications that are listed under the section entitled "REPORTABLE OUTCOMES". These scientific manuscripts have been published in peer review publications. We are currently editing a new manuscript describing our work on diabetes complications and anticipate having that paper ready for submission to a scientific journal prior to the end of 2008.

The So What Section. What are the implications of this research? Diabetes affects 16 million Americans and 800,000 new cases annually. African, Hispanic, Native and Asian Americans are particularly susceptible to its most severe complications. Costs associated with diabetes may be as high as \$132 billion. Diabetes accounts for 42% of new cases of ESRD with over 100,000 cases per year at an average cost of \$55,000 per patient annually.

What are the military significance and public purpose of this research? As the military is a reflection of the US population, improved prediction of risk for developing diabetes and diabetic complications among active duty members of the military, their families, and retired military personnel will potentially allow focused preventative treatment of at-risk individuals, providing significant healthcare savings and improved patient well being.

REFERENCES:

1. Ringquist, S., Nichol, L., Trucco, M. Transplantation Genetics. (2007) *In: Emery and Rimoin's Principles and Practice of Medical Genetics.* eds. D.L. Rimoin, M. Conner, R.E. Pyeritz, B.R. Korf, and A.E. Emery 5th Edition, Elsevier Books, Oxford.
2. Ringquist, S., Pecoraro, C., Trucco, M. (2007) Web-based program for pyrosequencing primer design. *ASHI Quarterly* 31:50-52.
3. Ringquist S, Pecoraro C, Lu Y, Styche A, Rudert WA, Benos PV, Trucco M. (2007) Web-based primer design software for genome-scale genotyping by pyrosequencing. *Methods Mol Biol* 373:25-38.
4. Ringquist S, Styche A, Rudert WA, Trucco M. (2007) Pyrosequencing-based strategies for improved allele typing of human leukocyte antigen loci. *Methods Mol Biol* 373:115-134.
5. Pasquali L, Bedeir A, Ringquist S, Styche A, Bhargava R, Trucco G. (2007) Quantification of CpG island methylation in progressive breast lesions from normal to invasive carcinoma. *Cancer Lett* 257:136-144.
6. Pasquali L, Trucco M, Ringquist S. (2007) Navigating pathways affecting type 1 diabetic kidney disease. *Pediatr Diabetes* 8:307-322.
7. Luca D, Ringquist S, Klei L, Lee AB, Gieger C, Wichmann HE, Schreiber S, Krawczak M, Lu Y, Styche A, Devlin B, Roeder K, Trucco M. (2008) On the use of general control samples for genome-wide association studies: genetic matching highlights causal variants. *Am J Hum Genet* 82:453-463.
8. Zhang L, Perdomo G, Kim DH, Qu S, Ringquist S, Trucco M, Dong HH. (2008) Proteomic analysis of fructose-induced fatty liver in hamsters. *Metabolism* 57:1115-1124.
9. Lu, L., Boehm, J., Nichol, L., Trucco, M., and Ringquist, S. (2008) Multiplex HLA typing by pyrosequencing. *Methods in Molecular Biology* (in press).

APPENDICES:

We have included the following as appendix materials:

Appendix 1: T1D GWAS p-values

Appendix 2: Wellcome Trust Information

We have also included the following published manuscripts:

Ringquist, S., Pecoraro, C., Trucco, M. (2007) Web-based program for pyrosequencing primer design. ASHI Quarterly 31:50-52.

Ringquist S, Pecoraro C, Lu Y, Styche A, Rudert WA, Benos PV, Trucco M. (2007) Web-based primer design software for genome-scale genotyping by pyrosequencing. *Methods Mol Biol* 373:25-38.

Pasquali L, Trucco M, Ringquist S. (2007) Navigating pathways affecting type 1 diabetic kidney disease. *Pediatr Diabetes* 8:307-322.

Luca D, Ringquist S, Klei L, Lee AB, Gieger C, Wichmann HE, Schreiber S, Krawczak M, Lu Y, Styche A, Devlin B, Roeder K, Trucco M. (2008) On the use of general control samples for genome-wide association studies: genetic matching highlights causal variants. *Am J Hum Genet* 82:453-463.

SUPPORTING DATA:

None

T1D GWAS p-values <0.001 (Revised 122807)

3	141,676,092	rs10513115	5.9E-04	1.6E-01	3.1E-01	5,231,644			GM2AP	18,363	GM2AP
3	146,907,736	rs2459136	8.7E-05	5.4E-03	1.5E-03	18,363	Pass				GM2AP
3	146,926,096	rs2687861	2.1E-04	1.2E-02	6.6E-03	4,918,331			SELT		SELT
3	151,844,430	rs6440690	8.6E-05	3.6E-02	4.4E-02	785,991	Pass				MED12L
3	152,630,421	rs6771904	1.8E-02	5.3E-04	2.7E-03	1,137,684		MED12L	152,287,366	152,634,500	
3	153,768,105	rs11925597	4.9E-02	5.5E-04	1.6E-01	4,576,339					
3	158,344,444	rs6809003	2.7E-03	9.1E-05	7.1E-03	88,982	Pass		CCNL1		CCNL1
3	158,433,426	rs13081038	4.6E-03	1.9E-04	1.2E-02	1,462				1,462	
3	158,434,888	rs10451916	3.1E-03	1.5E-04	1.1E-02	551				551	CCNL1
3	158,435,439	rs1392799	1.2E-03	2.1E-05	4.3E-03	10,853	Pass		CCNL1	10,853	CCNL1
3	158,446,292	rs9831830	3.0E-03	1.6E-04	1.1E-02	2,637				2,637	VEPH1
3	158,448,929	rs7642179	3.0E-03	1.0E-04	6.3E-03	7,569				7,569	VEPH1
3	158,456,498	rs1500925	3.4E-03	1.8E-04	1.1E-02	627				627	VEPH1
3	158,457,125	rs9289980	1.5E-02	7.1E-04	1.2E-02	7,054				7,054	VEPH1
3	158,464,179	rs924517	1.5E-02	8.9E-04	8.4E-03	9,907				9,907	VEPH1
3	158,474,086	rs12633429	2.5E-02	9.6E-04	8.9E-03	17,521				17,521	VEPH1
3	158,491,607	rs2874616	2.7E-02	9.6E-04	1.3E-02	35,260				35,260	VEPH1
3	158,526,867	rs10936081	8.7E-03	2.8E-04	9.7E-03	1,677				1,677	VEPH1
3	158,528,544	rs1522392	2.3E-02	8.5E-04	2.1E-02	293,539					VEPH1
3	158,822,083	rs11709879	1.7E-02	7.6E-03	5.8E-04	2,018					
3	158,824,101	rs9876844	1.7E-02	9.2E-03	5.6E-04	1,657,233					
3	160,481,334	rs9831067	5.4E-02	6.1E-04	1.6E-02	194,103					
3	160,675,437	rs9824310	1.7E-02	3.4E-03	9.4E-04	1,799,688					
3	162,475,125	rs9828189	3.9E-02	7.9E-02	2.2E-04	37,361				37,361	NMD3
3	162,512,486	rs9811833	3.6E-02	7.9E-02	2.2E-04	29,825				29,825	NMD3
3	162,542,311	rs336546	3.0E-02	7.6E-02	2.5E-04	5,683,665					NMD3
3	168,225,976	rs1949532	1.7E-05	9.4E-05	1.3E-04	216,996	Pass		Intergenic		Intergenic
3	168,442,972	rs11923256	4.1E-04	1.2E-02	8.0E-03	141,846					
3	168,584,818	rs1564568	3.6E-04	3.1E-03	2.5E-02	1,487				1,487	SERPINI2
3	168,586,305	rs11714970	6.9E-04	5.0E-03	2.9E-02	7,778				7,778	SERPINI2
3	168,594,083	CG03028974	9.9E-04	8.4E-03	2.8E-02	8,944,150					SERPINI2
3	177,538,233	rs2128850	4.1E-04	8.7E-02	2.8E-02	659				659	LOC730168
3	177,538,893	rs13100792	8.1E-04	1.4E-01	2.4E-02	22,262				22,262	LOC730168
3	177,561,154	rs2170808	9.0E-04	1.2E-01	7.6E-02	8,056,977					LOC730168
3	185,618,131	rs1533678	3.2E-04	4.8E-02	1.2E-01	19,971					
3	185,638,102	rs7429010	9.8E-04	5.1E-02	2.2E-01	200,280					
3	185,838,382	rs7646910	6.1E-03	3.0E-02	8.0E-04	667				4,365	ETV5
3	185,839,049	rs4686705	8.4E-03	3.8E-02	8.0E-04	1,445,273				5,502	ETV5
3	187,284,322	rs7433760	5.9E-02	9.1E-04	2.6E-03	4,365					ETV5
3	187,288,687	rs4686730	6.4E-02	1.9E-04	1.3E-03	5,502					ETV5
3	187,294,189	rs6444106	7.0E-02	2.8E-04	1.4E-03	303,984					ETV5
3	187,598,173	rs9851300	2.4E-02	1.9E-02	5.4E-04	1,677,592					
3	189,275,763	rs9813167	6.5E-04	3.1E-04	1.5E-03	458,465					
3	189,734,230	rs17605260	1.2E-03	1.7E-02	8.8E-04	9,012				9,012	LPP
3	189,743,242	rs1426261	5.0E-04	1.1E-02	3.1E-04	155				155	LPP
3	189,743,397	rs1426260	1.0E-03	1.2E-02	6.2E-04	7,909				7,909	LPP
3	189,751,306	rs4263285	1.1E-03	2.1E-02	3.4E-04	1,716,531					LPP
3	191,467,837	rs17427694	2.3E-01	7.0E-02	5.0E-04	4,543,255					
3	196,011,092	rs4434099	1.9E-03	9.3E-04	1.9E-03	1,380,958					
3	197,392,050	rs4916483	3.7E-02	5.9E-04	7.2E-02						
4	5,820,851	rs6817935	5.4E-03	6.1E-04	1.6E-01	205,170					
4	6,026,021	rs117333383	1.0E-01	8.0E-04	4.9E-02	1,712,997					
4	7,739,018	rs1557818	2.4E-03	3.6E-04	7.1E-04	3,075					
4	7,742,093	rs929264	4.6E-04	1.8E-04	4.0E-04	847,788					
4	8,589,881	rs3103091	4.4E-04	8.3E-02	1.0E-01	7,458,654					
4	16,048,535	rs4698487	1.3E-04	3.7E-03	1.1E-03	284,523					
4	16,333,058	rs1514645	6.9E-04	7.6E-05	6.5E-04	2,246			LDB2	2,246	LDB2
4	16,335,304	rs2645255	5.8E-04	9.3E-05	8.9E-04	580	Pass		LDB2	580	LDB2
4	16,335,864	rs2658509	2.2E-02	7.7E-04	6.6E-03	10,844				10,844	LDB2
4	16,346,728	rs283021	1.2E-02	6.1E-04	7.3E-03	6,454				6,454	LDB2
4	16,353,182	rs883086	5.3E-04	4.7E-04	1.4E-03	1,314,537					LDB2
4	17,667,719	rs9784574	1.6E-01	7.1E-03	9.7E-04	1,157,874					
4	18,825,593	rs10516333	1.3E-03	7.6E-04	8.5E-03	6,374,818					
4	25,200,411	rs939352	2.1E-04	6.2E-03	4.7E-02	3,863,633					
4	29,064,044	rs13118914	3.2E-03	7.2E-04	5.2E-02	3,508,968					
4	32,573,012	rs6531531	1.0E-05	1.7E-03	1.9E-04	3,408,030	Pass		Intergenic		Intergenic
4	35,981,042	rs10001947	4.7E-02	8.5E-04	4.8E-02	6,514,171					
4	42,495,213	rs2575515	8.2E-05	6.9E-03	1.1E-03	14,833	Pass		LOC389207	14,833	LOC389207
4	42,510,046	rs4861224	7.8E-04	2.5E-02	3.6E-03	99,351					
4	42,609,397	rs4861237	1.3E-03	1.9E-04	2.2E-02	25,052				25,052	LOC389207
4	42,634,449	rs2345759	6.5E-03	3.8E-04	1.0E-01	20,976				20,976	LOC389207
4	42,655,425	rs99213	4.0E-03	2.3E-04	6.4E-02	64,587					LOC389207
4	42,720,012	rs10938230	8.6E-03	5.2E-04	1.1E-01	17,151				17,151	LOC389207
4	42,737,163	rs920153	5.2E-03	3.7E-04	6.1E-02	6,839				6,839	LOC389207
4	42,744,002	rs10938235	7.2E-03	3.0E-04	9.8E-02	5,412				5,412	LOC389207
4	42,749,414	rs720961	9.0E-03	3.6E-04	1.1E-01	4,307				4,307	LOC389207
4	42,753,721	rs6865602	9.1E-03	3.6E-04	1.1E-01	7,773				7,773	LOC389207
4	42,761,494	rs1595187	7.2E-03	3.4E-04	1.3E-01	12,833,910					LOC389207
4	55,595,404	rs4864949	9.7E-04	1.3E-01	3.1E-02	339,640					
4	55,935,044	rs4864984	1.8E-02	3.6E-04	1.1E-02	12,537					
4	55,947,581	rs7664496	3.5E-02	8.3E-04	3.4E-02	5,144,943					

6	28,641,925	rs418092	9.3E-05	6.5E-05	2.8E-02	41,226	Pass	HLA Region
6	28,683,151	rs1474986	1.8E-04	1.3E-03	2.9E-02	159,504		HLA Region
6	28,842,655	rs1233604	1.0E-03	2.8E-04	5.0E-02	61,180		HLA Region
6	28,903,835	rs135296	8.0E-05	5.6E-05	1.7E-02	235,286	Pass	HLA Region
6	29,139,121	rs3117143	1.8E-04	4.5E-05	2.7E-02	26,497	Pass	HLA Region
6	29,165,618	rs3129788	6.0E-05	4.2E-05	2.3E-02	15,455	Pass	HLA Region
6	29,181,073	rs3131091	3.1E-04	1.2E-03	9.8E-02	94,481		HLA Region
6	29,275,554	rs3116830	3.4E-05	4.1E-05	1.2E-02	10,939	Pass	HLA Region
6	29,286,493	rs2206040	5.2E-04	1.9E-03	1.2E-01	16,497		HLA Region
6	29,302,990	rs3130813	7.8E-05	3.6E-04	8.7E-03	30,784	Pass	HLA Region
6	29,333,774	rs317330	7.5E-04	5.5E-03	6.3E-02	30,625		HLA Region
6	29,364,399	rs1884123	9.3E-04	5.2E-03	4.2E-02	4,011		HLA Region
6	29,368,410	rs317425	2.0E-05	5.1E-06	2.9E-03	82,344	Pass	HLA Region
6	29,450,754	rs3749971	7.2E-05	1.0E-05	7.7E-03	22,176	Pass	HLA Region
6	29,472,930	rs2073151	7.8E-04	1.9E-03	5.9E-03	11,434		HLA Region
6	29,484,364	rs406511	4.9E-06	2.8E-07	4.4E-04	39,079	Pass	HLA Region
6	29,523,443	rs2523443	1.1E-05	6.3E-06	1.3E-03	28,657	Pass	HLA Region
6	29,552,100	rs1233495	9.2E-03	8.2E-04	9.4E-02	102,678		HLA Region
6	29,654,778	rs1233396	3.0E-04	1.4E-04	8.0E-03	1,290		HLA Region
6	29,656,068	rs926552	9.4E-04	4.1E-04	3.2E-03	438,235		HLA Region
6	30,094,303	rs3115631	6.6E-06	6.9E-06	2.6E-03	106,813	Pass	HLA Region
6	30,201,116	rs2517592	8.8E-03	6.5E-04	1.9E-02	10,223		HLA Region
6	30,211,339	rs1541269	5.9E-06	1.4E-06	4.5E-04	49,107	Pass	HLA Region
6	30,260,446	CG06006774	1.4E-06	2.0E-06	4.4E-04	5,660	Pass	HLA Region
6	30,266,106	rs2517618	5.9E-04	1.0E-04	5.9E-03	11,200		HLA Region
6	30,277,306	rs2517611	1.8E-03	9.1E-04	6.2E-03	62,502		HLA Region
6	30,339,808	rs3094070	1.1E-03	6.8E-04	2.4E-02	421		HLA Region
6	30,340,229	rs3130404	9.3E-04	5.3E-04	2.0E-02	1,902		HLA Region
6	30,342,131	rs3130405	7.7E-04	6.7E-04	2.9E-02	516		HLA Region
6	30,342,647	rs2844764	1.6E-03	7.6E-04	1.6E-02	86,389		HLA Region
6	30,429,036	rs3132649	6.4E-08	6.5E-06	2.1E-04	132	Pass	HLA Region
6	30,429,168	rs3094061	3.6E-06	2.3E-05	1.2E-03	147	Pass	HLA Region
6	30,429,315	rs3130374	7.2E-06	4.3E-05	8.6E-04	146	Pass	HLA Region
6	30,429,461	rs3094627	5.0E-07	7.5E-06	5.2E-04	6,710	Pass	HLA Region
6	30,436,171	rs3130351	1.2E-06	2.5E-06	1.8E-04	165	Pass	HLA Region
6	30,436,336	rs3130352	1.1E-06	1.1E-06	1.2E-04	1,609	Pass	HLA Region
6	30,437,945	rs3094057	4.8E-06	6.6E-06	2.6E-04	2,180	Pass	HLA Region
6	30,440,125	rs3094055	4.3E-05	7.1E-04	2.1E-03	409	Pass	HLA Region
6	30,440,534	rs1012411	1.1E-05	6.8E-05	1.1E-03	9,957	Pass	HLA Region
6	30,450,491	rs3132636	9.4E-04	1.6E-03	3.9E-03	739		HLA Region
6	30,451,230	rs3129819	7.2E-04	1.2E-03	4.5E-03	3,988		HLA Region
6	30,455,218	rs970269	6.8E-04	9.5E-04	3.9E-03	1,962		HLA Region
6	30,457,180	rs3094623	8.1E-04	9.8E-04	5.1E-03	9,390		HLA Region
6	30,466,570	rs3094050	5.6E-11	7.1E-09	7.0E-06	366	Pass	HLA Region
6	30,466,936	rs3094703	4.0E-10	2.1E-08	1.7E-05	4,394	Pass	HLA Region
6	30,471,330	rs3094034	7.3E-07	1.5E-06	7.7E-05	88,553	Pass	HLA Region
6	30,559,883	rs3094694	1.4E-07	1.3E-07	6.7E-05	176,178	Pass	HLA Region
6	30,736,061	rs3130000	3.3E-05	1.3E-03	1.6E-03	65,734	Pass	HLA Region
6	30,801,795	rs3095329	2.6E-08	7.3E-07	8.3E-06	3,631	Pass	HLA Region
6	30,805,426	rs3094127	3.3E-09	1.0E-07	1.3E-06	29,492	Pass	HLA Region
6	30,834,918	rs3095340	1.8E-04	1.1E-06	4.8E-05	1,421	Pass	HLA Region
6	30,836,339	rs3094122	1.2E-03	4.8E-04	1.5E-03	18,856		HLA Region
6	30,855,195	rs10947091	6.4E-03	2.7E-04	2.3E-04	7,324		HLA Region
6	30,862,519	rs12527415	1.6E-03	1.5E-04	6.7E-05	3,808	Pass	HLA Region
6	30,866,327	rs11756868	1.7E-03	1.4E-04	5.1E-05	1,677	Pass	HLA Region
6	30,868,004	rs3131050	1.9E-09	2.1E-09	8.8E-07	3,266	Pass	HLA Region
6	30,871,270	rs3131060	2.5E-09	4.1E-09	1.2E-06	3,654	Pass	HLA Region
6	30,874,924	rs4587207	5.0E-02	1.6E-03	9.4E-04	5,433		HLA Region
6	30,880,357	rs3094123	2.3E-05	1.9E-04	3.7E-03	936	Pass	HLA Region
6	30,881,293	rs4713376	3.3E-04	6.7E-02	2.5E-02	16,294		HLA Region
6	30,897,587	rs12195469	5.2E-04	8.0E-02	2.4E-02	13,646		HLA Region
6	30,911,233	rs3130649	8.5E-04	4.9E-05	4.8E-05	14,612	Pass	HLA Region
6	30,925,845	rs3095350	2.1E-03	7.3E-05	3.9E-05	77,814	Pass	HLA Region
6	31,003,659	rs4711247	4.8E-03	1.3E-03	6.9E-04	6,215	DPCR1	HLA Region
6	31,009,874	rs3131785	1.8E-04	3.1E-03	3.8E-02	2,053	DPCR1	DPCR1
6	31,011,927	rs3131784	1.8E-04	3.7E-03	4.9E-02	36,439	DPCR1	HLA Region
6	31,048,366	rs2530710	1.9E-06	1.5E-05	8.6E-05	32,202	Pass	DPCR1
6	31,080,568	rs1634717	2.8E-04	1.3E-05	4.9E-04	276	Pass	HLA Region
6	31,080,844	rs1634718	1.1E-06	5.4E-08	3.9E-05	2,784	Pass	HLA Region
6	31,083,628	rs1632854	2.1E-04	1.2E-05	4.2E-04	37,892	Pass	HLA Region
6	31,121,520	rs2517538	3.4E-04	1.2E-05	3.1E-03	4,907	Pass	HLA Region
6	31,126,427	rs2523865	2.1E-09	3.3E-10	5.1E-07	7,265		HLA Region
6	31,133,692	rs2517524	4.6E-03	1.9E-02	2.3E-04	32,627		HLA Region
6	31,166,319	rs3130544	6.2E-17	1.7E-14	5.4E-10	22,131	Pass	HLA Region
6	31,188,450	rs1265052	2.6E-06	6.5E-07	6.1E-05	1,367	Pass	HLA Region
6	31,189,817	rs3130975	9.3E-08	2.0E-07	2.2E-05	1,975	Pass	HLA Region
6	31,191,792	rs3130981	5.8E-06	1.8E-05	1.6E-04	3,320	Pass	HLA Region
6	31,195,112	rs3095324	1.1E-07	1.2E-07	1.8E-05	2,498	Pass	HLA Region
6	31,197,610	rs3095314	2.9E-06	2.9E-06	1.2E-04	7,552	Pass	HLA Region
6	31,205,162	rs3130558	5.3E-06	6.5E-06	7.3E-05	4,491	Pass	HLA Region
6	31,209,653	rs3130564	4.6E-12	1.0E-10	1.4E-08	28,404	Pass	HLA Region

6	32,481,210	rs10947261	5.9E-05	3.4E-05	3.8E-05	1,390	Pass	BTNL2	32,470,491	32,482,878	HLA Region	BTNL2
6	32,482,600	rs3763307	6.3E-09	2.7E-08	1.3E-08	8,788	Pass	BTNL2	32,470,491	32,482,878	HLA Region	BTNL2
6	32,491,388	rs6930933	3.2E-08	2.8E-06	5.2E-07	448	Pass	BTNL2	32,470,491	32,482,878	HLA Region	BTNL2
6	32,491,836	rs2001097	3.8E-08	2.8E-06	3.8E-07	669	Pass	BTNL2	32,470,491	32,482,878	HLA Region	BTNL2
6	32,492,505	rs9268541	7.7E-04	3.9E-02	3.2E-01	572		BTNL2	32,470,491	32,482,878	HLA Region	BTNL2
6	32,493,077	rs3135378	3.1E-08	3.3E-06	5.2E-07	300	Pass	BTNL2	32,470,491	32,482,878	HLA Region	BTNL2
6	32,493,377	rs3135377	5.0E-18	2.1E-11	1.7E-10	71	Pass	BTNL2	32,470,491	32,482,878	HLA Region	BTNL2
6	32,493,448	rs3135376	3.9E-08	3.5E-06	5.2E-07	2,282	Pass	BTNL2	32,470,491	32,482,878	HLA Region	BTNL2
6	32,495,730	rs2395161	2.4E-08	3.3E-06	4.8E-07	108	Pass	BTNL2	32,470,491	32,482,878	HLA Region	BTNL2
6	32,495,838	rs2395164	1.4E-09	6.0E-07	1.8E-07	448	Pass	BTNL2	32,470,491	32,482,878	HLA Region	BTNL2
6	32,496,286	rs2395167	1.8E-07	2.2E-06	6.0E-07	266	Pass	BTNL2	32,470,491	32,482,878	HLA Region	BTNL2
6	32,496,552	rs2213580	2.6E-07	2.0E-05	2.7E-06	938	Pass	BTNL2	32,470,491	32,482,878	HLA Region	BTNL2
6	32,497,490	rs9268560	1.2E-05	2.1E-04	3.4E-03	7,103	Pass	BTNL2	32,470,491	32,482,878	HLA Region	BTNL2
6	32,504,593	rs3135342	2.9E-06	6.9E-05	3.5E-06	7,520	Pass	BTNL2	32,470,491	32,482,878	HLA Region	BTNL2
6	32,512,113	rs5000563	2.8E-06	6.7E-05	1.3E-06	3,018	Pass	BTNL2	32,470,491	32,482,878	HLA Region	BTNL2
6	32,515,131	rs3129872	1.8E-06	5.7E-05	1.2E-06	1,374	Pass	BTNL2	32,470,491	32,482,878	HLA Region	BTNL2
6	32,516,505	rs9268645	1.1E-06	1.6E-05	1.6E-04	70	Pass	BTNL2	32,470,491	32,482,878	HLA Region	BTNL2
6	32,516,575	rs3129877	6.5E-06	9.4E-05	1.9E-06	245	Pass	BTNL2	32,470,491	32,482,878	HLA Region	BTNL2
6	32,516,820	rs3135393	6.1E-08	6.0E-06	4.9E-07	3,750	Pass	BTNL2	32,470,491	32,482,878	HLA Region	BTNL2
6	32,520,570	rs1051336	1.8E-07	8.2E-06	1.7E-06	17,051	Pass	BTNL2	32,470,491	32,482,878	HLA Region	BTNL2
6	32,537,621	rs9268853	1.3E-13	6.1E-13	5.9E-11	115	Pass	HLA-DRA	32,515,625	32,520,801 Strong	HLA Region	HLA-DRA
6	32,537,736	rs9268855	5.0E-13	7.9E-13	3.0E-10	1,389	Pass	HLA-DRA	32,515,625	32,520,801 Strong	HLA Region	HLA-DRA
6	32,539,125	rs9268877	9.1E-19	8.9E-16	2.6E-12	11,205	Pass	HLA-DRA	32,515,625	32,520,801 Strong	HLA Region	HLA-DRA
6	32,652,330	rs2027852	1.4E-33	0.0E+00	4.6E-14	29,708	Fail	HLA-DRB5	32,593,129	32,605,984 Mixed	Tunisian, Trinidadian, Thai	HLA Region
6	32,682,038	rs9270986	5.8E-16	2.2E-10	5.2E-11	21,023	Pass	HLA-DRB1	32,654,527	32,665,559 Mixed	African, Japanese, Caucasian, Icelandic, Indian, Majorcan, C	HLA Region
6	32,703,061	rs3129768	1.2E-21	8.7E-14	1.7E-13	7,186	Pass	HLA-DRB1	32,654,527	32,665,559 Mixed	African, Japanese, Caucasian, Icelandic, Indian, Majorcan, C	HLA Region
6	32,710,247	rs2272219	9.3E-05	3.1E-03	5.4E-02	7,158	Pass	HLA-DRB1	32,654,527	32,665,559 Mixed	African, Japanese, Caucasian, Icelandic, Indian, Majorcan, C	HLA Region
6	32,717,405	rs9272723	9.0E-27	0.0E+00	5.8E-14	16,845	Pass	HLA-DQA1	32,713,161	32,719,407 Strong	Russian, African, Taiwanese, European American, Indian, Ict	HLA Region
6	32,734,250	rs9273363	7.1E-89	0.0E+00	0.0E+00	28,368	Pass	HLA-DQA1	32,713,161	32,719,407 Strong	Russian, African, Taiwanese, European American, Indian, Ict	HLA Region
6	32,762,618	rs2856688	2.9E-17	9.9E-15	3.0E-10	3,439	Pass	HLA-DQA1	32,713,161	32,719,407 Strong	Russian, African, Taiwanese, European American, Indian, Ict	HLA Region
6	32,766,057	rs7775228	8.0E-06	5.6E-06	1.5E-05	231	Pass	HLA-DQA1	32,713,161	32,719,407 Strong	Russian, African, Taiwanese, European American, Indian, Ict	HLA Region
6	32,766,288	rs496220	4.9E-19	4.4E-16	6.6E-13	11,690	Pass	HLA-DQA1	32,713,161	32,719,407 Strong	Russian, African, Taiwanese, European American, Indian, Ict	HLA Region
6	32,777,978	rs285308	2.2E-05	2.9E-05	2.4E-04	14,029	Pass	HLA-DOB1	32,735,642	32,742,419 Strong	Japanese, Mixageneted population (caucasian, african, ame	HLA Region
6	32,792,007	rs9366863	7.0E-17	3.4E-14	2.4E-11	1,521	Pass	HLA-DOB1	32,735,642	32,742,419 Strong	Japanese, Mixageneted population (caucasian, african, ame	HLA-DOB1
6	32,793,528	rs3916765	5.2E-30	0.0E+00	6.7E-14	3,774	Pass				HLA Region	
6	32,797,302	rs9275765	4.2E-07	2.1E-07	8.5E-06	179	Pass				HLA Region	
6	32,797,481	rs9275772	4.1E-07	2.4E-07	1.1E-05	26	Pass				HLA Region	
6	32,797,507	rs9461799	7.9E-10	8.8E-11	2.2E-09	498	Pass				HLA Region	
6	32,798,005	rs9275793	3.7E-07	1.3E-07	4.7E-06	21,755	Pass				HLA Region	
6	32,819,760	rs2227127	9.0E-11	2.2E-11	1.7E-10	322	Pass				HLA Region	
6	32,820,082	rs9276429	1.2E-10	1.7E-10	1.0E-09	143	Pass				HLA Region	
6	32,820,225	rs9276431	1.2E-10	1.9E-10	1.6E-09	137	Pass				HLA Region	
6	32,820,362	rs9276432	1.2E-10	1.7E-10	1.0E-09	883	Pass				HLA Region	
6	32,821,245	rs2239800	2.3E-06	1.6E-07	6.4E-08	600	Pass				HLA Region	
6	32,821,845	rs9276435	7.8E-04	7.9E-03	1.1E-03	916					HLA Region	
6	32,822,761	rs9276440	3.9E-10	7.5E-10	3.6E-09	15,038	Pass				HLA Region	
6	32,837,799	rs7768530	2.0E-10	1.1E-10	7.9E-10	191	Pass				HLA Region	
6	32,837,990	rs7453920	1.6E-10	1.2E-10	1.4E-09	1,948	Pass				HLA Region	
6	32,839,938	rs6902723	2.9E-08	3.0E-07	6.3E-08	250	Pass	HLA-DOB	32,888,527	32,892,762	HLA Region	HLA-DOB
6	32,840,188	rs6903130	1.0E-07	7.3E-07	1.3E-07	3,934	Pass	HLA-DOB	32,888,527	32,892,762	HLA Region	HLA-DOB
6	32,844,122	rs9296044	2.8E-09	1.5E-09	3.7E-10	9,383	Pass	HLA-DOB	32,888,527	32,892,762	HLA Region	HLA-DOB
6	32,853,505	rs12661352	7.0E-04	2.3E-05	2.2E-02	6,087	Fail	HLA-DOB	32,888,527	32,892,762	HLA Region	HLA-DOB
6	32,859,592	rs17429127	4.0E-04	3.4E-05	8.5E-03	29,940	Pass	HLA-DOB	32,888,527	32,892,762	HLA Region	HLA-DOB
6	32,889,532	rs2070121	1.9E-04	7.0E-04	4.9E-04	595	Pass	HLA-DOB	32,888,527	32,892,762	HLA Region	HLA-DOB
6	32,890,127	rs17501267	8.7E-04	1.9E-03	5.2E-03	433	Pass	HLA-DOB	32,888,527	32,892,762	HLA Region	HLA-DOB
6	32,890,560	rs2071474	2.6E-07	3.1E-09	8.0E-07	4,454	Pass	HLA-DOB	32,888,527	32,892,762	HLA Region	HLA-DOB
6	32,895,014	rs1894407	3.4E-02	1.2E-04	2.9E-03	139	Pass	HLA-DOB	32,888,527	32,892,762	HLA Region	HLA-DOB
6	32,895,153	rs9784858	7.4E-06	5.3E-04	8.1E-03	7,857	Pass	HLA-DOB	32,888,527	32,892,762	HLA Region	HLA-DOB
6	32,903,010	rs10484565	6.0E-05	5.0E-03	2.4E-02	8,808	Pass	HLA-DOB	32,888,527	32,892,762	HLA Region	HLA-DOB
6	32,911,818	rs2414249	1.2E-02	1.7E-04	1.4E-03	574	Pass	HLA-DOB	32,888,527	32,892,762	HLA Region	HLA-DOB
6	32,912,392	rs2414247	1.8E-13	6.6E-11	9.4E-08	62,578	Pass	HLA-DOB	32,888,527	32,892,762	HLA Region	HLA-DOB
6	32,974,970	rs2414043	3.1E-09	3.1E-07	6.1E-07	3,065	Pass	TAP1	32,920,964	32,929,726 Weak	Finnish, German, Japanese and Caucasian	TAP1
6	32,978,035	rs3101942	4.8E-12	6.2E-10	3.5E-08	33,843	Pass	TAP1	32,920,964	32,929,726 Weak	Finnish, German, Japanese and Caucasian	TAP1
6	33,011,878	rs151719	8.4E-10	6.5E-07	1.3E-05	13,957	Pass	HLA-DMB	33,010,393	33,016,795 Weak	HLA Region	HLA-DMB
6	33,025,835	rs1050391	9.0E-05	4.0E-04	4.3E-03	123	Pass	HLA-DMB	33,010,393	33,016,795 Weak	HLA Region	HLA-DMB
6	33,025,958	rs1539216	1.6E-04	2.9E-03	1.7E-02	20,219	Pass	HLA-DMB	33,010,393	33,016,795 Weak	HLA Region	HLA-DMB
6	33,046,177	rs17840186	4.9E-04	1.5E-02	3.7E-02	27,743	Pass	HLA-DMB	33,010,393	33,016,795 Weak	HLA Region	HLA-DMB
6	33,073,920	rs176248	1.8E-06	7.1E-08	4.0E-06	7,801	Pass	HLA-DMA	33,024,373	33,028,831	HLA Region	HLA-DMA
6	33,081,721	rs3129304	1.2E-05	4.5E-06	1.3E-03	135	Pass				HLA Region	
6	33,081,856	rs3129303	1.0E-05	3.0E-06	8.1E-04	4,709	Pass				HLA Region	
6	33,086,565	rs429916	1.8E-08	2.8E-07	3.6E-05	18,990	Pass				HLA Region	
6	33,105,555	rs3135196	2.0E-05	5.7E-06	2.2E-03	27,029	Pass	HLA-DPA1	33,140,772	33,149,356 Mixed	HLA Region	HLA-DPA1
6	33,132,584	rs376877	1.9E-05	2.0E-05	3.6E-03	22,425	Pass	HLA-DPA1	33,1			

9	32,175,642	rs10970830	3.3E-03	4.4E-04	4.9E-05	1,669,496	Pass	Intergenic	Intergenic	
9	33,845,138	rs10971738	2.1E-02	1.6E-02	2.5E-04	727,745				
9	34,572,883	rs7032335	8.6E-04	4.5E-03	2.2E-03	36,738				
9	34,609,621	rs10972168	3.6E-04	5.6E-03	6.2E-03	855,770				
9	35,465,391	rs10972486	4.7E-04	1.2E-02	1.4E-02	50,679				
9	35,516,070	rs13298415	6.7E-04	1.1E-03	1.1E-03	416,336				
9	35,932,406	rs7863401	2.2E-03	3.6E-04	1.2E-03	3,569				
9	35,935,975	rs7019283	2.7E-03	4.1E-04	1.6E-03	215,458				
9	36,151,433	rs7851615	6.8E-04	2.6E-02	5.7E-04	2,577,056				
9	38,728,489	rs11794651	8.2E-03	4.4E-04	2.1E-02	628				
9	38,729,117	rs7861857	4.2E-02	7.7E-04	3.8E-02	34,060,528				
9	72,789,645	rs1895063	6.2E-03	4.2E-03	7.3E-04	4,962,801				
9	77,752,446	rs2377425	1.6E-03	2.5E-04	7.2E-04	10,942,416				
9	88,694,862	rs10868500	5.6E-04	6.1E-03	4.3E-02	814,372				
9	89,509,234	rs3118860	4.8E-02	6.0E-02	8.2E-04	7,681				
9	89,516,915	rs3128499	6.6E-02	5.6E-02	9.2E-05	CTSL	7,681	CTSL		
9	89,528,325	rs9410942	1.7E-02	1.3E-02	1.0E-04	11,410	Pass	11,410	CTSL	
9	89,532,495	rs2274611	1.4E-02	3.4E-02	4.3E-04	4,170		4,170	CTSL	
9	89,544,048	rs3128514	2.6E-03	3.3E-03	8.8E-05	8,858	Pass	11,553	CTSL	
9	89,552,906	rs3118840	9.0E-03	6.7E-02	6.5E-04	2,191,882		8,858	CTSL	
9	91,744,788	rs7864499	2.0E-04	5.1E-04	2.6E-03	12,260		12,260	CTSL	
9	91,757,048	rs749194	1.1E-03	9.1E-04	8.1E-03	7,716		7,716	CTSL	
9	91,764,764	rs10993230	5.7E-04	6.4E-04	6.2E-03	716		716	CTSL	
9	91,765,480	rs10993257	7.0E-04	6.5E-04	6.2E-03	804		804	CTSL	
9	91,766,284	rs10821382	8.8E-04	8.6E-04	7.0E-03	495		495	CTSL	
9	91,766,779	rs10993330	6.7E-04	6.5E-04	5.3E-03	28		28	CTSL	
9	91,766,807	rs10993331	7.4E-04	9.0E-04	4.6E-03	630		630	CTSL	
9	91,767,437	rs10761354	6.3E-04	6.3E-04	5.1E-03	1,973		1,973	CTSL	
9	91,769,410	rs1992544	5.8E-04	6.3E-04	5.2E-03	1,130		1,130	CTSL	
9	91,770,540	rs10993476	7.7E-04	6.5E-04	6.2E-03	8,526,301				
9	100,296,841	rs10125760	7.4E-04	3.9E-03	2.0E-03	3,388,068				
9	103,684,909	rs9299353	7.7E-03	7.8E-04	1.0E-01	2,604,506				
9	106,289,415	CG09016047	5.9E-02	4.0E-02	3.2E-04	3,811,369				
9	110,100,784	rs10816654	5.8E-04	2.3E-02	3.6E-03	1,163,780				
9	111,264,564	rs3935785	2.0E-02	3.3E-04	5.1E-04	6,468,906				
9	117,733,470	rs6478214	4.0E-04	1.2E-04	2.8E-03	4,266,411				
9	121,999,881	rs10984868	3.4E-03	3.0E-02	4.0E-04	10,749				
9	122,010,630	rs10217145	2.7E-03	6.7E-02	7.5E-04	509,887				
9	122,520,517	rs4617229	1.2E-03	6.6E-04	6.2E-03	5,262,168				
9	127,782,685	rs10987704	3.3E-02	2.8E-04	6.1E-02	5,385				
9	127,788,070	rs1571570	3.4E-02	9.8E-04	7.3E-02	521,597				
9	128,309,667	rs16929088	2.1E-03	5.6E-05	4.0E-02	9,009	Pass	9,009	FAM125B	
9	128,318,676	rs4837098	1.4E-03	3.6E-04	3.2E-02	6,806,253			FAM125B	
9	135,124,929	rs8176707	2.7E-04	1.5E-02	6.1E-03	2,259,942	ABO	135,120,384	135,140,451	ABO
9	137,384,871	rs11789038	8.0E-04	2.3E-03	2.4E-01					
10	3,172,026	rs4880598	6.5E-04	7.0E-03	1.2E-02	1,721		1,721	PITRM1	
10	3,173,747	rs7094698	8.2E-04	4.0E-03	2.5E-03	5,065		5,065	PITRM1	
10	3,178,812	rs7898290	7.3E-04	2.6E-03	8.5E-03	2,715		2,715	PITRM1	
10	3,181,527	rs2388557	9.8E-04	9.2E-03	5.1E-03	14,838		14,838	PITRM1	
10	3,196,365	rs4620624	7.8E-04	2.2E-02	3.8E-02	2,935,734			PITRM1	
10	6,132,099	rs10905669	6.1E-02	1.0E-03	3.9E-02	216,553			PITRM1	
10	6,348,652	rs4750200	2.0E-02	1.6E-02	9.7E-04	2,646,631			PITRM1	
10	8,995,283	rs1822801	5.6E-02	8.6E-04	5.6E-04	1,293,750			PITRM1	
10	10,289,033	rs2759640	2.1E-02	3.2E-03	6.1E-04	836,137			PITRM1	
10	11,125,170	rs1291870	2.5E-03	1.9E-02	3.6E-04	60,089			PITRM1	
10	11,185,259	rs1080845	6.7E-04	7.9E-03	6.1E-02	2,517,758			PITRM1	
10	13,703,017	rs10906425	1.8E-02	7.7E-04	7.1E-03	4,767		4,767	PRPF18	
10	13,707,784	rs7098243	9.4E-03	3.1E-04	4.9E-03	11,930		11,930	PRPF18	
10	13,719,714	rs1541019	9.2E-03	4.7E-04	6.3E-03	26,659		26,659	PRPF18	
10	13,746,373	rs4750396	2.3E-02	7.0E-04	2.5E-02	41		41	PRPF18	
10	13,746,414	rs4748050	2.8E-02	8.2E-04	2.0E-02	825,122			PRPF18	
10	14,571,536	rs10508474	7.3E-04	1.7E-02	7.8E-03	2,951,657			PRPF18	
10	17,523,193	rs11254600	2.6E-04	1.0E-02	9.8E-02	1,096,550			PRPF18	
10	18,619,743	rs10828424	9.8E-03	2.3E-04	1.5E-02	4,856,772			PRPF18	
10	23,476,515	rs10828412	8.9E-03	6.1E-04	2.8E-03	118,507			PRPF18	
10	23,595,022	rs4074209	3.0E-03	9.9E-04	2.5E-02	5,104,424			PRPF18	
10	28,699,446	rs1249575	8.8E-04	6.1E-03	1.6E-01	1,393,112			PRPF18	
10	30,092,558	rs1013610	8.8E-06	4.4E-05	2.2E-05	57,963	Fail		CKS1BP2	
10	30,150,521	rs11007760	1.1E-04	1.6E-04	6.7E-03	14,259			CKS1BP2	
10	30,164,780	rs2150556	1.6E-04	2.8E-04	7.0E-03	577,042			CKS1BP2	
10	30,741,822	rs6481677	1.7E-02	5.7E-03	5.3E-04	2,665,988	MAP3K8	30,762,872	30,790,767	MAP3K8
10	33,407,810	rs2666275	7.2E-03	9.8E-04	7.0E-03	43,631			LOC401640	
10	33,451,441	rs2070302	1.6E-01	8.5E-03	3.1E-04	12,258		12,258	LOC401640	
10	33,463,699	rs2093055	3.7E-03	3.4E-04	3.1E-01	444,681	NRP1	33,506,432	33,663,839	NRP1
10	33,908,380	rs6481861	6.8E-04	2.3E-03	1.3E-03	16,060,147				
10	49,968,527	rs7074818	7.6E-04	2.4E-03	7.5E-03	609,543				
10	50,578,070	rs1258323	5.3E-04	8.5E-03	7.2E-04	3,975,296				
10	54,553,366	rs1006677	2.5E-02	7.8E-04	2.9E-03	2,076		2,076	Intergenic	
10	54,555,442	rs10762926	2.8E-02	7.8E-04	2.9E-03	16,283		16,283	Intergenic	
10	54,557,125	rs4408237	5.3E-02	9.1E-04	1.5E-03	423		423	Intergenic	
10	54,572,148	rs10824900	5.8E-02	9.5E-04	4.2E-03	17,517		17,517	Intergenic	

11	106,848,172	rs7924419	6.0E-04	1.3E-02	9.6E-02	144		144		CWF19L2		
11	106,848,316	rs1943682	5.6E-04	5.7E-03	2.3E-02	1,076,313				CWF19L2		
11	107,924,629	rs1940212	7.1E-03	4.8E-04	8.9E-02	13,216				EXPH5		
11	107,937,845	rs2256362	1.3E-03	8.7E-05	1.0E-02	142,277	Pass			EXPH5		
11	108,080,122	rs7130825	2.1E-04	3.0E-04	3.8E-03	2,653,186						
11	110,733,308	rs2228637	2.5E-04	2.0E-03	5.8E-03	4,543,710						
11	115,277,018	rs11215719	3.4E-04	4.9E-03	1.4E-02	729,876						
11	116,006,894	rs11216058	1.6E-02	7.5E-04	6.0E-04	700,065						
11	116,706,959	rs609663	2.1E-04	1.4E-02	1.5E-02	3,514,135						
11	120,221,094	rs6598947	7.1E-04	6.4E-03	7.2E-02	4,175,211						
11	124,396,305	rs11219869	9.4E-04	2.3E-01	7.8E-02	31,673		31,673		CCDC15		
11	124,427,978	rs11219878	4.4E-04	1.2E-01	1.2E-01	16,466		16,466		CCDC15		
11	124,444,444	rs4935903	6.8E-04	1.3E-01	1.3E-01	1,085,299				CCDC15		
11	125,529,743	rs4937107	8.5E-03	5.5E-04	6.0E-04	2,568,960						
11	128,098,703	rs947930	1.4E-04	2.9E-02	1.1E-02	680,541						
11	128,779,244	rs4937426	4.8E-04	5.9E-03	3.3E-03	1,034,845						
11	129,814,089	rs10894199	2.5E-03	8.2E-04	2.7E-02	2,802,621						
11	132,616,710	rs4937758	5.2E-03	1.8E-02	5.1E-04	35,899	OPCML	131,790,085	132,907,613	OPCML		
11	132,652,609	rs1941217	1.1E-01	7.9E-02	8.8E-04	118,932	OPCML	131,790,085	132,907,613	OPCML		
11	132,771,541	rs10894675	4.8E-03	1.0E-03	5.6E-04	205,993	OPCML	131,790,085	132,907,613	OPCML		
11	132,977,534	rs11606737	2.2E-03	2.6E-04	1.3E-03	738,205						
11	133,715,739	rs1258852	8.6E-04	2.0E-01	1.0E-01	6,336						
11	133,722,075	rs1223765	2.0E-04	2.4E-03	7.8E-03							
12	1,809,513	rs12301312	1.0E-02	1.4E-02	7.0E-04	375,067						
12	2,184,580	rs12423277	1.8E-02	8.9E-04	8.4E-03	4,591,231						
12	6,775,811	rs1075836	6.0E-02	2.7E-04	5.9E-02	1,878,419	CD4	6,768,912	6,800,237	Strong	Belgian, Danish	CD4
12	8,654,230	rs1561560	3.3E-03	6.8E-03	1.6E-04	2,005,483						
12	10,659,713	rs12306757	1.1E-02	4.3E-04	1.3E-02	6,252						
12	10,665,965	rs2900467	1.6E-02	8.6E-04	5.1E-02	1,434,071						
12	12,100,036	rs2909003	6.3E-08	5.0E-05	4.6E-04	5,035,616	Fail					
12	17,135,652	rs7974666	4.0E-03	6.4E-04	3.3E-03	302,563						
12	17,438,215	rs10840701	2.5E-02	3.5E-02	1.1E-04	30,967						
12	17,469,182	rs7133850	1.1E-02	3.6E-02	1.0E-03	10,635						
12	17,479,817	rs11043458	2.4E-03	1.5E-02	9.4E-04	7,654,045						
12	25,133,862	rs7969931	5.2E-03	4.1E-04	9.9E-03	36,764						
12	25,170,626	rs17387444	6.2E-03	6.9E-04	1.0E-02	975,390						
12	26,146,016	rs12367830	3.6E-04	4.4E-03	1.9E-02	597,395						
12	26,743,411	rs10771294	1.4E-03	6.4E-04	4.5E-04	4,343,128						
12	31,086,539	rs12822390	6.1E-05	2.7E-03	5.7E-03	2,361,952	Poor					
12	33,448,491	rs7309981	3.3E-02	1.2E-03	8.0E-04	29,657						
12	33,478,148	rs7971226	6.0E-02	4.6E-03	9.8E-04	3,683,630						
12	37,161,778	rs11609286	3.6E-02	1.7E-02	9.3E-04	579						
12	37,162,357	rs7963716	2.3E-02	1.2E-02	9.0E-04	13,248						
12	37,175,605	rs11168238	1.7E-04	4.9E-03	7.5E-03	49,719						
12	37,225,324	rs11168505	1.8E-02	1.7E-02	7.0E-04	2,381,434						
12	39,606,758	rs10784951	2.5E-04	4.1E-02	3.6E-02	3,879						
12	39,610,637	rs11179084	1.6E-04	7.4E-02	2.1E-02	138,463						
12	39,749,100	rs11179687	2.8E-04	4.8E-01	1.4E-01	891,796						
12	40,640,896	rs1234032	1.5E-01	2.8E-04	5.7E-02	53,030						
12	40,693,926	rs1882139	2.5E-01	3.9E-04	3.3E-02	63,541						
12	40,757,467	rs6582378	2.4E-01	3.2E-04	5.6E-02	27,200						
12	40,784,667	rs665420	2.9E-01	7.1E-04	6.0E-02	5,225,758						
12	46,409,425	rs11183856	3.0E-02	7.1E-04	7.6E-02	399,405						
12	46,409,830	rs7484827	9.5E-04	6.2E-04	7.2E-03	4,868,145						
12	51,277,975	rs4103862	5.8E-03	7.0E-04	2.6E-03	1,324,599						
12	52,602,574	rs1443504	3.9E-03	5.4E-04	9.2E-03	152,719						
12	52,755,293	rs4999382	6.3E-04	1.1E-01	2.5E-01	112,038						
12	52,867,331	rs2279402	8.3E-04	1.4E-01	9.5E-02	419						
12	52,867,750	rs2279399	8.9E-04	1.3E-01	1.1E-01	4,431,176						
12	57,298,926	rs885278	1.9E-02	6.8E-04	2.6E-03	4,303						
12	57,303,229	rs2137461	2.3E-02	8.7E-04	3.2E-03	543,477						
12	57,846,706	rs12308619	1.5E-02	5.4E-03	1.2E-04	18,633						
12	57,865,339	rs11172932	4.9E-02	1.7E-02	2.1E-04	1,777						
12	57,867,116	rs11172934	7.4E-02	3.7E-02	2.5E-04	21,053						
12	57,888,169	rs2173646	1.4E-01	4.2E-02	8.3E-04	3,704,833						
12	61,593,002	rs772564	4.0E-02	1.0E-02	6.4E-04	517,880						
12	62,110,882	rs11174970	4.5E-03	8.5E-04	1.3E-03	4,367,506						
12	66,478,388	rs7976772	4.0E-04	4.0E-03	3.3E-02	1,515,045						
12	67,993,433	rs1456233	2.6E-03	5.1E-03	4.3E-04	7,432,788						
12	75,426,221	rs12298661	2.4E-04	9.8E-04	6.9E-03	4,425,187						
12	79,851,408	rs7310000	2.9E-04	2.6E-03	2.5E-05	165,438	Pass					
12	80,016,846	rs10862237	5.8E-02	3.5E-02	8.0E-04	59,623						
12	80,076,469	rs11835646	1.1E-03	9.2E-03	1.0E-04	15,246						
12	80,091,715	rs7964978	2.4E-03	1.2E-02	9.5E-05	289	Pass					
12	80,092,004	rs7135822	8.5E-03	2.7E-02	5.0E-04	10,653,582						
12	90,745,586	rs7304552	9.0E-04	6.9E-02	2.0E-01	53,400						
12	90,798,986	rs10507004	6.8E-03	6.4E-04	2.6E-03	2,108,743						
12	92,907,729	rs669493	3.0E-04	6.8E-03	8.7E-04	770,904						
12	93,678,633	rs6538534	5.6E-04	1.3E-02	8.7E-03	8,369,052						
12	102,047,685	rs1818702	1.5E-03	8.5E-04	2.4E-03	401,685						
12	102,449,370	rs10778260	2.6E-02	1.9E-02	2.7E-04	1,443,454						

12	103,892,824	rs11112269	3.4E-05	3.3E-04	2.3E-03	6,756,274	Pass	KTR18P20	KTR18P20
12	110,649,098	rs634389	1.9E-03	9.6E-04	2.0E-03	25,723			
12	110,674,821	rs6490294	8.0E-03	3.5E-03	8.5E-04	146,924			
12	110,821,745	rs9971746	5.7E-04	4.5E-04	5.3E-04	123,387			
12	110,945,132	rs7114	1.5E-03	9.6E-03	6.9E-04	56,893			
12	111,002,025	rs1980364	9.6E-04	9.4E-03	5.3E-04	190,784			
12	111,192,803	rs2285809	3.6E-04	1.3E-02	3.6E-04	31,889	TRAFD1 C12orf51	111,047,764 111,082,375	111,075,795 111,169,738
12	111,224,698	rs1859246	6.4E-04	2.1E-02	5.0E-04	237,462			
12	111,462,160	rs10850053	6.7E-04	9.2E-03	5.5E-04	292,948	PTPN11	111,340,919	111,432,100
12	111,755,108	rs10850084	1.3E-04	3.4E-03	8.0E-03	2,325			
12	111,757,433	rs10492025	1.4E-04	1.6E-04	6.4E-04	270,778			
12	112,028,211	rs1732771	1.5E-02	9.4E-04	1.2E-01	632,949			
12	112,661,160	rs1114886	9.7E-02	6.7E-05	4.0E-03	2,310,075	Pass	RBM19	RBM19
12	114,971,235	rs3214009	7.3E-04	4.0E-03	7.2E-03	495,870			
12	115,467,105	rs10774871	2.2E-04	1.8E-03	2.7E-03	1,903,600			
12	117,370,705	rs6490178	5.0E-04	1.1E-03	8.4E-02	808,780			
12	118,179,485	rs2727688	5.8E-03	1.6E-03	3.9E-04	1,320,359			
12	119,499,844	rs16950293	1.1E-02	8.1E-04	5.2E-03	7,772,996			
12	127,272,840	rs10847578	9.9E-04	1.1E-02	6.1E-03	1,135			
12	127,273,975	rs9795848	2.2E-03	3.0E-02	5.4E-04	1,811,788			
12	129,085,763	rs628195	1.2E-03	3.6E-04	3.3E-02	314,915			
12	129,400,678	rs3736332	9.7E-04	7.7E-04	5.4E-02	732,908			
12	130,133,586	rs7138155	6.1E-02	6.8E-04	2.1E-02				
13	23,550,171	rs9553161	2.5E-04	1.2E-01	4.6E-02	378			
13	23,550,549	rs912151	5.0E-04	1.6E-01	7.4E-02	1,169,054			
13	24,719,603	rs8262	2.4E-04	7.3E-03	1.5E-03	2,655,037			
13	27,374,640	rs9554196	6.5E-04	1.8E-02	9.5E-03	3,340			
13	27,377,980	rs9319399	3.8E-04	1.6E-02	7.5E-03	376	PDX1	27,392,177	27,397,410 Mixed
13	27,378,356	rs9551419	7.4E-04	2.2E-02	9.5E-03	1,706,388	PDX1	27,392,177	27,397,410 Mixed
13	29,084,744	rs590377	4.6E-04	6.4E-02	4.3E-02	38,942	SLC7A1	28,961,551	29,067,721
13	29,123,686	rs550984	6.3E-04	7.0E-02	3.7E-02	237,026			
13	29,360,712	rs9551767	8.4E-04	1.7E-01	1.0E-02	1,323			
13	29,362,035	rs9578147	6.8E-04	1.5E-01	7.6E-03	948,093			
13	30,310,128	rs7328020	1.4E-03	4.7E-04	1.7E-02	5,046,703			
13	35,356,831	rs9574777	1.0E-01	3.0E-04	6.3E-02	3,223,201			
13	38,580,032	rs2324129	3.2E-04	2.8E-02	1.1E-03	540,612			
13	39,120,644	CG13004816	1.7E-02	2.9E-03	2.6E-04	4,305,486			
13	43,426,130	rs7331414	3.4E-03	3.4E-02	7.8E-04	2,206			
13	43,428,336	rs7322264	4.3E-03	2.2E-02	9.2E-04	8,016	PDX1	27,392,177	27,397,410 Mixed
13	43,436,352	rs9525895	2.2E-03	1.6E-02	7.8E-04	1,804,878	PDX1	27,392,177	27,397,410 Mixed
13	45,241,230	rs9590025	1.6E-02	2.0E-04	5.8E-04	1,515,422	PDX1	27,392,177	27,397,410 Mixed
13	46,756,652	rs7333102	3.0E-03	9.4E-04	1.6E-03	434,390			
13	47,191,042	rs6561402	4.7E-05	1.2E-02	1.3E-02	3,929,181	Pass	LOC730174	LOC730174
13	51,209,223	rs17597531	1.8E-04	3.5E-03	5.4E-02	89,259			
13	51,209,482	rs9535744	2.9E-04	1.0E-02	9.8E-02	14,996			
13	51,224,478	rs12146894	3.7E-04	9.9E-03	6.8E-02	543	PDX1	27,392,177	27,397,410 Mixed
13	51,225,021	rs9526793	3.8E-04	1.1E-02	9.8E-02	14,161	PDX1	27,392,177	27,397,410 Mixed
13	51,239,182	rs9526795	1.0E-04	6.1E-03	4.3E-02	4,456	PDX1	27,392,177	27,397,410 Mixed
13	51,243,638	rs2296028	4.0E-04	9.1E-03	6.3E-02	1,018,249	PDX1	27,392,177	27,397,410 Mixed
13	52,261,887	rs402583	1.1E-01	4.9E-03	7.6E-04	3,572	PDX1	27,392,177	27,397,410 Mixed
13	52,265,459	rs886347	2.0E-02	6.8E-03	3.9E-04	69,940	PDX1	27,392,177	27,397,410 Mixed
13	52,335,399	rs489654	2.2E-03	1.6E-03	2.4E-04	50,760	PDX1	27,392,177	27,397,410 Mixed
13	52,386,159	rs17052520	1.4E-02	3.4E-02	2.8E-04	2,016,241	PDX1	27,392,177	27,397,410 Mixed
13	54,402,400	rs1993777	3.6E-04	3.6E-02	2.8E-02	10,481,498	PDX1	27,392,177	27,397,410 Mixed
13	64,883,898	rs2038825	1.2E-03	6.4E-04	3.6E-02	1,936,375	PDX1	27,392,177	27,397,410 Mixed
13	66,820,273	rs2991432	8.6E-04	7.0E-03	1.3E-02	1,363,320	PDX1	27,392,177	27,397,410 Mixed
13	68,183,593	rs287485	6.8E-04	1.2E-03	3.0E-02	3,519,207	PDX1	27,392,177	27,397,410 Mixed
13	71,702,800	rs7328519	2.4E-04	2.2E-03	1.2E-02	8,263	PDX1	27,392,177	27,397,410 Mixed
13	71,711,063	rs2483837	5.0E-05	3.3E-03	1.0E-02	3,688	Pass	Intergenic	Intergenic
13	71,714,751	rs340523	7.0E-04	6.7E-03	1.0E-01	170	PDX1	27,392,177	27,397,410 Mixed
13	71,714,921	rs340524	6.6E-05	2.0E-03	1.4E-02	1,081,145	Pass	Intergenic	Intergenic
13	72,796,066	rs17191385	2.9E-04	3.1E-04	3.2E-04	439,153	PDX1	27,392,177	27,397,410 Mixed
13	73,235,219	rs9318213	1.3E-03	2.0E-03	4.3E-04	1,239,166	PDX1	27,392,177	27,397,410 Mixed
13	74,474,385	rs17337503	1.4E-01	2.4E-02	8.5E-04	5,613,231	PDX1	27,392,177	27,397,410 Mixed
13	80,087,616	rs1772573	1.8E-02	1.8E-02	9.6E-03	283,872	PDX1	27,392,177	27,397,410 Mixed
13	80,371,484	rs6563196	1.1E-04	1.6E-03	5.2E-02	11,877	PDX1	27,392,177	27,397,410 Mixed
13	80,383,365	rs4310745	9.8E-05	1.9E-03	5.3E-02	2,331,766	Pass	Intergenic	Intergenic
13	82,715,131	rs1512771	7.4E-04	8.6E-03	1.0E-01	2,519,561	PDX1	27,392,177	27,397,410 Mixed
13	85,234,692	rs9566093	3.8E-03	2.0E-02	6.3E-04	1,026	PDX1	27,392,177	27,397,410 Mixed
13	85,235,718	rs9579547	3.2E-03	1.8E-02	5.1E-04	5,870	PDX1	27,392,177	27,397,410 Mixed
13	85,241,588	rs666540	4.5E-03	2.5E-02	6.1E-04	953	PDX1	27,392,177	27,397,410 Mixed
13	85,242,541	rs652258	3.7E-03	2.0E-02	6.1E-04	952	PDX1	27,392,177	27,397,410 Mixed
13	85,243,493	rs637400	3.8E-03	1.9E-02	7.6E-04	375	PDX1	27,392,177	27,397,410 Mixed
13	85,243,868	rs617544	3.8E-03	2.0E-02	7.6E-04	1,944	PDX1	27,392,177	27,397,410 Mixed
13	85,245,812	rs588777	3.6E-03	2.2E-02	5.9E-04	17	PDX1	27,392,177	27,397,410 Mixed
13	85,245,829	rs606646	3.8E-03	2.5E-02	7.2E-04	33	PDX1	27,392,177	27,397,410 Mixed
13	85,245,862	rs606300	3.5E-03	2.0E-02	5.9E-04	381	PDX1	27,392,177	27,397,410 Mixed
13	85,246,243	rs694502	4.4E-03	2.7E-02	8.7E-04	1,103	PDX1	27,392,177	27,397,410 Mixed
13	85,247,346	rs669668	2.1E-03	1.3E-02	5.6E-04	7,320	PDX1	27,392,177	27,397,410 Mixed
13	85,254,666	rs673100	4.0E-03	1.5E-02	8.4E-04	3,842	PDX1	27,392,177	27,397,410 Mixed
13	85,258,508	rs598507	4.8E-03	2.6E-02	6.1E-04	46,596	PDX1	27,392,177	27,397,410 Mixed

13	85,305,104	rs449704	1.3E-03	3.4E-02	7.5E-04	1,952,945				SLTRK6
13	87,258,049	rs1953341	8.1E-04	5.1E-03	1.3E-03	5,627,934				GPC6
13	92,885,983	rs7338402	6.8E-03	5.1E-04	3.4E-02	12,122				GPC6
13	92,898,105	rs9524070	1.1E-02	4.3E-04	3.5E-02	18,471				GPC6
13	92,916,576	rs895193	2.0E-04	3.2E-05	1.5E-03	51,326	Pass			GPC6
13	92,967,902	rs9524111	4.9E-03	2.0E-04	5.8E-03	637,764				GPC6
13	93,605,666	rs1328822	7.4E-04	1.2E-03	4.6E-02	3,616				GPC6
13	93,609,282	rs9561507	1.9E-04	2.5E-04	9.0E-03	12,798				GPC6
13	93,622,080	rs16949539	7.9E-04	1.2E-03	1.1E-02	212,699				GPC6
13	93,834,779	rs17196184	6.1E-03	1.1E-03	2.1E-05	32,358	Pass			GPC6
13	93,867,137	rs6650322	3.4E-01	1.1E-01	7.1E-04	2,689,635				GPC6
13	96,556,772	rs2055424	3.4E-04	2.9E-02	2.1E-03	6,473,442				GPC6
13	103,030,214	rs12865443	1.2E-01	1.2E-02	9.8E-04	4,656				4,656
13	103,034,870	rs12584285	1.1E-01	1.1E-02	9.8E-04	802				802
13	103,035,672	rs12876017	1.3E-01	1.2E-02	9.8E-04	88,161				Intergenic
13	103,123,833	rs9519133	1.8E-03	4.0E-04	2.0E-04	1,830,289				Intergenic
13	104,954,122	rs11618600	3.2E-02	1.2E-04	1.8E-02	2,834,883				Intergenic
13	107,789,005	rs9520845	1.2E-03	2.9E-04	3.3E-02	1,253,397				Intergenic
13	109,042,402	rs11069790	3.3E-05	2.0E-03	1.5E-03	187,225	Pass			IRS2
13	109,229,627	rs4771648	3.3E-03	3.5E-04	1.7E-04	77,719				IRS2
13	109,307,346	rs1041637	1.6E-03	6.0E-06	1.8E-04	572,812	Pass			IRS2
13	109,880,158	rs4551896	7.2E-02	2.9E-02	9.4E-04	61,694				
13	109,941,852	rs402661	3.2E-04	1.2E-02	2.1E-03					
14	20,744,204	rs17102539	2.1E-02	9.8E-03	6.6E-04	5,719,075				
14	26,463,279	rs1956073	1.8E-02	8.1E-04	4.0E-02	1,085				UNGP2
14	26,464,364	rs12584803	6.4E-04	2.4E-03	1.4E-03	10,257				UNGP2
14	26,474,621	rs1956075	1.0E-02	7.2E-04	4.0E-02	1,220				UNGP2
14	26,475,841	rs11160092	9.9E-03	3.3E-04	1.8E-02	8,224				UNGP2
14	26,484,065	rs10431641	6.1E-03	8.1E-04	2.1E-02	3,626				UNGP2
14	26,487,691	rs12881169	6.6E-05	3.9E-04	2.0E-03	686	Pass			UNGP2
14	26,498,377	rs8011593	8.9E-05	2.8E-04	1.4E-03	5,927	Pass			UNGP2
14	26,494,304	rs2332880	2.1E-04	7.0E-04	2.1E-03	7,007				UNGP2
14	26,501,311	rs1977165	5.6E-03	6.7E-04	2.1E-02	740				UNGP2
14	26,502,051	rs4983208	1.6E-05	1.0E-04	1.1E-03	282,611	Pass			UNGP2
14	26,784,662	rs10873462	5.4E-04	4.9E-03	7.3E-02	94,109				
14	26,878,771	rs7145681	8.8E-04	3.4E-02	7.2E-02	93,495				
14	26,972,266	rs2061262	3.3E-04	4.8E-03	2.5E-02	31,103				
14	27,003,369	rs17112718	3.1E-04	5.4E-04	3.1E-02	4,482,662				
14	31,486,031	rs1278930	8.9E-04	1.7E-04	1.3E-02	626,405				
14	32,112,436	rs8016916	2.0E-04	1.0E-03	5.4E-03	5,357,409				
14	37,469,845	rs8013747	6.8E-04	2.5E-02	1.7E-02	250				
14	37,470,095	rs4597229	6.0E-04	3.2E-02	2.9E-02	16,264,143				
14	53,734,238	rs1043189	3.8E-03	6.4E-02	4.5E-04	1,352,219				
14	55,086,457	rs3742571	1.6E-02	5.4E-03	6.6E-04	2,011,989				
14	57,098,446	rs7156767	2.6E-03	2.3E-04	6.7E-03	2,791,778				
14	59,890,224	rs932606	8.1E-03	1.5E-03	8.1E-04	15,266				
14	59,905,490	rs1254260	4.6E-03	8.4E-04	1.4E-03	7,202,158				
14	67,107,648	rs10138094	3.3E-04	2.8E-03	1.1E-02	4,360				
14	67,112,008	rs4902490	6.3E-04	3.2E-03	6.3E-03	9,227,533				
14	76,339,541	rs2075773	8.7E-02	1.9E-02	7.7E-04	12,763,651				
14	89,103,192	rs10146976	3.5E-04	4.1E-03	4.0E-03	575,768				
14	89,678,960	rs12432204	6.1E-03	5.4E-04	2.0E-02	2,873,091				
14	92,552,051	rs3783904	8.0E-04	6.0E-05	3.0E-04	1,359,343	Fail			ITPK1
14	93,911,394	rs1243167	9.5E-04	7.0E-03	5.2E-03	102,471				ITPK1
14	94,013,865	rs17825644	3.8E-03	7.1E-04	8.9E-04	6,009				
14	94,019,874	rs8008729	3.2E-03	4.9E-04	6.5E-04	702,004				
14	94,721,787	rs8005908	4.1E-03	2.4E-04	2.2E-03	1,028,449				
14	95,750,327	rs4905462	6.7E-02	1.0E-01	5.7E-04	1,840,758				
14	97,591,085	rs857058	2.2E-02	2.5E-04	2.0E-03	534,991				
14	98,126,076	rs4900406	1.4E-05	2.0E-04	7.5E-04	94,903	Fail			Intergenic
14	98,220,979	rs12432577	5.2E-04	4.0E-04	1.5E-04	1,062,083				Intergenic
14	99,283,062	rs9324014	9.4E-03	1.0E-02	1.7E-04					
15	22,220,838	rs11161090	3.7E-03	3.2E-02	9.5E-04	2,855,810				
15	25,076,648	rs11636700	2.1E-06	2.4E-04	1.4E-04	11,234	Pass			Intergenic
15	25,087,882	rs6606891	7.0E-06	4.3E-05	1.3E-03	26,953	Pass			Intergenic
15	25,114,835	CG15000874	8.6E-04	1.3E-02	6.9E-02	599,102				Intergenic
15	25,713,937	rs3930739	8.5E-04	5.1E-03	1.9E-02	415				
15	25,714,352	rs17674017	6.9E-04	6.6E-03	1.0E-02	7,978				
15	25,722,330	rs6497234	5.7E-05	9.8E-04	1.4E-03	2,847				OCA2
15	25,725,177	rs6497236	1.5E-04	1.6E-03	2.1E-03	26,380				OCA2
15	25,751,557	rs1391623	7.9E-05	2.8E-04	4.9E-04	474				OCA2
15	25,752,031	rs10162623	4.3E-04	8.1E-05	1.2E-02	1,625				OCA2
15	25,753,656	rs4778192	5.1E-04	9.3E-03	1.4E-02	105				OCA2
15	25,753,761	rs4778193	1.3E-04	3.5E-04	6.4E-04	1,444,120				OCA2
15	27,197,881	rs4779798	1.4E-04	5.0E-04	1.2E-04	3,008,156				OCA2
15	30,206,037	rs904952	8.0E-04	3.7E-03	2.5E-03	673,989				OCA2
15	30,880,026	rs17816387	8.6E-04	2.5E-02	2.5E-02	65,365				OCA2
15	30,945,391	rs8040135	6.8E-04	1.2E-03	1.5E-02	8,961				FMN1
15	30,954,352	rs12591087	2.8E-05	7.3E-04	3.2E-04	14,521	Pass			FMN1
15	30,968,873	rs347937	3.0E-02	2.3E-02	6.0E-04	124,261				FMN1
15	31,093,134	rs11633931	7.2E-03	1.3E-03	2.6E-04	375,795				FMN1

16	88,366,807	rs12599180	1.1E-02	6.1E-04	2.8E-02	6,744		6,744		FANCA
16	88,373,551	rs3743859	1.3E-02	6.6E-04	3.1E-02	119,792				FANCA
16	88,493,343	rs10153055	6.8E-02	9.9E-04	1.0E-01	164,128				
16	88,657,471	rs4493039	2.5E-02	2.2E-04	1.6E-01					
17	1,278,556	rs8070640	2.7E-05	9.4E-04	5.7E-05	4,576	Pass		CRK	4,576
17	1,283,132	rs8064892	5.6E-05	3.6E-03	1.8E-04	25	Pass		CRK	25
17	1,283,157	rs8073032	3.0E-04	1.6E-02	4.2E-04	26,873			CRK	26,873
17	1,310,030	rs7211083	3.3E-05	2.2E-03	1.0E-04	1,282,591	Pass		CRK	
17	2,592,621	rs17834974	3.8E-02	1.1E-02	1.0E-04	2,774,805				
17	5,367,426	rs11656183	2.0E-03	1.3E-02	7.7E-04	417,892				
17	5,785,318	rs1783141	8.3E-04	1.3E-03	3.0E-03	1,117,917				
17	6,903,235	rs4796366	5.4E-03	4.6E-03	4.6E-04	2,368,497				
17	9,271,732	rs17808941	1.4E-04	4.2E-02	1.3E-04	5,651				
17	9,277,383	rs9916292	3.6E-04	7.0E-02	1.5E-04	4,563,229				
17	13,840,612	rs9893391	6.6E-03	8.8E-04	1.7E-02	45,915				
17	13,886,527	rs8077837	4.9E-03	5.4E-04	8.5E-03	387,184				
17	14,273,711	rs6502358	1.3E-02	4.8E-04	8.2E-02	422,324				
17	14,696,035	rs11652535	1.2E-04	4.4E-04	3.2E-02	318,971				
17	15,015,006	rs8082487	9.0E-02	9.8E-04	2.8E-02	8,747,009			SLC46A1	SLC46A1
17	23,762,015	rs6505081	4.1E-03	7.8E-04	6.2E-05	4,932,612	Pass			
17	28,694,627	rs12449721	1.4E-02	9.6E-04	8.1E-02	1,248,264				
17	29,942,891	rs11654085	2.9E-04	9.4E-03	6.8E-03	3,202,256				
17	33,145,147	rs3110648	6.5E-02	9.4E-04	7.9E-02	81,065				
17	33,226,212	rs9900825	2.7E-03	1.0E-03	2.8E-06	949,510	Pass		HNF1B	HNF1B
17	34,175,722	rs1043515	5.2E-04	1.0E-01	8.0E-04	7,382				
17	34,183,104	rs2338115	3.3E-04	6.2E-02	6.6E-04	4,126,667				
17	38,309,771	rs2593595	1.9E-04	1.0E-02	8.0E-04	1,547,447				
17	39,857,218	rs1869495	7.3E-02	7.5E-04	9.5E-03	4,485,825				
17	44,343,043	rs999475	7.6E-02	5.0E-04	8.1E-02	20,502				
17	44,363,545	rs4793993	3.3E-02	2.2E-04	5.6E-02	1,009,789				
17	45,373,334	rs271661	7.5E-04	4.6E-03	1.2E-01	7,720,314				
17	53,093,648	rs8065120	6.7E-03	1.8E-03	1.1E-04	526,368				
17	53,620,016	rs917606	1.1E-01	1.5E-02	7.0E-04	1,896,265				
17	55,516,281	rs7211063	1.9E-03	4.6E-04	1.6E-03	7,193,754				
17	62,710,035	rs6504495	1.4E-04	6.7E-05	9.9E-03	3,601,756	Pass		PSMD12	PSMD12
17	66,311,791	rs3859276	5.6E-04	3.5E-03	5.0E-03	5,457				
17	66,317,248	rs16976275	1.5E-04	7.9E-04	1.6E-03	1,220,156				
17	67,537,404	rs2193054	9.1E-04	3.1E-04	1.9E-02					
18	3,732,572	rs3745050	6.5E-03	6.1E-04	1.2E-02	182,768		621	DLGAP1	DLGAP1
18	3,915,340	rs935118	9.0E-04	1.6E-02	1.3E-02	621			DLGAP1	DLGAP1
18	3,915,961	rs4076011	6.6E-05	2.1E-03	1.9E-02	157,339	Pass			
18	4,073,300	rs9963455	2.8E-04	3.9E-04	5.0E-03	261				
18	4,073,561	rs9955521	3.8E-04	5.5E-04	6.9E-03	2,434,273				
18	6,507,834	rs7504263	9.9E-06	1.6E-04	1.6E-03	924,770	Pass		LOC645387	LOC645387
18	7,432,604	rs16951745	1.3E-03	4.2E-04	6.1E-03	258		258	PTPRM	PTPRM
18	7,432,862	rs4798567	4.5E-04	1.0E-02	1.9E-02	5,779		5,779	PTPRM	PTPRM
18	7,438,641	rs16951794	2.2E-04	4.5E-03	8.1E-03	3,362,835				
18	10,801,476	rs8095854	6.6E-02	1.0E-01	1.6E-04	7,102,886				
18	17,904,362	rs16962762	2.0E-02	7.2E-04	7.2E-03	3,089,416				
18	20,993,778	rs9959583	2.9E-03	4.7E-04	8.7E-03	5,050				
18	20,998,828	rs8085678	6.3E-03	6.3E-04	8.2E-03	590,495				
18	21,589,323	rs1971613	3.1E-03	4.9E-04	2.1E-03	2,813,219				
18	24,402,542	rs16944936	2.7E-02	9.5E-04	1.2E-02	276,907				
18	24,679,449	rs1941195	3.1E-02	3.9E-04	2.1E-03	4,864,390				
18	29,543,839	rs7237757	6.0E-04	6.7E-03	2.5E-02	6,240,719				
18	35,784,558	rs2862294	2.9E-04	5.5E-02	2.6E-03	24,870		24,870		
18	35,809,428	rs17632270	3.2E-04	8.9E-02	5.2E-03	3,808		3,808		
18	35,813,236	rs2568472	1.4E-04	5.3E-02	2.2E-03	14,801		14,801		
18	35,828,037	rs394365	2.8E-04	9.3E-02	5.9E-03	959,659				
18	36,787,696	rs7240599	3.3E-03	2.2E-04	2.9E-03	2,873,517				
18	39,661,213	rs17677611	3.0E-02	8.5E-04	1.0E-02	2,721,636				
18	42,382,849	rs4133665	2.1E-03	4.9E-04	1.2E-02	2,453,249				
18	44,836,098	rs2044550	1.8E-04	2.7E-03	1.0E-01	113,449				
18	44,949,547	rs1943000	9.1E-04	4.9E-03	1.0E-01	55,044				
18	45,004,591	rs12606493	6.9E-04	2.8E-03	8.9E-02	13,220				
18	45,017,811	rs16950465	4.2E-04	2.1E-03	7.5E-02	88,302				
18	45,106,113	rs12606466	3.4E-04	2.9E-02	1.5E-02	44,246				
18	45,150,359	rs12455199	2.7E-04	2.7E-02	1.5E-02	87,659				
18	45,238,018	rs12457899	7.3E-04	5.2E-02	2.0E-02	5,324				
18	45,243,342	rs12456474	6.9E-04	4.3E-02	2.0E-02	206,230				
18	45,449,572	rs12970803	3.3E-04	1.6E-03	3.8E-03	383,581				
18	45,833,153	rs17801909	9.0E-04	5.4E-03	3.7E-03	369				
18	45,833,522	rs17728885	2.5E-04	2.3E-03	7.0E-04	416,034				
18	46,249,556	rs17803514	4.7E-04	1.3E-02	1.0E-02	1,017,362				
18	47,266,918	rs1656747	3.5E-04	2.3E-01	1.6E-01	6,045,862				
18	53,312,780	rs2290118	6.2E-03	3.8E-03	2.8E-04	960,003				
18	54,272,783	rs9490706	6.3E-03	3.1E-04	2.1E-02	1,362,493				
18	55,635,276	rs9551126	1.8E-04	3.3E-02	1.1E-01	5,991,803				
18	61,627,079	rs1994230	3.4E-04	2.1E-03	4.5E-04	4,447,184				
18	66,074,263	rs8088698	5.5E-04	3.9E-02	1.0E-01	2,398,554				
18	68,472,817	rs12962531	2.7E-03	9.5E-04	4.9E-04	18,204				

21	39,267,210	rs2836795	2.8E-05	2.7E-03	4.3E-03	51	Pass	FLJ45139	51	FLJ45139
21	39,267,261	rs2836796	3.5E-05	3.2E-03	2.7E-03	93	Pass	FLJ45139	93	FLJ45139
21	39,267,354	rs2836797	9.9E-05	6.1E-03	4.9E-03	4,177	Pass	FLJ45139	4,177	FLJ45139
21	39,271,531	rs2836801	8.1E-05	5.3E-03	1.3E-02	99,228	Pass	FLJ45139	FLJ45139	FLJ45139
21	39,370,759	rs17231256	5.2E-04	4.5E-03	5.6E-03	486,752		FLJ45139	FLJ45139	FLJ45139
21	39,857,511	rs571227	9.3E-02	3.0E-01	9.9E-04	2,288		2,288	FLJ45139	FLJ45139
21	39,859,799	rs523372	1.7E-01	3.6E-01	8.9E-04	8,195		8,195	FLJ45139	FLJ45139
21	39,867,994	rs1734930	1.6E-01	9.6E-02	4.2E-04	2,638,268		FLJ45139	FLJ45139	FLJ45139
21	42,506,262	rs221948	6.9E-04	3.9E-02	1.5E-01	573,947		FLJ45139	FLJ45139	FLJ45139
21	43,080,209	rs683471	7.8E-04	1.3E-01	1.7E-01	1,917,610		FLJ45139	FLJ45139	FLJ45139
21	44,997,819	rs690260	3.3E-04	3.7E-03	9.5E-04	1,842,295		FLJ45139	FLJ45139	FLJ45139
21	46,840,114	rs2839342	3.6E-06	1.9E-05	3.4E-04		Fail			
22	19,542,090	rs178067	6.6E-04	1.0E-03	2.4E-05	5,096,146	Fail			
22	24,638,236	rs1476053	2.5E-08	5.3E-06	3.9E-05	3,186,388	Fail			
22	27,824,624	rs2294242	7.7E-03	3.6E-04	7.3E-02	144,466				
22	27,969,090	rs5763087	3.1E-06	1.2E-05	1.4E-03	549,155	Poor	EMID1	EMID1	EMID1
22	28,518,245	rs5752962	9.7E-04	2.9E-02	5.9E-03	62,067				
22	28,580,312	rs5752972	3.0E-04	3.9E-02	8.5E-03	63,780				
22	28,644,092	rs713718	1.4E-04	2.6E-02	4.4E-03	79,411				
22	28,723,503	rs5763688	2.5E-04	1.5E-02	9.5E-03	12,480				
22	28,735,983	rs41158	2.0E-05	1.5E-03	2.0E-03	1,381	Pass	S100B	S100B	S100B
22	28,737,364	rs41159	4.2E-04	2.1E-02	1.2E-02	25,039		SNAP29	SNAP29	SNAP29
22	28,762,403	rs41176	3.5E-04	2.2E-02	1.6E-03	39,851		MYO18B	MYO18B	MYO18B
22	28,802,254	rs1989870	2.4E-04	1.5E-02	2.7E-03	58,837				
22	28,861,091	rs4820830	6.0E-04	3.5E-02	7.5E-03	36,816				
22	28,897,907	rs2412976	4.2E-04	2.6E-02	4.5E-03	5,892,113		MTMR3	MTMR3	MTMR3
22	34,790,020	rs5995203	5.0E-03	2.7E-04	4.7E-05	1,350,633	Pass	APOL3	APOL3	APOL3
22	36,140,653	rs133738	2.8E-04	1.3E-02	5.2E-02	1,463				
22	36,142,116	rs133736	5.6E-04	3.7E-02	6.1E-02	1,687,434				
22	37,829,550	rs139314	2.0E-03	9.7E-03	6.9E-04	8,068,718				
22	45,898,268	rs738662	4.7E-03	2.3E-04	5.8E-02	11,341				
22	45,909,609	rs5767523	3.2E-03	4.4E-04	4.9E-02	3,526,470				
22	49,436,079	rs6009945	2.1E-04	3.0E-03	1.6E-02					
23	11,715,814	rs5935164	8.6E-04	2.1E-02	1.2E-01	4,763,948				
23	16,479,762	rs2428447	3.4E-02	5.6E-02	5.3E-04	641,837				
23	17,121,599	rs7049284	7.5E-04	1.4E-02	5.2E-04	10,344,080				
23	27,465,679	rs221406	8.2E-04	2.0E-03	1.9E-02	5,041,354				
23	32,507,033	rs5928369	9.0E-04	9.6E-03	1.3E-02	1,069,617				
23	33,576,650	rs232963	9.1E-04	6.0E-03	2.2E-02	47,480,190				
23	31,056,840	rs4131395	2.1E-04	5.3E-04	1.1E-02	833,095				
23	81,889,935	rs4828519	5.2E-04	2.6E-03	9.6E-04	1,668,266				
23	83,558,201	rs4437785	1.0E-05	2.3E-05	8.0E-04	667,407	Pass	HDX	HDX	HDX
23	84,225,608	rs5923256	1.9E-04	3.4E-03	5.8E-03	730,966				
23	84,956,574	rs2206006	1.8E-05	6.6E-03	3.1E-02	409,559	Pass	CHM	CHM	CHM
23	85,366,133	rs5923512	6.8E-04	1.9E-02	1.3E-02	590,578				
23	85,956,711	rs11797054	4.7E-04	9.3E-03	1.3E-03	289,260				
23	86,245,971	rs5923792	1.8E-07	4.8E-06	5.1E-04	394,107	Pass	Intergenic	Intergenic	Intergenic
23	86,640,078	rs2213671	2.5E-06	2.5E-04	2.8E-02	778,740	Pass	KLHL4	KLHL4	KLHL4
23	87,418,818	rs5969586	2.7E-04	4.9E-03	3.0E-02	96,500				
23	87,515,318	rs6522030	1.6E-04	8.4E-04	5.8E-03	82,174				
23	87,597,492	rs12842964	2.7E-04	2.0E-03	2.5E-02	469,070				
23	88,066,562	rs621716	3.0E-06	7.2E-04	8.8E-04	73,854				
23	88,140,416	rs3850155	1.5E-05	5.8E-04	5.5E-03	151,629	Pass			
23	88,292,045	rs5944240	2.9E-05	1.8E-03	1.3E-02	3,026,341	Pass			
23	91,318,386	rs4358964	9.2E-05	2.2E-02	8.7E-02	519,886	Pass			
23	91,838,273	rs594213	9.9E-06	3.4E-03	1.2E-04	469,497	Pass	PCDH11X	PCDH11X	PCDH11X
23	92,307,769	rs785754	5.8E-06	1.7E-06	4.8E-05	166,584	Pass	LOC401602	LOC401602	LOC401602
23	92,474,353	rs5940144	2.4E-08	1.4E-07	6.5E-05	369,783	Pass	LOC643310	LOC643310	LOC643310
23	92,844,136	rs2312033	4.3E-04	3.1E-02	6.7E-02	158,907				
23	93,003,043	rs1797020	4.5E-04	1.5E-03	1.2E-01	618,270				
23	93,621,313	rs2782710	2.2E-04	1.3E-03	1.3E-01	607				
23	93,621,920	rs1582247	2.1E-04	1.9E-03	1.1E-01	640,017				
23	94,261,937	rs7061674	6.1E-06	3.3E-03	2.4E-03	59,436		Intergenic	59,436	Intergenic
23	94,321,373	rs6169774	9.9E-06	1.7E-06	1.3E-05	16,569	Pass	Intergenic	16,569	Intergenic
23	94,337,942	rs10855336	9.1E-03	6.2E-04	5.8E-04	22,841			22,841	
23	94,360,783	rs5950249	6.6E-07	2.5E-05	3.3E-06	410,820	Pass	Intergenic	Intergenic	Intergenic
23	94,771,603	rs2153931	1.1E-04	1.3E-04	2.2E-03	1,175,421				
23	95,947,024	rs233655	3.9E-04	6.2E-03	7.3E-03	1,360,032				
23	97,307,056	rs1458782	4.5E-06	4.3E-03	2.8E-04	53,894		LOC392505	53,894	LOC392505
23	97,360,950	rs1458780	5.4E-06	2.7E-03	4.4E-04	2,394,686		LOC392505		LOC392505
23	99,755,636	rs736550	3.8E-06	2.8E-03	1.3E-02	1,465,954		TSPAN6		TSPAN6
23	101,221,590	rs5944840	7.0E-04	1.9E-02	3.2E-03	1,666,251				
23	102,887,841	rs532860	7.2E-06	1.5E-05	3.6E-04	5,810,170	Pass	PLP1	PLP1	PLP1
23	108,698,011	rs542602	3.4E-04	1.5E-02	2.4E-02	461,501				
23	109,159,512	rs2066364	4.3E-06	1.5E-06	9.1E-06	2,708,220	Pass	TMEM164	TMEM164	TMEM164
23	111,867,732	rs16987072	9.2E-05	2.4E-03	1.1E-03	194,988	Pass	LOC203510	LOC203510	LOC203510
23	112,062,720	rs5974328	5.5E-05	6.5E-04	1.1E-05	123,665	Pass	Intergenic	Intergenic	Intergenic
23	112,186,385	rs3125994	8.6E-07	2.5E-05	4.5E-04	461,253	Pass	Intergenic	Intergenic	Intergenic
23	112,647,638	rs5929302	1.1E-05	9.9E-04	3.6E-05	458,450		LOC139466	LOC139466	LOC139466
23	113,106,088	rs6642665	1.2E-04	3.8E-04	4.8E-04	2,603,900		LOC653155	41,418	LOC653155
23	115,709,988	rs5909877	2.6E-05	7.6E-04	1.9E-03	41,418	Pass	LOC653155	41,418	LOC653155

Application for Access to Genotype Data

Name of applicant and co-applicant(s), including affiliations and contact details.

Please ensure that both telephone numbers and email addresses are included.

Massimo Trucco, MD (Applicant)
Children's Hospital of Pittsburgh
Pittsburgh, PA 15213 USA
TEL: (412) 692-6570
FAX: (412) 692-5809
E-mail: mnt@pitt.edu

Bernie Devlin, Ph.D. (Co-Applicant)
Department of Psychiatry
University of Pittsburgh School of Medicine
Pittsburgh, PA 15213 USA
TEL: (412) 246-6642
FAX: (412) 624-8181
E-mail: devlinbj@upmc.edu

Kathryn Roeder, Ph.D. (Co-Applicant)
Department of Statistics
Carnegie Mellon University
Pittsburgh, PA 15213
TEL: (412) 268-2513
FAX: (412) 268-7828
E-mail: roeder@stat.cmu.edu

Title of Project

In less than 30 words.

DETECTION OF SUSCEPTIBILITY LOCI IN MULTIFACTORIAL DISEASE

Genotype Data Requested

Please indicate which disease and/or control genotypes you require.

Type 1 Diabetes
Type 2 Diabetes
Bipolar Disorder
Rheumatoid Arthritis
Coronary Heart Disease
Hypertension
Inflammatory Bowel Disease

1958 British Birth Cohort controls
UK Blood Service controls
Quantile Normalised Data for Control and Disease Samples

Research Question

Please give a brief description of the project and its specific aims in no more than 500 words. This should include specific details of what you plan to do with the data and include key references.

As platforms for genome-wide association studies (GWAS) become standardized, numerous resources will become available. Analyses of GWAS are enhanced by the availability of large, well characterized, populations such as the WTCCC cohort. How to exploit these datasets effectively is an open question. As part of our work into the genetics of Type 1 Diabetes (T1D) we have developed a method to match, by genetic ancestry, controls to cases (1). Applying the method to the GWAS obtained from our cohort of T1D (N=394) and non-T1D (N=2,144) participants we have shown that GEnetic Matching (GEM) resulted in a reduced rate of false positives as well as highlighting of true positive signals for association.

The goal is to exploit our genetic data by combining it with the WTCCC resource while developing approaches that improve power of association studies to identify true signals. We are proceeding with a staged analysis for T1D using an independent cohort of cases (N=1,300) and controls (N=2,500) recruited among European-Americans and residents from Germany. Development of GEM as a method for elucidating association between SNP and T1D has led us to anticipate that combining our cohort with the WTCCC dataset will result in improved power to detect genes influencing disease.

Substantial progress has been made toward the completion of our goal. In our recent publication (1) we developed GEM as a means to control for the impact of ancestry on association testing, and showed how using GEM allows multiple datasets to be combined for discovery of genetic association. We contrasted this approach with other popular methods for controlling the spurious effects of ancestral heterogeneity, namely Eigenstrat (2). Compared with Eigenstrat, the GEM algorithm improved data analysis, highlighting true associations by reducing the number of confounding signals linked to false positives. In fact, genetic matching identified confirmed T1D loci *CTLA4*, *IL2RA*, and *PTPN22*.

Our experimental plan is to use the combined results from GWAS performed in Pittsburgh and by WTCCC to optimize GEM methodology, and apply the GEM algorithm during analysis of the complete WTCCC dataset. We anticipate that, when the Pittsburgh 'common' controls are combined with the WTCCC dataset, the method will increase power to detect true association. In order to accomplish these goals we request access to the complete WTCCC dataset of common diseases and controls. Our initial focus will be to enhance the power of the GWAS performed in Pittsburgh and by WTCCC. We will then direct our efforts towards exploiting the complete WTCCC dataset delivering an analysis with increased power to detect true signals for association with T1D. This will be our primary analysis. If our results are promising, secondary analyses will target each of the disease sets in turn, using the other, appropriate data sets as controls. Finally it is possible that some of the WTCCC common diseases have etiological factors in common. For example it is plausible that T1D, rheumatoid arthritis, and inflammatory bowel disease inherit risk from a common locus. Joint analyses using GEM methods will be useful to evaluate this possibility.

1. Luca et al. On the use of general control samples for genome-wide association studies: genetic matching highlights causal variants. *Am J Hum Genet* (in press).
2. Price et al. Principal components analysis corrects for stratification in genome-wide association studies. *Nat Genet* 2006 38:904-909.

Feasibility

Please describe your experience and expertise, and that of your collaborators, and how this will be applied to the proposed study. Relevant publications should be cited.

Massimo Trucco, MD (Applicant) is Chief of the Division of Immunogenetics at Children's Hospital of Pittsburgh, Hillman Professor of Pediatric Immunology and professor of Pediatrics at the University of Pittsburgh School of Medicine. Dr. Trucco's research is focused on the genetic and immunologic mechanisms underlying susceptibility to Type 1 Diabetes.

Bernie Devlin, Ph.D. (Co-Applicant) is Associate Professor of Psychiatry and Human Genetics and Director of the Western Psychiatric Institute and Clinic Computational Genetics Program. Dr. Devlin's research is focused on developing statistical approaches for examining genetic polymorphisms associated with human disease. He has pioneered methods for developing predictive models of linkage disequilibrium and genomic structure as well as novel analytical solutions for identifying positive genetic signatures from genome-wide analyses.

Kathryn Roeder, Ph.D. (Co-Applicant) is Professor of Statistics at Carnegie Mellon University. Dr. Roeder's research is focused on population genetic and statistical issues surrounding how best to identify disease associated genomic variants. Dr. Roeder has been awarded a National Young Investigator Prize from the National Science Foundation and has been the recipient of the Myrto Lefkopoulos Distinguished Lectureship at the Harvard School of Public Health. She is currently an associated editor for the Journal of the American Statistical Association and the American Journal of Human Genetics.

Relevant Publications (Applicant and Co-Applicant are indicated in bold font):

Devlin B, Roeder K, Wasserman L. (2001) Genomic control, a new approach to genetic-based association studies. *Theor Popul Biol* 60:155-166.

Devlin B, Roeder K, Bacanu SA. (2001) Unbiased methods for population-based association studies. *Genet Epidemiol* 21:273-284.

Luca D, Ringquist S, Klei L, Lee AB, Gieger C, Wichmann H-E, Schreiber S, Krawczak M, Lu Y, Styche A, **Devlin B, Roeder K, Trucco M.** (in press) On the use of general control samples for genome-wide association studies: genetic matching highlights causal variants. *Am J Hum Genet*.

Morel PA, Dorman JS, Todd JA, McDevitt HO, **Trucco M.** (1988) Aspartic acid at position 57 of the HLA-DQ beta chain protects against type I diabetes: a family study. *Proc Natl Acad Sci USA* 85:8111-8115.

I have read and agree to abide by the terms and conditions outlined in the Data Access Agreement and the Publication Policy?

Yes	<input checked="" type="checkbox"/>
No	<input type="checkbox"/>



Table of Contents

American Society for Histocompatibility and Immunogenetics

Features

SCIENTIFIC COMMUNICATIONS

A Web-Based Program for Pyrosequencing Primer Design 50
Steven Ringquist, Christopher Pecoraro, and Massimo Trucco

HLA Class II Antibodies in Potential Renal Transplant Recipients 54
Judith E. Baker and Jenifer Williams

An Innovative Twist in Transplanting Multiple Patients 56
Jeffrey T. Sholander

Highlights

Summary of Board of Directors Meeting 62
ASHI 2006 Financial Summary 65
2007 Regional Meetings Retrospective 66

Departments

EDITORIAL

From the Editor-in-Chief 46
President's Column 48

ASHI QUARTERLY CONTINUING EDUCATION QUIZ 60

COMMITTEE ACTIVITIES

Accreditation News 68

Editor's Note

Individuals interested in submitting articles for the *ASHI Quarterly* should observe the following requirements (see p.38 for additional details):

- All articles must be submitted via e-mail in Microsoft Word format
- All articles must be double-spaced

Article submissions should be forwarded to:

Editor-in-Chief
Francesco Marincola
E-mail: fmarincola@cc.nih.gov

Copy deadlines for future issues:

Fourth Quarter 2007: November 5, 2007

ASHI Quarterly

Volume 31, Number 3

Editor-in-Chief

Francesco M. Marincola, MD

Deputy Editor-in-Chief

Sharon Adams

Section Editors

Raja Rajalingam, PhD

Clinical Science

Laura Underwood, MT (ASCP), CHS (ABHI)

Technological Issues

Thalachallour Mohanakumar, PhD

Basic Science Editor

Executive Director

Kimberly Glenn

Publication Manager

Frank Scussa

Graphic Designer

Anthony N. Mungiali

ASHI Quarterly is published quarterly by the American Society of Histocompatibility and Immunogenetics, 15000 Commerce Parkway, Mount Laurel, New Jersey 08054. Subscription rates are \$35 within the United States and Canada, \$40 outside the United States and Canada. Subscriptions are accepted on a calendar year basis. Remittance should be made by check, draft or money order in U.S. currency, payable to the American Society for Histocompatibility and Immunogenetics. Notify ASHI of change of address at least 30 days before date of issue by sending both the old and new address. Multiple reproductions of any material in this publication is permitted only under license from the American Society of Histocompatibility and Immunogenetics with the written permission of the authors. Fair use of such material by individual readers and non-profit libraries, such as making single copies of an article for use in teaching or research, is allowed. Consent of the authors and ASHI must be obtained to reprint figures, tables or excerpts from the printed matter. The statements and opinions are not necessarily those of ASHI. ASHI does not endorse any products.

Copyright © 2007. American Society for Histocompatibility and Immunogenetics.

www.ashi-hla.org

A Web-Based Program for Pyrosequencing Primer Design

Steven Ringquist, Christopher Pecoraro, & Massimo Trucco

Division of Immunogenetics

Department of Pediatrics

Rangos Research Center

Children's Hospital of Pittsburgh

University of Pittsburgh School of Medicine

*Address correspondence to: Massimo Trucco, MD,
Division of Immunogenetics, Rangos Research Center,
Children's Hospital of Pittsburgh, 3460 Fifth Avenue,
Pittsburgh, PA, 15213. E-mail: mnt@pitt.edu;
Tel: (412) 692-6570; Fax: (412) 692-5809.*

Introduction

This review presents a brief description of the Selection of Oligonucleotide Primer for PCR and Pyrosequencing (SOP3) software. The web-based application enables efficient design of polymerase chain reaction (PCR) and pyrosequencing primers that can be used for analysis of genetic polymorphisms, including single nucleotide polymorphisms (SNPs). The software automates the process of retrieving genomic DNA sequences and locations of SNPs from the human genome database, and takes into consideration specific restrictions necessary during the design of pyrosequencing assays.^{1,2} The application aids in the sorting of SNPs for biologically interesting properties (e.g., the association of a SNP with a particular genetic structural element and whether it codes for an amino acid change in the resulting protein, as well as its heterozygosity within a population) that, in turn, adds to the usefulness of particular primer sets during physical mapping studies.

Pyrosequencing was developed for the analysis of expressed sequence tags (EST), enabling accurate sequencing of short stretches of DNA. This methodology has found increasing acceptance as a method for analysis of SNPs, insertion/deletion polymorphisms, and for investigating sites of DNA methylation. Sequencing of a maximum length of 40 nucleotides is commonly performed while a maximum of 150 nucleotides sequenced has been reported.^{3,4} When applied to genotyping human leukocyte antigen (HLA), the method is capable of distinguishing between allelic pairs commonly found to be ambiguous using other methods [e.g., sequence specific oligonucleotide probe (SSOP) and sequence base typing (SBT) genotyping methods].⁴ Pyrosequencing allows increased resolution of allelic pairs due to its ability to accurately resolve heterozygous nucleotides by enabling out-of-phase sequencing.⁵ Performed by stepwise addition of dNTPs, pyrosequencing enables synthesis of the nascent nucleotide chain that is extended one nucleotide residue per dispensation step. Detection of the nucleotide sequence is performed by way of a chain of enzymatic reactions involving DNA polymerase, apyrase, ATP sulfurylase, as well as luciferase.^{3,6} Each nucleotide is dispensed independently into the reaction mix. The graphic display, depicting the incorporation of a particular nucleotide, is in the form of a nucleotide dispensation event (x-axis) versus the intensity of emitted light (y-axis) and is referred to as a pyrogram (Figure

1). The pyrosequencing reaction is quantitative, in that increased light intensity is produced upon incorporation of multiple nucleotides. Thus, DNA sequence is determined by examination of light intensity emitted immediately after nucleotide dispensation and is known as sequencing by synthesis. Positions of polymorphic sequence are identified due to their exhibiting variable incorporation patterns as determined by the genotype.

Software for Pyrosequence Primer Design

SOP3 is a web-based software application (<http://imgen.cccb.pitt.edu/sop3>) that has been specifically developed for use in pyrosequence assay design.^{1,2} The webserver hosts an integrated biological database consisting of genetic variants as well as the DNA sequence of the human and mouse genomes, including validated human SNPs contained within the HapMap comparative genome project. The software provides a batch analysis tool that accepts the names of as many as 100 genetic loci, 100 SNP identifiers, or a 100 kb section of genomic DNA under investigation. The application returns a set of primer trios for PCR (2 primers) and pyrosequencing (1 primer) for the corresponding genetic variants listed in dbSNP. Genomic DNA sequences are stored on the web server making them readily accessible to the application. Detailed instructions for using SOP3 are available online using the Assay Design User Guide (http://imgen.cccb.pitt.edu/sop3/entry_box.html).

The graphical interface for the SOP3 application provides an array of user-defined settings to allow customization of primer trio design. Genomic sequences from queried polymorphisms and their flanking sequences are returned to the SOP3 application's core algorithm and enable the selection of suitable primer trios. Choice of PCR primers is based on multiple criteria including the distance between PCR primer annealing sites and the SNP, as well as allowing for the selection of optimal genomic flanking sequence for annealing of sequencing primer. Additional criteria for maximizing PCR amplification yield are included. For example, the search identifies suitable primers at multiple annealing sequences on either side of the SNP. The list of candidate PCR primers is evaluated for their ability to form a competing secondary structure that may interfere with primer annealing; the

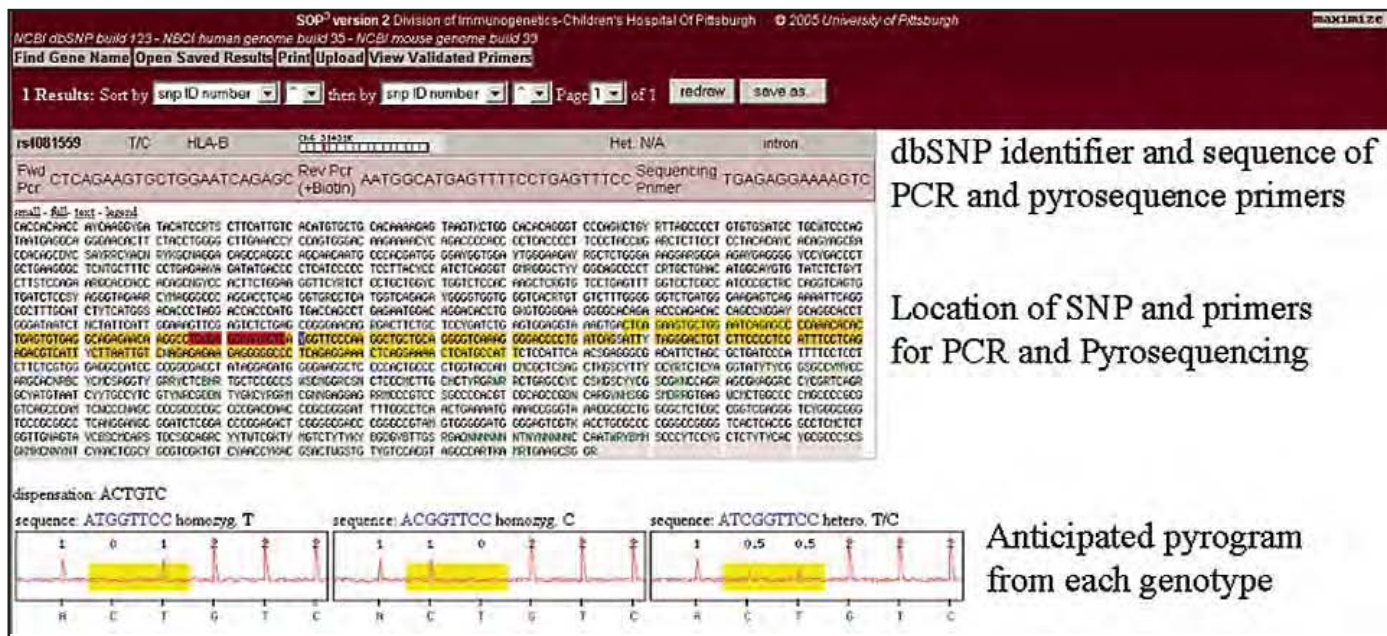


Figure 1

Results of the query for SNP rs4081559 contained within intron 2 of HLA-B as obtained from the SOP3 application. Upper Panel. The output summarizes the SNP under consideration by referencing the dbSNP identifier (i.e., rs4081559) and provides the recommended sequence of primers for PCR and pyrosequencing. Middle Panel. The location of SNP and primers are indicated in blue (query SNP), red (pyrosequencing primer), and yellow (PCR primers). The region amplified during PCR is indicated in gold. The locations of nearby SNPs are indicated (pink). Bottom Panel. The anticipated pyrograms from each genotype are shown. Pyrograms plot the nucleotide dispensation order (x-axis) versus the light emitted (y-axis) during sequencing by synthesis steps of pyrosequencing.

predicted stability of primer annealing is monitored by calculating the melting temperature (T_m); sequence complexity is measured by maintaining representative frequencies of each nucleotide residue in the final primer sequence. Identification of nearby polymorphic sites is performed in order to improve the design of primer trios for sequencing as well as to enable possible multiplexing of assays for genotyping these residues.

The software generates lists of candidate forward and reverse PCR primers that pass the individual tests. These oligonucleotide sequences are then compared in order to obtain compatible primer pairs for use during PCR amplification. This is accomplished by analyzing primers for regions of reverse complementary sequence that may initiate primer dimer amplification. Final optimization of PCR primers is accomplished by modifying the PCR forward primer by addition of an extra-genomic nucleotide motif to the 5'-end. This results in suppression of competing sequencing reactions during genotyping analysis that may occur whenever the template strand 3'-end is capable of annealing to an internal sequence motif, thus repressing initiation of intra-molecular sequencing.⁷ The resulting PCR primers are returned to the user as oligonucleotide sequences recommended for laboratory testing which are either presented graphically or in a tab-delimited format (Figure 1, top panel).

Computer software for designing primers for use during polymerase chain reaction (PCR) is available from a number of sources (Table 1). A principle use of these applications is to aid assay design when evaluating the association between phenotypic changes and the inheritance of genetic markers, such as single nucleotide polymorphisms (SNPs) and nucleotide insertions and deletions. Commercial software is also available

for generating PCR and sequencing primers (Table 1). For example, the manufacturer of the pyrosequence instrument Biotage LLC provides assay design software aimed at developing primer sets suitable for use during pyrosequencing. These applications provide access to PCR and sequencing primer design algorithms but require the manual input of sequence along with identification of the polymorphic residues to be evaluated. For genetic studies where many polymorphisms are being investigated, such as in the investigation of a set of candidate markers for association with a disease, this requirement creates a bottleneck during assay development. Thus, improved approaches to assay design that provide integrated genomic sequence, genetic variant, and functional information increase the efficiency by which genotyping assays can be developed and validated by laboratory testing.⁸

The objective of the SOP3 application has been to provide a method to effectively search genomic databases for SNPs and insertion/deletion polymorphisms in order to design genotyping assays. The application has been used to design primers that have been validated for a variety of SNPs within loci suspected of correlating with risk towards developing disease as well as HLA genotyping.^{9,12} Localizing the NCBI dbSNP database and the data from University of California Santa Cruz (UCSC) GoldenPath for the human genome allowed the creation of structured query language (SQL) to present genomic variation data as well as annotation of functional genomic elements in a customized format. Using the SOP3 application for a multi-loci genetic marker association study is aided by the use of the integrated Entrez Gene annotation, which identifies the start and end markers of a gene, as well as the start and end markers of exons, introns, and the location of polymorphisms associated with splice site regions. SOP3 designed primer trios continue to be evaluated

Website	Web Address	Description
Primer Design Software:		
Integrated DNA Technologies	http://www.idtdna.com	Supplier of oligonucleotides. The website also contains an extensive selection of scientific tools for PCR primer design.
Primer3	http://frodo.wi.mit.edu/cgi-bin/primer3/primer3_www.cgi	Primer3 is a widely used program for designing primers for PCR.
SOP3	http://imgen.ccbb.pitt.edu/sop3	Web-based software specifically tailored for designing primers for pyrosequencing.
Human Genome Resources:		
NCBI	http://www.ncbi.nlm.nih.gov/	The National Center for Biotechnology Information (NCBI) is a national resource for molecular biology information containing public databases and software tools for analyzing genome data.
dbSNP	http://www.ncbi.nlm.nih.gov/SNP/	The dbSNP database serves as a central repository for both single base nucleotide substitutions and short deletion and insertion polymorphisms.
Entrez Gene	http://www.ncbi.nlm.nih.gov/entrez/query.fcgi?db=gene	Entrez Gene is a searchable database of genes maintained by the National Center for Biotechnology Information.
HapMap	http://www.hapmap.org/	The HapMap Project is an effort to identify and catalog genetic similarities and differences in human beings.
Pyrosequencing Resources:		
Biotage, AB	http://www.biotage.com	Leading supplier of pyrosequencing reagents & instruments.

Table 1. Websites and Internet Resources Related to Pyrosequencing.

in the laboratory as part of ongoing research into the genetics of complex diseases using human cohorts as well as mouse model systems.^{4,13}

Summary

The ability to generate high resolution sequence data and throughput of hundreds of sequencing reactions per day make pyrosequencing an important method for identification of known genetic markers. Based on finding a short sequence in each allele of interest that occurs only once within the PCR generated fragment, the pyrosequencing protocol allowed rapid identification of alleles for analysis of genetic predisposition to autoimmune disease as well as for histocompatibility typing. Pyrosequencing is an ideal tool for rapid and accurate identification of genotypes in studies of the genetic association of certain HLA alleles with the likelihood of developing autoimmune disease, as well as during clinical genotyping of patients and donors for histocompatibility matching during transplantation.

Acknowledgements

The authors thank Alexis Styche for a critical reading of the manuscript. This work was supported by grants from the NIH-NLM, U19-AI056374-01 Autoimmunity Centers of Excellence (SR and MT), RO1DK24021(MT) from the National Institutes of Health, and ERHS #00021010 (SR and MT) from the Department of Defense.

References

1. Ringquist S, Pecoraro C, Gilchrist MS, Styche A, Rudert WA, Benos PV, Trucco M. SOP3v2: web-based selection of oligonucleotide primer trios for genotyping of human and mouse polymorphisms. *Nucl Acids Res* 2005;33:W548-W552.
2. Ringquist S, Pecoraro C, Lu Y, Styche A, Rudert WA, Benos PV, Trucco M.
3. Gharizadeh B, Nordstrom T, Ahmadian A, Ronaghi M, Nyren P. Long-read pyrosequencing using pure 2'-deoxyadenosine-5'-O'-(1-thiophosphosphate) sp-isomer. *Anal Biochem* 2002;301:82-90.
4. Ringquist S, Alexander AM, Styche A, Pecoraro C, Rudert WA, Trucco M. HLA class II DRB high resolution genotyping by pyrosequencing: comparison of group specific PCR and pyrosequencing primers. *Hum Immunol* 2004;65:163-174.
5. Garcia CA, Ahmadian A, Gharizadeh B, Lundeberg J, Ronaghi M, Nyren P. Mutation detection by pyrosequencing: sequencing of exons 5-8 of the p53 tumor suppressor gene. *Gene* 2000;253:249-257.
6. Ronaghi M, Karamohamed S, Pettersson B, Uhlen M, Nyren P. Real-time DNA sequencing using detection of pyrophosphate release. *Anal Biochem* 1996;242:84-89.
7. Ronaghi M, Pettersson B, Uhlen M, Nyren P. PCR-introduced loop structure as primer in DNA sequencing. *Biotechniques* 1998;25:876-878.
8. Stein LD. Integrating biological databases. *Nature Rev Genet* 2003;4:337-345.
9. Todd JA, Bell JI, McDevitt HO. HLA-DQ beta gene contributes to susceptibility and resistance to insulin-dependent diabetes mellitus. *Nature* 1987;329:599-604.
10. Morel PA, Dorman JS, Todd JA, McDevitt HO, Trucco M. Aspartic acid at position 57 of the HLA-DQ beta chain protects against type I diabetes: a family study. *Proc Natl Acad Sci USA* 1988;85:8111-8115.
11. Sollid LM. Celiac disease: dissecting a complex inflammatory disorder. *Nat Rev Immunol* 2002;2:647-655.
12. Zanelli E, Breedveld FC, de Vries RR. HLA class II association with rheumatoid arthritis: facts and interpretations. *Hum Immunol* 2000;61:1254-1261.
13. Mathews CE, Leiter EH, Spirina O, Bykhovskaya Y, Gusdon AM, Ringquist S, Fischel-Ghodsian N. mt-Nd2 Allele of the ALR/Lt mouse confers resistance against both chemically induced and autoimmune diabetes. *Diabetologia* 2005;48:261-267.

Web-based primer design software for genome scale SNP mapping by pyrosequencing. In: *Methods in Molecular Biology*, vol 373: Pyrosequencing Protocols. ed. S. March. Humana Press Inc., Totowa, New Jersey (2006).

1. Ringquist S, Pecoraro C, Gilchrist MS, Styche A, Rudert WA, Benos PV, Trucco M. SOP3v2: web-based selection of oligonucleotide primer trios for genotyping of human and mouse polymorphisms. *Nucl Acids Res* 2005;33:W548-W552.
2. Ringquist S, Pecoraro C, Lu Y, Styche A, Rudert WA, Benos PV, Trucco M.
3. Gharizadeh B, Nordstrom T, Ahmadian A, Ronaghi M, Nyren P. Long-read pyrosequencing using pure 2'-deoxyadenosine-5'-O'-(1-thiophosphosphate) sp-isomer. *Anal Biochem* 2002;301:82-90.
4. Ringquist S, Alexander AM, Styche A, Pecoraro C, Rudert WA, Trucco M. HLA class II DRB high resolution genotyping by pyrosequencing: comparison of group specific PCR and pyrosequencing primers. *Hum Immunol* 2004;65:163-174.
5. Garcia CA, Ahmadian A, Gharizadeh B, Lundeberg J, Ronaghi M, Nyren P. Mutation detection by pyrosequencing: sequencing of exons 5-8 of the p53 tumor suppressor gene. *Gene* 2000;253:249-257.
6. Ronaghi M, Karamohamed S, Pettersson B, Uhlen M, Nyren P. Real-time DNA sequencing using detection of pyrophosphate release. *Anal Biochem* 1996;242:84-89.
7. Ronaghi M, Pettersson B, Uhlen M, Nyren P. PCR-introduced loop structure as primer in DNA sequencing. *Biotechniques* 1998;25:876-878.
8. Stein LD. Integrating biological databases. *Nature Rev Genet* 2003;4:337-345.
9. Todd JA, Bell JI, McDevitt HO. HLA-DQ beta gene contributes to susceptibility and resistance to insulin-dependent diabetes mellitus. *Nature* 1987;329:599-604.
10. Morel PA, Dorman JS, Todd JA, McDevitt HO, Trucco M. Aspartic acid at position 57 of the HLA-DQ beta chain protects against type I diabetes: a family study. *Proc Natl Acad Sci USA* 1988;85:8111-8115.
11. Sollid LM. Celiac disease: dissecting a complex inflammatory disorder. *Nat Rev Immunol* 2002;2:647-655.
12. Zanelli E, Breedveld FC, de Vries RR. HLA class II association with rheumatoid arthritis: facts and interpretations. *Hum Immunol* 2000;61:1254-1261.
13. Mathews CE, Leiter EH, Spirina O, Bykhovskaya Y, Gusdon AM, Ringquist S, Fischel-Ghodsian N. mt-Nd2 Allele of the ALR/Lt mouse confers resistance against both chemically induced and autoimmune diabetes. *Diabetologia* 2005;48:261-267.

Web-Based Primer Design Software for Genome-Scale Genotyping by Pyrosequencing®

Steven Ringquist, Christopher Pecoraro, Ying Lu, Alexis Styche,
William A. Rudert, Panayiotis V. Benos, and Massimo Trucco

Summary

Design of locus-specific primers for use during genetic analysis requires combining information from multiple sources and can be a time-consuming process when validating large numbers of assays. Data warehousing of genomic DNA sequences and genetic variations when coupled with software applications for optimizing the generation of locus-specific primers can increase the efficiency of assay development. Selection of oligonucleotide primers for PCR and Pyrosequencing® (SOP³) software allows user-directed queries of warehoused data collected from the human and mouse genome sequencing projects. The software automates collection of DNA sequence flanking single-nucleotide polymorphisms (SNPs) as well as the incorporation of locus-associated functional information, such as whether the SNP occurs in an exon, intron, or untranslated region. SOP³ software accepts three types of user-directed input consisting of gene locus symbols, SNP reference sequence numbers, or chromosomal physical location. For human polymorphisms, SOP³ incorporates haplotype, ethnicity, and SNP validation attributes. The output is a list of oligonucleotide primers recommended for Pyrosequencing-based typing of genetic variations. SOP³ is available at the Division of Immunogenetics computational server found at <http://imgen.cccb.pitt.edu>.

Key Words: Bioinformatics; genetics; genomics; genotyping; sequencing.

1. Introduction

Computer software for designing primers for use during PCR are available from a number of sources (1–3). A principle use of these applications is to aid assay design when evaluating the association between phenotypical changes and the inheritance of genetic markers, such as single-nucleotide polymorphisms (SNPs) including nucleotide insertions and deletions. Commercial software is also available for generating PCR and sequencing primers and for use

From: *Methods in Molecular Biology*, vol. 373: Pyrosequencing® Protocols
Edited by: S. Marsh © Humana Press Inc., Totowa, NJ

during DNA sequencing. For example, the manufacturer of the Pyrosequencing® instrument Biotage, LLC provides assay design software aimed at developing primer sets suitable for use during Pyrosequencing. These applications provide access to PCR and sequencing primer design algorithms, but require user input of FASTA-formatted sequences along with identification of polymorphic residues that are to be evaluated. For genetic studies where many polymorphisms are being investigated, such as is necessary when investigating a set of candidate markers for association with a disease phenotype, this requirement creates a bottleneck during assay development. Improved approaches to assay design that provide integrated genomic sequence, genetic variant, and functional information increase the efficiency by which genotyping assays can be developed and validated by laboratory testing (4).

SOP³ is a web-based software application that has been developed for use in Pyrosequencing assay design and is available at <http://imgen.cccb.pitt.edu> (5). The computational webserver warehouses an integrated biological database comprised of genetic variants, as well as DNA sequence of the human and mouse genomes, including validation of human SNPs within the HapMap comparative genome project. The software provides a batch analysis tool that accepts the names of as many as 100 genetic loci, 100 SNP identifiers, or a 100-kb section of genomic DNA under investigation. The application returns a set of primers for PCR and Pyrosequencing for all corresponding genetic variants listed in dbSNP along with flanking genomic DNA sequences contained within the human and mouse genome resources. Local warehousing of genomic sequences, making them accessible to the application, enables the software to provide the choice of locus-specific primer trios for PCR and Pyrosequencing for use in rapid genotype analysis.

2. Materials

2.1. System Configuration

1. The SOP³ application, genomic sequence, and genetic variation data from the human and mouse genome projects are warehoused on a computational webserver purchased from @Xi Computer (San Clemente, CA). The software application is written in preprocessor hypertext protocol v5.0.3 and is associated with a MySQL 4.1 database developed on a Linux SuSE Enterprise Server 8 for the AMD64 operating system with Apache web server v2.0.48. The computational server consists of dual AMD Opteron 246 64-bit processors with 1024 KB Cache, 8192 MB random access memory, and four 250 GB hard drives.

2.2. Connecting to the Webserver

1. The SOP³ website can be accessed over the internet at <http://imgen.cccb.pitt.edu>. The application works best when viewed in Internet Explorer v6 or higher but can

Primer Design Software Uncorrected Proof Copy

27

also be viewed in Firefox as well as Netscape. Internet browsers are available for download from <http://www.microsoft.com/windows/ie>, <http://browser.netscape.com>, and <http://www.mozilla.org>, respectively.

3. Methods

The SOP³ application has been designed for use with genotyping protocols and enables locus-specific PCR amplification of candidate SNPs for sequence analysis. Filtering of genetic variations for validated and HapMap-associated SNPs improves the efficiency of assay development for studying the role of DNA polymorphisms in determining the phenotype in models of genetic inheritance (**Table 1**). An advantage of the SOP³ application is that design of genotyping studies can be developed using the assay design algorithm by filtering all available genetic variants for those specified by user-directed query, such as specifying human or mouse and using only validated nucleotide polymorphisms (see **Note 1**). The application accepts multiple queries of gene loci, SNPs, as well as chromosomal regions for analysis. SOP³ provides multiple choices for selecting the most suitable genetic markers for evaluation during genotyping. The User Guide for operation of SOP³ software is available online at <http://imgen.cccb.pitt.edu/sop3/userguide>.

3.1. Basic Functions

1. Searching human or mouse genetic variations. The web interface to the SOP³ application allows the user to specify whether to search for SNPs within the human or mouse genome. The default setting is for human genetic variants and is indicated on the website by the filled in button adjacent to the label for “Human.” To specify searching of the mouse database the user should click the button next to “Mouse” provided on the website (**Fig. 1**).
2. Searching by locus name. To query the SOP³ database for SNPs associated with up to 100 locus symbols the user can enter the symbol or a list of locus symbols into the textbox. Locus symbols can be typed directly into the text box, entered using the copy and paste function on the user’s computer, or by uploading from a text file. Queries are restricted to no more than 100 entries per batch. Use the check boxes provided to specify whether the query is for human or mouse genomes. Click the “Search” button to activate the application. Results will appear at the bottom of the page. Selecting the “Clear” button will refresh the application to the default settings.
3. Searching by SNP identifier. To query the SOP³ database by SNP identifier the user can enter either a single reference sequence number or a list of polymorphism reference sequence numbers. Queries are restricted to no more than 100 entries per batch. Use the check boxes provided to specify whether the query is for human or mouse genomes. Click the “Search” button to activate the application. Results will appear at the bottom of the page. Selecting the “Clear” button will refresh the application to the default settings.

FIG 1

Table 1
Classification of Human and Mouse Genetic Variants

Classification	Number of human SNPs	Number of mouse SNPs	Description
<i>Validation status</i>			
HapMap	35,126	NA	The genetic variant has been genotyped by the International HapMap Consortium and incorporated into the dbSNP resource.
Validated	384,831	464,137	Multiple submissions of the genetic variant has been reported within the dbSNP resource.
<i>Function type</i>			
Coding: syn. unknown	34	9	The genetic variant is within the coding region of a gene. The location of the polymorphism cannot be resolved because of an error in the alignment of the exon.
Intron	3,704,388	213,968	The variant is in the intron of a gene but not within two residues from the intron/exon boundary.
Nonsynonymous change	61,963	5478	The genetic variant is nonsynonymous for the codon within the gene. This class of allele is defined by a substitution and translation of the allele into the codon that results in a change to the amino acid specified by the exon reading frame.
No RNA_acc / Protein_acc	357,606	30,373	The polymorphism is within 2000 nucleotides 5' or 500 nucleotides 3' of a gene feature. The variant is not in the transcript for the gene.
Splice site	971	23	The variant is in the first two or last two nucleotides on the intron of a gene.
Synonymous change	48,702	9548	The genetic variant is synonymous for the codon within the gene. This class of allele is defined by a substitution and translation of the allele into the codon that results in no change to the amino acid specified by the exon reading frame.
Untranslated region	668,282	43,414	The nucleotide polymorphism is in the transcript of a gene but not in the coding region of the mRNA.

<i>Geographic population</i>			
Cent. Asia	46	NA	Samples from Russia and its satellite republics and from nations bordering the Indian Ocean between East Asia and the Persian Gulf regions.
Cent/S. Africa	30	NA	Samples from nations south of the Equator, Madagascar, and neighboring island nations.
Cent/S. America	11	NA	Samples from Mainland Central and South America and island nations of the western Atlantic, Gulf of Mexico, and Eastern Pacific.
E. Asia	7447	NA	Samples from eastern and south eastern Mainland Asia and from Northern Pacific island nations.
Europe	535	NA	Samples from Europe north and west of Caucasus Mountains, Scandinavia, and Atlantic Islands.
Multinations	13,004	NA	Samples that were designated to maximize measures of heterogeneity or sample human diversity in a global fashion.
N. America	11,438	NA	All samples north of the Tropic of Cancer, including defined samples of US caucasians, African Americans, Hispanic Americans, and the National Human Genome Research Initiative (NHGRI) polymorphism discovery resource.
N.E. Africa and Mid. East	27	NA	Samples collected from North Africa (including the Sahara desert), East Africa (south to the Equator), Levant, and the Persian Gulf.
Pacific	144	NA	Samples from Australia, New Zealand, Central and Southern Pacific Islands, and Southeast Asian peninsular/island nations.
Unknown	479	NA	Samples with unknown geographic provinces that are not global in nature.
W. Africa	174	NA	Sub-Saharan nations bordering the Atlantic north of the Congo River and central/southern Atlantic nations.

SOP³, version 2 Division of Immunogenetics-Children's Hospital Of Pittsburgh © 2005 University of Pittsburgh
NCBI dbSNP build 123 - NCBI human genome build 35 - NCBI mouse genome build 33

Find Gene Name [Open](#) [Saved Results](#) [Print](#) [Upload](#) [View Validated Primers](#)

Search by SNP id or Locus Name Info

Human Mouse advanced options

Enter list of gene names or ref.seq's

Guide me [SEARCH](#) [CLEAR](#)

(Optional) Limit Results to: [Validated snp's \(384,831\)](#) [INFO](#) [HapMap \(35,126\)](#) [INFO](#)

Search by Location/Range Info

Chromosome number [▼](#)

From Lower Limit (base pairs) [▼](#)

To Upper Limit (base pairs) [▼](#)

Limit by Population Criteria Info

N. America (11,438) Cent/S. America (146) Europe (635) no ma. acc/ protein. acc hs-357.806 mm-30.373

N/E Africa & Mid. East (rate) W. Africa (174) Cent. S. Africa (rate) nonsynonymous change hs-61.963 mm-5.478 hs-698.282 mm-43.414

E. Asia (7,447) Cent. Asia (rate) Pacific (144) intron hs-3.709.388 mm-213.968 hs-971 mm-23

Multiple Nations (13,004) Unknown (479) coding, syn. unknown hs-34 mm-9

Limit by Function Type Info

synonymous change hs-48.702 mm-9.548

untranslated region

splice-site

Sort by [snp ID number](#) [▼](#) [then by](#) [snp ID number](#) [▼](#) [redraw](#) [save as..](#)

AU: Is GCK referring to a gene in Figs. 1 and 2?

Fig. 1. User interface to the SOP³ web-based software application. The example illustrates a search for polymorphisms associated with the human glucokinase locus, GCK. The query is limited to single-nucleotide polymorphisms linked to the HapMap project, filtered for genetic variants found in populations within North America, and for polymorphisms associated with intron elements of the RNA transcript.

Primer Design Software Uncorrected Proof Copy

31

Table 2

Maximum Allowable Upper Limit for Screening Chromosome Range

Human chromosome	Maximum range	Mouse chromosome	Maximum range
1	245,442,500	1	195,198,653
2	242,818,021	2	181,685,801
3	199,450,386	3	160,571,871
4	191,400,945	4	154,132,574
5	180,837,593	5	149,217,787
6	170,972,421	6	149,553,910
7	206,556,958	7	133,031,105
8	146,272,185	8	128,674,990
9	138,428,984	9	124,140,960
10	135,412,916	10	130,567,357
11	134,451,003	11	121,607,694
12	132,389,146	12	114,933,529
13	114,127,336	13	116,456,691
14	106,360,250	14	117,011,917
15	100,337,960	15	104,102,711
16	88,821,548	16	98,800,952
17	80,652,345	17	93,538,550
18	76,116,152	18	90,878,013
19	63,806,020	19	60,667,351
20	62,435,629	X	160,070,598
21	46,943,948	Y	47,759,179
22	49,534,318		
X	154,823,225		
Y	57,700,652		

Values for maximum range were determined using the highest chromosomal position number associated with a SNP on the human or mouse genomes using build 35 or 33, respectively.

4. Searching by chromosomal location and range. To query the SOP³ database by chromosomal range use the check boxes to specify whether the search will focus on human or mouse genomes. Next, use the “Chromosome Number” dropdown menu to specify which chromosome is to be used. Enter lower and upper limits for the nucleotide positions that should be screened. Queries are restricted to regions no greater than 100,000 nucleotides. The maximum allowable upper limit for screening a range of nucleotides on each chromosome corresponds to the length of the chromosome and is indicated in **Table 2**. Click the “Search” button to activate the application. Results will appear at the bottom of the page. Selecting the “Clear” button will refresh the application to the default settings.
5. Filtering the results to show only validated SNPs. Selection of the “Validated SNPs” search filter directs the application to screen genetic polymorphisms for inclusion in the list of validated polymorphisms provided by dbSNP. There are

TABLE 2

currently 384,831 human and 464,137 mouse polymorphisms associated with this attribute. Validation status is defined as a genetic variant that has been reported by multiple submissions, is linked to frequency data for the SNP in a population, or was submitter validated by an updated submission from the original report.

6. Filtering the results to show only HapMap-genotyped SNPs. Selection of the “HapMap” search filter directs the application to screen genetic polymorphisms for those validated polymorphisms that are also included in the International HapMap Consortium haplotyping mapping project incorporated into the dbSNP database. There are currently 35,126 human polymorphisms associated with this attribute.
7. Filtering the results by limiting the population criteria. Selection of the “Limit By Population Criteria” filter directs the application to screen genetic polymorphisms by geographic origin of the sample. Selection of more than one population filter will return those polymorphisms that meet either of the criteria (i.e., a Boolean OR operation). The number of polymorphisms associated with each population group is indicated on the application’s homepage.
8. Limiting the search by function type. Genetic variants may be filtered by whether they are near a gene (locus region), in a UTR (untranslated region), in an intron (intron), or in a splice site (splice site). If the variation is in a coding region, then the functional class of the variation depends on how each allele may affect the translated peptide sequence, e.g., nonsynonymous change or synonymous change. Selection of more than one of the function-type filters will return those polymorphisms that meet either of the criteria (i.e., a Boolean OR operator). A definition of these filters as well as the number of polymorphisms associated with each function type, for human and mouse, is indicated in **Table 1**.
9. Initiating design of primers for PCR and Pyrosequencing. Selecting the “Search” button will activate the application. Locus-specific primers for PCR and Pyrosequencing will be returned for those SNPs that meet the filtering criteria selected in the user input section of the web interface.
10. Reporting the results. After submitting a search the application will present the results at the bottom frame of the website. Each report consists of four sections, attribute bar, candidate primer bar, DNA sequence flanking the polymorphism, and computer-simulated Pyrosequencing data for heterozygous and each homozygous genotype (**Fig. 2**).
11. The locus attribute bar provides information linked to the polymorphism consisting of reference sequence number, identity of the polymorphism, locus symbol, physical location on the chromosome, heterozygosity value, and function attribute. If the filters for “Validated SNPs,” “HapMap,” or “Limit By Population Criteria” were selected that information will also appear in the attribute bar.
12. The candidate primer bar contains the oligonucleotide sequence (written 5' to 3') for the candidate PCR forward and reverse primers as well as the Pyrosequencing primer (see **Note 2**). The nomenclature used for designating a forward PCR primer is that it is on the same side of the SNP as the Pyrosequencing primer. The nomenclature for designating a reverse PCR primer is that it is on the opposite side of the SNP as the Pyrosequencing primer. The reverse PCR primer should be synthesized with a 5' biotin-TEG modification during the Pyrosequencing protocol.

FIG 2

AU: Pls
spell out
TEG, if
appropriate.

AU: Is GCK referring to a gene in Figs. 1 and 2?

AU: Pls
modify
Fig. 2
caption;
there is to
be no
color.

Fig. 2. Results of the query for single-nucleotide polymorphisms (SNPs) linked to the human glucokinase locus, GCK. There are two entries in SOP³ v2 corresponding to the query. The attribute bar, candidate primer bar, DNA sequence, and simulated Pyrosequencing[®] data are shown. The color code in the DNA sequence box indicates the location of the PCR primers (yellow), Pyrosequencing primer (red), region of amplified DNA (orange), and location of the SNP (blue).

13. The DNA sequence flanking the SNP is indicated in the third panel of the results frame. The user may view the “Full” sequence that was evaluated, consisting of the polymorphism and 1000 flanking residues. The DNA sequence may also be viewed in FASTA format by selecting the “Text” button. The option for viewing the flanking sequence as “Small” will display only the sequence amplified by the locus-specific PCR primers (*see Note 3*). The color code in the bottom frame shows PCR primers indicated in yellow, Pyrosequencing primer in red, the SNP is colored blue, the amplified region in orange, and nearby polymorphisms shown in gray. Lowercase characters indicate the location of repeat masker-identified genomic regions. A “Legend” button providing a key to the color coding is also provided.
14. Simulated Pyrosequencing data is displayed in the bottom panel of each result. A simulated Pyrogram is drawn for each genotype, i.e., heterozygous and both homozygous genotypes. A nucleotide dispensation order for evaluating these data in the Pyrosequencing software is illustrated above the Pyrogram charts. Informative dispensations for distinguishing the genotypes are indicated in yellow (*see Note 4*).
15. Minimization and maximization of the input/output frames can be accomplished by clicking the “Minimize/Maximize” button located in the upper right-hand corner of the web interface. A full-screen view of the results of the SOP³ application is available, allowing easier browsing of the results frame.
16. Sorting the results by reference SNP number, heterozygosity value, physical position on the chromosome, gene name, or function can be accomplished using the “Sort By” dropdown menus. The “Sort By” function is located in the horizontal bar found along the middle of the web interface. Results may be viewed in ascending “^” or descending “v” order. Results on the web interface are presented 20 at a time. When greater than 20 results are returned they can be viewed by choosing the “Page” dropdown menu. The total number of results and pages of results is also indicated. After selection of functions for sorting and page display the results can be refreshed by clicking the “Redraw” button located on the middle toolbar.
17. Results from the SOP³ application can be saved in an Excel formatted text file. Select this function by clicking the “Save As.” This will open a text box for designating a file name and a “Save” button for uploading the results to the SOP³ server. The saved file can be viewed by selecting the “Open Saved Results” button located at the top of the page. Saved files are listed alphabetically and each file contains a tab-delimited list of PCR and sequencing primers, as well as SNP attributes such as reference sequence number, heterozygosity value, and function attribute. Selection of the “Save All” button will allow all the results to be transferred to the web server. Unselecting of the “Save All” button will allow only the page of results presently displayed in the bottom frame to be saved.
18. Selecting the “Clear” button located in the upper frame of the web interface will refresh the application to the default settings.

3.2. Advanced Options for PCR Primer Design

1. Selection of the “Advanced Options” button opens a list of PCR and sequencing primer design settings used in the assay design algorithm. This function allows

Primer Design Software Uncorrected Proof Copy

35

the user to specify customized settings for primer selection that are different from the default settings. Clicking the “Advanced Options” a second time will hide these values. Selecting the “Clear” button will refresh the application to the default settings.

2. The display for PCR primer design settings allows the user to adjust the primer selection criteria.
3. “Melting Temperature (T_m) °C” default setting is 60°C. T_m is calculated using the relationship ($T_m = 16.6 \cdot \log[\text{cation concentration}] + 41 \cdot [\text{fraction of GC}] + 81.5$, where the concentration of cation was estimated to be 0.1 M) described by Schildkraut and Lifson (6). User-directed changes to this value instruct the application to design primers to the indicated minimum T_m value.
4. The “Minimum Foldover” filter is set at a default of five. This value reflects the minimum allowable number of contiguous base-paired residues that can occur within a candidate PCR primer. The function allows user-directed input in order to minimize the formation of potential primer secondary structure that can interfere with PCR efficiency.
5. The “Unique N’mer Maximum Length” filter default setting is six and specifies the maximum number of 3'-end residues that meet the requirement of only occurring once within 1000 nucleotides flanking either side of the polymorphism.
6. The “A/T Test” filter specifies that at least one A or T residue will occur in the last three 3' nucleotides of the PCR primer.
7. The “Residue Thresholds” filter specifies the frequency range for each A, T, C, G nucleotide residue in the candidate PCR primer. The default setting for this filter is minimum 14% and maximum 40% nucleotide composition.
8. The “Flank Length (Maximum 1000)” setting default setting is 1000 and denotes the length of DNA flanking the polymorphism that is used to screen for suitable PCR primers.
9. The filter “Use Repeat Masker” indicates whether the results of RepeatMasker (repeatmasker.org) will be used when evaluating the DNA sequence flanking the SNP. When selected, residues that are identified as being included in a repetitive region will be masked off and will not be considered when making the PCR primer, thus generating primers that will not anneal to regions of repetitive DNA. Using this option will generally decrease the number of primers found, but will better ensure that primers do not anneal to multiple sites.
10. The filter for “PCR Product Size” determines the range of length of an acceptable amplified PCR product. The default setting for this filter is minimum 200 bp and maximum 500 bp.

3.3. Advanced Options for Pyrosequencing Primer Design

1. User-directed changes to the Pyrosequencing primer design settings are accomplished using the three interactive boxes available on the lower panel of the “Advanced Options” window.
2. The “Melting Temperature (T_m) °C” default setting is 40°C. T_m is calculated using the relationship ($T_m = 16.6 \cdot \log[\text{cation concentration}] + 41 \cdot [\text{fraction of GC}] + 81.5$, where the concentration of cation was estimated to be 0.1 M) described

by Schildkraut and Lifson (6). User-directed changes to this value instruct the application to design each sequencing primer to the indicated minimum T_m value.

3. The filter for “T+A Percentage” evaluates the design of the candidate sequencing primer for % AT content ensuring that this value falls within the specified range. The default range is minimum 30% and maximum 65%.
4. The interactive box for designating the “Distance From SNP” provides a tool for specifying the minimum number of bases away from the SNP to initiate the design of the Pyrosequencing primer. The default range is minimum 1 and maximum 30 nucleotides. The software algorithm is designed to choose the closest Pyrosequencing primer to the SNP but with the range of distance designated by the “Distance From SNP” function.

3.4. Exploring the Website

1. General information regarding warehoused genomic and genetic variant data is indicated in the masthead of the web interface. For example, the build of dbSNP and human and mouse DNA sequences used for v2 of SOP³ are build 123, 35, and 33, respectively. Updates to the SOP³ database are performed twice a year and are indicated in the masthead.
2. The “Find Gene Name” button opens a link to the search page for determining the locus symbol for either human or mouse genes as specified by the user. The “Find Gene Name” search box allows simple Boolean searches. It allows and, or, not. It uses “*” to indicate a wildcard character and quotation marks to designate a phrase. Queries are submitted using the “Submit Query” button.
3. The “Open Saved Results” button opens a link to the list of saved files available on the SOP³ web server. Selection of a file provides a tab-delimited document consisting of the locus symbol, reference sequence number, allele, heterozygosity value, chromosome location, primer sequences, and size of expected PCR product. The tab-delimited document can be saved to the user’s computer and opened in Microsoft Excel.
4. The “Print” button provides a link to the user’s print command for use in obtaining a hardcopy of the results.
5. The “Upload” button opens a “Text Box,” “Browse” button, “Submit” button, and “Cancel” button for uploading to the web server a text file containing a batch of locus symbols or reference sequence numbers from a file located on the user’s computer. Selection of the “Browse” button prompts the user to indicate the location of a carriage return delimited text file. Selection of the “Submit” button uploads the query batch to “Search By SNP ID Or Locus Name,” i.e., the application’s main entry box. The application is initiated by selecting the “Search” button. Selection of the “Cancel” button removes the upload feature from the web interface and allows the user to query genomic SNPs using the basic functions available on the website.
6. The “View Validated Primers” button opens a link to the primer trios that have been made available for general use. They are listed in a tabulated format and include reference sequence, locus, forward PCR primer, reverse PCR primer, Pyrosequencing primer, and PCR product length.

Primer Design Software

Uncorrected Proof Copy

37

3.5. Online User Guide

1. The “Guide Me” button opens a link to the online user guide for the SOP³ application. The user guide is updated along with changes to the application and the warehoused database (see Note 5). Explanations of the choices available when using the application are indicated in alphabetical order.
2. The “Info” buttons open information links for selected functions available on the web interface. For example, selection of the “Info” button next to the “Limit By Function Type” heading opens a new browser window to the online user guide describing the use of this filter when selecting SNPs for genetic analysis.

4. Notes

1. Software applications for primer design are available from several sources. Commonly used web-based applications for designing PCR primers are available at the Primer3 (<http://www.primer3.org>) and IDT Corporation (<http://www.idtdna.com>) websites (1). Both applications generate oligonucleotide sequences for locus-specific PCR amplification. They are limited, however, in that they do not provide a sequencing primer for Pyrosequencing. Another application, specific for Pyrosequencing, is Assay Design Software available commercially from Biotage, LLC. This application provides access to a primer design algorithm for locus-specific PCR and SNP-specific Pyrosequencing. The application, however, requires user input of each SNP and DNA flanking sequence. The Biotage Assay Design Software can be operated using a batch mode once the sequences are arranged in a text file on the user’s computer. These applications and the SOP³ software provide complimentary solutions for selecting robust primers for use during pyrosequencing-based typing of genetic variants.
2. Addition of a unique nucleotide motif to the 5'-end of the forward PCR primer occurs in order to avoid formation of secondary structure in the biotinylated template strand, which can lead to competing sequencing signal owing to self-priming during Pyrosequencing (7–9). The nucleotide motif is chosen from a list of all possible nucleotide combinations that do not occur within the DNA sequence flanking the SNP.
3. Validating PCR primers designed by the computer application should be performed by PCR amplification followed by analysis of the product with agarose gel electrophoresis. Selection of primers assumes a standard PCR condition using an annealing temperature of 60°C. It is recommended that, when possible, PCR product yield be examined at 1 and 2 mM MgCl₂ and over an annealing temperature range from 54 to 65°C using a gradient thermal cycler instrument. PCR primers are considered validated if they result in a single amplified DNA product of the expected size as visualized by agarose gel electrophoresis.
4. Validating Pyrosequencing primers is accomplished by performing the Pyrosequencing reaction using a control DNA of known quality and combined with a set of negative control Pyrosequencing reactions. The negative control reactions are designed to allow troubleshooting of the sequencing reaction by analyzing the level of background signal associated with the sequencing primer, biotinylated reverse PCR primer, and possible alternative PCR products. Recom-

mended negative control reactions are as follows: (1) PCR product without the addition of Pyrosequencing primer; (2) PCR negative control reaction with Pyrosequencing primer; (3) PCR negative control reaction without Pyrosequencing primer; (4) Biotinylated reverse PCR primer alone; (5) Pyrosequencing primer alone; (6) Biotinylated PCR primer with Pyrosequencing primer. Failure to positively genotype samples using SOP³ designed primers for PCR and Pyrosequencing can often be the result of background signal associated with the negative control reactions. Isolation of the background signal can be helpful in redesigning assays for selection of new primer trio sets.

5. Contact information for web server administration. The SOP³ application is maintained by the Division of Immunogenetics at the Children's Hospital of Pittsburgh. Inquiries concerning customized searches of the database or reports of errors in the application should be addressed to Steven Ringquist (email: smr73@pitt.edu).

Acknowledgments

This work was supported by grants from the NIH-NLM, U19-AI056374-01 Autoimmunity Centers of Excellence (SR and MT), RO1DK24021(MT) from the National Institutes of Health, and ERHS no. 00021010 (SR and MT) from the Department of Defense. PVB was supported partially by the NSF grant MCB0316255.

References

1. Rozen, S. and Skaletsky, H. (2000) Primer3 on the WWW for general users and for biologist programmers. In: *Bioinformatics Methods and Protocols*, (Krawetz, S. and Misener S., eds.), Humana Press, Totowa, NJ, pp. 365–386.
2. Varotto, C., Richly, E., Salamini, F., and Leister, D. (2001) GST-PRIME: a genome-wide primer design software for the generation of gene sequence tags. *Nucl. Acids Res.* **29**, 4373–4377.
3. Emrich, S. J., Lowe, M., and Delcher, A. L. (2003) PROBEmer: a web-based software tool for selection optimal DNA oligos. *Nucl. Acids Res.* **31**, 3746–3750.
4. Stein, L. D. (2003) Integrating biological databases. *Nat. Rev. Genet.* **4**, 337–345.
5. Ringquist, S., Pecoraro, C., Gilchrist, M. S., et al. (2005) SOP³v2: web-based selection of oligonucleotide primer trios for genotyping of human and mouse polymorphisms. *Nucl. Acids Res.* **33**, W548–W552.
6. Schildkraut, C. and Lifson, S. (1965) Dependence of the melting temperature of DNA on salt concentration. *Biopolymers* **3**, 195–208.
7. Ronaghi, M., Pettersson, B., Uhlen, M., and Nyren, P. (1998) PCR-introduced loop structure as primer in DNA sequencing. *Biotechniques* **25**, 876–878.
8. Ringquist, S., Alexander, A. M., Rudert, W. A., Styche, A., and Trucco, M. (2002) Pyrosequence based typing of alleles of the HLA-DQB1 gene. *Biotechniques* **33**, 166–175.
9. Utting, M. J., Hampe, J., Platzer, M., and Huse, K. (2004) Locking of 3' ends of single-stranded DNA templates for improved Pyrosequencing performance. *BioTechniques* **37**, 66–73.

Review Article

Navigating pathways affecting type 1 diabetic kidney disease

Pasquali L, Trucco M, Ringquist S. Navigating pathways affecting type 1 diabetic kidney disease.
Pediatric Diabetes 2007; 8: 307–322.

Lorenzo Pasquali^{a,b},
Massimo Trucco^a and
Steven Ringquist^a

^aDivision of Immunogenetics,
Department of Pediatrics, Rangos
Research Center, Children's Hospital of
Pittsburgh, University of Pittsburgh
School of Medicine, Pittsburgh, PA, USA;
and ^bDepartment of Pediatrics, Institute
G Gaslini, University of Genoa, Genoa,
Italy

Key words: diabetes – genetics –
insulin – nephropathy – renal disease

Corresponding author:
Massimo Trucco, MD
Division of Immunogenetics
Department of Pediatrics
Rangos Research Center, Children's
Hospital of Pittsburgh
University of Pittsburgh School of
Medicine
3460 Fifth Avenue
Pittsburgh, PA 15213
USA.
Tel: (412) 692-6570;
fax: (412) 692-5809;
e-mail: mnt@pitt.edu

Submitted 4 April 2007. Accepted for
publication 10 May 2007

Complications of type 1 diabetes (T1D), even with reduction in risk as a result of better glycemic control, are still the major concern for pediatricians dealing with young patients who during their lifetime will eventually have to face impaired vision, reduced peripheral sensitivity, and kidney disease. T1D is associated with increased risk of nephropathy, a clinical syndrome usually accompanied by other diabetic-related complications such as retinopathy and neuropathy. Blood pressure elevation, cerebrovascular disease and high risk of cardiovascular morbidity and mortality accompany the renal symptoms, completing the picture of the syndrome (1). An estimated 20–40% of T1D patients will develop diabetic nephropathy (DN), clinically first evidenced by microalbuminuria, during their lifetime. If untreated, nearly all T1D

patients experiencing microalbuminuria will progress to overt nephropathy, evidenced by macroalbuminuria, followed by declining kidney function, and culminating in end-stage renal disease (ESRD) (2, 3). In addition to frequent morbidity linked to treating complications of the kidney (e.g., dialysis and kidney transplantation), patients experience a high rate of mortality, with a 5-yr survival rate of 21% once ESRD has developed. An estimated 45% of new patients requiring dialysis and kidney transplant are diabetic (T1D and T2D), and diabetes is the most common and rapidly increasing cause of ESRD in the US and European populations.

The prevalence and course of DN are similar in T1D and T2D patients when matched for duration of the disease (4). T2D incidence is increasing in children

and has become a major concern for pediatricians. DN follows an established natural history. The cardinal clinical feature of the syndrome is the progressive increase in urine protein excretion rate (2). The clinical course starting with microalbuminuria through proteinuria and azotemia culminates with ESRD. Before the onset of overt nephropathy, a prolonged period of clinical silence hides various changes in renal function such as hyperfiltration, hyperinfusion, and increasing capillary permeability to macromolecules.

A progressive rise in arterial blood pressure and albuminuria accompanies glomerular filtration rate (GFR) decline. T1D patients predominantly develop diastolic hypertension, whereas T2D patients typically manifest systolic hypertension (1). Microalbuminuria remains the best predictor of DN in both T1D and T2D patients (5). Risk factors correlated with disease progression are poor glycemic control, hypertension, dyslipidemia, elevated serum cholesterol, and smoking (6–8). ESRD is the major cause of mortality in T1D patients and is the dominant indicator of fatality as a result of cardiovascular disease (9, 10).

Changes in kidney structure described in diabetic patients (T1D and T2D) include nodular glomerular sclerosis (Kimmelstiel–Wilson nodular disease) (11) and a diffuse, generalized process of mesangial expansion (diffuse diabetic glomerulosclerosis). In addition, ultrastructural changes such as thickening of the tubular and the glomerular basement membrane (GBM), arteriolar hyalinosis (afferent and efferent) and increase of mesangial matrix component have been observed in both T1D and T2D. Changes in the GBM and the mesangium already can be detected after 2 yr of diabetes during a period of clinical silence (12). However, in some T2D patients, a more heterogeneous renal pathology has been described (13, 14). The latter includes superimposed changes observed in T2DM such as chronic vascular (arteriosclerotic type) and tubulointerstitial lesions or glomerular changes unrelated to diabetes such as proliferative glomerulonephritis or membranous nephropathy (15). The atypical pattern in renal pathology described for T2D may underline the interplay of different factors acting as promoters of progression in the disease other than hyperglycemia.

Genetic risk of DN and ESRD

It is widely accepted that poorly controlled blood glucose while closely correlated with T1DN is insufficient to fully account for the incidence of kidney disease in this population. Approximately half of the patients with poor glycemic control do not develop nephropathy (16–18). Epidemiologic study of the disease has provided evidence supporting the hypothesis that there is a genetic predisposition. Among T1D patients who have healthy kidney

function 30 yr after onset of diabetes, the incidence of T1DN decreases, even among individuals experiencing retinopathy. New cases of T1DN are few among individuals with long-lasting T1D (3, 19, 20). Studies of siblings concordant for T1D have demonstrated familial clustering of DN. The increased familial incidence of T1DN allowed the estimation of the genetic risk ratio for a sibling ranging between roughly twofold for T1DN and threefold for T1D–ESRD (21–24).

T1DN is a complex genetic disease indicating that synergy among several genes, with varying individual effects, are contributing to the disease. Models of genetic susceptibility to T1DN are based primarily on the analysis of Rogus et al. (25) who used the data reported by Quinn et al. (23) to simulate the incidence of T1DN among siblings. Their analysis modeled the occurrence of T1DN assuming co-occurrence of 71.5% when the index case exhibited T1DN and 25.4% when the index case presented T1D but with normal kidney function. Comparison of these observations, when overlaid onto a genetic model of an autosomal dominant gene with 20% disease allele frequency and 100% penetrance, implied a 36% lifetime risk of developing nephropathy in the individuals with T1D. Risks of 66.2 and 19.0% were predicted for T1D siblings of the index cases with and without T1DN, respectively. In contrast, an autosomal recessive model assuming 60% disease allele frequency in the Caucasian population also accounted for the observed lifetime risk of T1DN and similar sibling risks of 64.0 and 23.3% for an index case with siblings who are T1DN or T1D, respectively.

Genome-wide mapping aimed at understanding the basis for inherited risk of diseases coincident with T1DN (i.e., T1D and hypertension) have identified genetic elements consistent with their etiology (Table 1). For example, T1D has been strongly linked to inheritance of histocompatibility leukocyte antigen (HLA) class II DRB1 and DQB1 loci expressing a non-aspartate residue at amino acid 57 (26, 27). An estimated 95% of T1D patients have inherited at least one copy of the DRB1*0301, DQB1*0201 or the DRB1*04, DQB1*0302 haplotype (28). Between 30 and 40% of T1D patients are heterozygous for the combined haplotype despite the expected frequency of 2% in their respective populations (29–31). However, HLA is estimated to account for only 40% of the genetic risk of developing T1D (32–34). Genetic analyses of affected individuals have identified additional T1D susceptibility loci, reproducibly implicating chromosomal regions 11p15.5 (insulin-dependent diabetes mellitus [IDDM]2, INS), 2q33 (IDDM12, CTLA4 region), and 1p13 (PTPN22) (34–36).

Comparison of biopsy tissues from the kidneys of T1DN patients supports the hypothesis that familial factors affect severity of the glomerular lesion. In fact

Table 1. Confirmed genetic elements influencing susceptibility to type 1 diabetes

Locus symbol	IDDM region	Cytogenetic band	Odds ratio	Sibling risk ratio	Description
HLA-DQB1	IDDM1	6p21.3	95	2.5–3.6	HLA class II locus DQB1 accounts for greater than 40% of the relative genetic risk associated with T1D
INS	IDDM2	11p15.5	2.7	1.29	Association between a VNTR marker located immediately 5' of the insulin gene locus
CTLA4	IDDM12	2q33	1.2	1.01	The CTLA4 locus along with ICOS and CD28 are each strong candidates for IDDM12-associated risk
PTPN22	–	1p13	1.8	1.23	The PTPN22 locus encodes a tyrosine phosphatase and is linked with an increased risk for T1D as well as other autoimmune diseases, e.g., rheumatoid arthritis, systemic lupus erythematosus, and thyroiditis

HLA, histocompatibility leukocyte antigen; ICOS, inducible t-cell costimulator; IDDM, insulin dependent diabetes mellitus; INS, insulin; T1D, type 1 diabetes; VNTR, variable number of tandem repeat. Data are summarized from genetic linkage analysis described by Onengut-Gumuscu and Concannon (36) and Motzo et al. (147).

significant similarities between glomerular lesions were identified even when sibling T1D patients were discordant for glycemic control (37). The correlation in severity of glomerular lesions among T1D siblings independent of hemoglobin A1C (HbA1C) levels is consistent with an underlying genetic predisposition. Development of lesions in normal kidneys transplanted into diabetic patients has been described in a long-term study of recipients 6–14 yr after transplantation. Wide variation in the rate of development of lesions in different kidneys was observed independently from the history of blood glucose levels. This suggests that in addition to glycemic control *per se* risk factors intrinsic to the kidney itself are present (38, 39).

In addition to T1D, hypertension is an inheritable risk factor linked to development of kidney disease,

indicating that the genetics of T1DN and essential hypertension may be linked (Tables 2 and 3). By controlling blood volume, the kidney is responsible for long-term blood pressure control. Impaired kidney function is a principal component underlying the physiology of essential hypertension (40, 41). Family-based studies have reported an increased incidence of hypertension, 30–40% higher in patients who develop T1DN (42, 43), whereas patients with uncomplicated T1D exhibit relatively lower blood pressures (41). Parents of T1DN patients frequently exhibit increased blood pressure when compared with parents of unaffected T1D patients, suggesting a familial basis linking hypertension with impaired kidney function (43). Studies designed to deconstruct the role of genetics on hypertension have indicated that different

Table 2. Genes linked to Mendelian hypertensive disorders

Locus symbol(s)	Mendelian disorder	Physiological role	Description
HSB11B1	Apparent mineralocorticoid excess	Salt–water homeostasis	11-beta-hydroxysteroid dehydrogenase, type I (autosomal recessive trait)
CYP11B1, CYP11B2	Glucocorticoid-remediable aldosteronism	Salt–water homeostasis	Cytochrome P450, subfamily XIB, polypeptide 1 and cytochrome P450, subfamily XIB, polypeptide 2 (autosomal dominant trait)
SCNN1B, SCNN1G	Liddle syndrome	Salt–water homeostasis	Sodium channel, nonvoltage-gated 1, beta subunit and sodium channel, nonvoltage-gated 1, gamma subunit (autosomal dominant trait)
NR3C2	Mutations in mineralocorticoid receptor	Salt–water homeostasis	Nuclear receptor subfamily 3, group C, member 2 (autosomal dominant trait)
WNK1, WNK4	Pseudohypoaldosteronism type II	Salt–water homeostasis	Protein kinase, lysine-deficient 1 and protein kinase, lysine-deficient 4 (autosomal dominant trait)

Data are summarized from Mullins et al. (45), Lifton et al. (119), and Cowley (148).

Table 3. Candidate loci influencing susceptibility to essential hypertension

Locus symbol	Cytogenetic band	Physiological role	Description
Candidate genes located on chromosome 1q			
AGT	1q42–q43	RAS	Angiotensin I
AVPR1B	1q32	Salt–water homeostasis	Arginine vasopressin receptor 1B
HSD11B1	1q32–q41	Steroid metabolism	11-beta-hydroxysteroid dehydrogenase, type I
NPR1	1q21–q22	Salt–water homeostasis	Natriuretic peptide A type receptor
REN	1q32	RAS	Renin
Candidate genes located on chromosome 3q			
AGTR1	3q21–q25	RAS	Angiotensin II receptor, type 1
CLCN2	3q27–q28	Salt–water homeostasis	Chloride channel 2
DRD3	3q13.3	adrenergic system	Dopamine receptor D3
ECE2	3q28–q29	Endothelin related	Endothelin-converting enzyme 2
KNG1	3q27	Kallikrein–Kinin system	Kininogen 1
MME	3q25.1–q25.2	Salt–water homeostasis	Membrane metallo-endopeptidase (neutral endopeptidase, enkephalinase)

RAS, renin–angiotensin system. Data are summarized from DeWan et al. (44), Hamet et al. (149), and Jeunemaitre et al. (150).

genes may contribute to increased incidence of hypertension in different ethnic groups (44, 45). Genome-wide scans have implicated different regions of chromosome 3 in Caucasian and African-American populations as well as genetic markers on chromosome 1 and 6 among Caucasians (43, 45, 46) (Table 3). Improved understanding of the inherited basis of T1DN may lead to deeper understanding of the molecular mechanisms underlying the disease, leading to improved therapeutic intervention as well as improved understanding of why the majority of T1D patients maintain normal kidney function while a substantial minority go on to exhibit T1DN.

A number of genome-wide linkage scans have been performed in order to evaluate the genetics underlying impaired kidney phenotype. The first genome scans were performed in a Pima Indian cohort with T2D and proteinuria. Genetic analysis of sib pairs identified significant linkage on chromosome 7. Additional loci were identified on chromosomes 3q and 9. Genome scans performed in an African-American cohort affected by T2D and ESRD revealed evidence for susceptibility on chromosomes 3q, 7p, and 18q (Table 4). However, as these studies were performed using DNA obtained from affected sib pairs concordant for both T2D and proteinuria or ESRD, positive signals may have cosegregated with T2D or nephropathy. Following nephropathy only, a study performed using a cohort of 18 large Turkish families with T2D and proteinuria showed strong linkage with chromosome 18q. A recent genome-wide association study has been performed genotyping greater than 80 000 single nucleotide polymorphisms (SNPs) using a cohort of T2DN (case) and T2D (control) patients, identifying genetic association with the engulfment and cell motility 1 gene (*ELMO1*) and a *p* value of less than 8×10^{-6} on chromosome 7p (47). Osterholm et al. (48) have recently performed a genome-wide

linkage analysis using T1D sib pairs discordant for nephropathy. The study identified five genomic regions with possible linkage to T1DN, implicating chromosomes 3q, 4p, 9p, 16q, and 22p. The overlap between chromosome 3q identified from this study and those performed with T2DN cohorts suggests a possible area of focus for future genetic analyses.

The complex etiology of DN reflects the intricate nature of the disease, requiring a combination of alleles of several genes in addition to exposure to environmental factors. The role of shared environmental risk factors has been extensively evaluated, and while their exact nature is unclear, it is likely that similar lifestyles such as eating and smoking habits are more prevalent among siblings compared with unrelated T1D patients. Glycemic control has been proposed to be a risk factor for nephropathy (49). Studies on diabetic twins have indicated that HbA1C levels are at least partially genetically determined, accounting for greater than 60% of the population variance of glycosylated hemoglobin (50). Individuals with good glycemic control, whether through genetics or as a result of rigorous testing and adjustment of insulin doses to control blood glucose levels, are able to reduce their risk of developing diabetic complications, including T1DN as was shown in the Diabetes Control and Complications Trial (DCCT), as explained later in this text.

Risk factors associated with the progression of T1DN

What factors contribute to onset of nephropathy as a complication in T1D patients? Early age of T1D onset may be linked to the increased risk of T1DN (51), but this conclusion has been controversial (52, 53). The observation that the risk for T1DN reaches a peak incidence at ages 25–29 yr and occurs equally in both males and females may indicate that the triggering

Table 4. Candidate loci influencing susceptibility to diabetic nephropathy

Locus symbol	Cytogenetic band	Physiological role	Description
Candidate genes located on chromosome 3q			
NCK1	3q21	Growth factor/cytokine/signal transduction	NCK adaptor protein 1
RAB7	3q21.3	GTP-binding protein related	RAB7, member RAS oncogene family
SLC2A2	3q26.1–q26.3	Carbohydrate transport/metabolism	GLUT2 (solute carrier family 2 (facilitated glucose transporter), member 2)
SUCNR1	3q24–q25.1	Metabolism	Succinate receptor 1
Candidate genes located on chromosome 4p			
ADD1	4p16.3	Cytoskeletal component	Adducin 1
Candidate genes located on chromosome 7p			
ELMO1	7p14.2	Apoptosis related	Engulfment and cell motility 1
IGFBP1	7p14–p12	Growth factor/cytokine/signal transduction	Insulin-like growth factor-binding protein 1
IL6	7p21	Growth factor/cytokine/signal transduction	Interleukin 6
NXPH1	7p22	Cell adhesion	Neurexophilin 1
RAC1	7p22	GTP-binding protein related	Ras-related C3 botulinum toxin substrate 1 (rho family, small GTP-binding protein Rac 1)
Candidate genes located on chromosome 16q			
BCAR1	16q23.1	Cell adhesion	Breast cancer anti-estrogen resistance 1
CDH1	16q22.1	Tight junction component	Cadherin 1, type 1, E-cadherin (epithelial)
CDH3	16q22.1	Tight junction component	Cadherin 3, type 1, P-cadherin (placental)
CETP	16q21	Fatty acid/cholesterol transport/metabolism	Cholesteryl ester transfer protein, plasma
CYBA	16q24	Reactive oxygen species metabolism	Cytochrome b(-245), alpha subunit
MAPK3	16q11.2	Growth factor/cytokine/signal transduction	Mitogen-activated protein kinase 3
MMP2	16q13	Extracellular matrix component	Matrix metalloproteinase 2
Candidate genes located on chromosome 18q			
BCL2	18q21.3	Apoptosis related	B-cell CLL/lymphoma 2
DSC2	18q12.1	Cell adhesion	Desmocollin 2
SERPINB7	18q21.33	Extracellular matrix component	Serpin peptidase inhibitor, clade b(ovalbumin), member 7
SMAD7	18q21.1	Growth factor/cytokine/signal transduction	SMAD family member 7

CLL, chronic lymphocytic leukemia; GLUT, glucose transporter; RAB, RAS-associated protein; RAS, renin-angiotensin system; SMAD, homolog of mothers against decapentaplegic. Data are summarized from Shimazaki et al. (47), Osterholm et al. (48), He et al. (143), and Ewens et al. (90).

event(s) may be independent of differences in T1D onset. The triggering event may, however, be linked to puberty and the beginning of adolescence. Puberty-associated deterioration in glycemic control, hormonal changes, as well as psychosocial pressures have come under increased scrutiny for their influence in patients who fail to maintain good blood glucose control (54). Glycemic control often deteriorates during adolescence in individuals with T1D and may result from developmental changes, especially increased growth hormone secretion during puberty, as well as the transition to more autonomous lifestyle typified by adulthood. In some female patients, there is also the emergence of eating disorders and the misuse of insulin as a means to control weight gain (54, 55).

Constitutional factors

Predisposition to the development of DN can be because of genetic susceptibility as well as factors operating *in utero*. Intra-uterine malnutrition has been associated with a reduced number of nephrons (56), increasing the risk of kidney diseases and hypertension in adult life (57). Exposure to unfavorable intra-uterine environment leading to intra-uterine growth retardation (IUGR) was proposed as a risk factor for DN progression. This conclusion follows from the hypothesis that reduced nephron number observed in IUGR patients (58) may lead to reduced functional reserve in those kidneys subjected to potentially toxic agents (e.g., hyperglycemia or smoking). Rossing et al. (59)

observed an increased risk of DN in women with IUGR and T1D. This was confirmed for both sexes in a cohort of Pima Indian type 2 diabetic patients (60). In contrast, the conclusion failed to be reproduced according to observations reported by Eshoj et al. (61) and in a recent study on Finnish T1D patients (62). Contradictory results from different studies have not yet clarified if there is a correlation between IUGR and DN; however, individuals with essential hypertension were shown to have a markedly reduced number of nephrons in addition to an inverse correlation between birth weight and adult systolic blood pressure (63). It is possible that intra-uterine factors may have a direct effect on DN progression later in life although the effect may be indirect, e.g., via hypertension.

Hyperglycemia

Rates of decline in GFR have been linked in T1D patients to increased levels of blood glucose and occur at a rate of roughly 10–14 ml/min/yr in patients with persistent albuminuria (64). This observation has been confirmed in several independent studies, indicating that HbA1C levels are predictive of the risk of subsequent onset of ESRD. In the absence of therapeutic intervention, the majority of patients with sustained microalbuminuria progress to overt nephropathy over a period of 10–15 yr (65–69).

Control of blood glucose levels is critical to the development of the characteristic complications of diabetes, including DN, as has been demonstrated by the outcome of the DCCT. The DCCT was carried out from 1983 to 1993 and assessed the relative effects of intensive and conventional insulin therapy treatments on preventing development and progression of complications (16). Enrolling greater than 1400 adult patients with T1D, the DCCT showed that HbA1C levels could be reduced from 9.1% to 7.2% with a corresponding reduction in progression of renal complications (16). At the end of the study, the incidence of microalbuminuria was reduced by 34% in a cohort in which no evidence of retinopathy or nephropathy was present at baseline. In a second cohort, mild and early complications were present and the DCCT reported a 43% reduction in the incidence of microalbuminuria. The success of intensive insulin therapy for the treatment of diabetes was confirmed by a follow-up study showing persistent long-term reduction in the incidence of T1DN (70).

Compliance with the intensive insulin therapy regime 2 yr after conclusion of the study indicated that 95% of the intensive therapy group reported following intensive therapy regime and 70% of the conventional treatment group now reported following intensive therapy regime. This means that 30% of the conventional treatment patients failed to adopt intensive therapy despite knowledge of the results.

Comparison of HbA1C levels after 2 yr post-DCCT indicated that the intensive therapy group experienced HbA1C levels of 7.2% during DCCT and 7.9% 2 yr after conclusion of the trial. Of these patients, 46% continued to monitor blood glucose four or more times a day. Patients from the conventional treatment group who converted to intensive therapy demonstrated HbA1C levels of 8.1% post-DCCT. Of these patients, 36% reported monitoring blood glucose four or more times a day. The benefits of intensive therapy 5 yr post-DCCT were disappointing in that both cohorts reported average HbA1C levels exceeding 8%. One conclusion of the study is that in the absence of a strong research motivation and monthly visits with a health care provider, the degree of intensive treatment shown in the DCCT was not maintained. Moreover, the availability of health insurance corresponded to success as measured by reduction of HbA1C levels. Patients receiving intensive therapy 5 yr post-DCCT without health insurance maintained an average HbA1C of 8.6%, while patients with health insurance maintained an average HbA1C of 8.1%.

Unfortunately, patients participating in intensive insulin therapy treatments for diabetes are more likely to experience severe adverse effects resulting from frequent injections of insulin. Severe hypoglycemic events occurred nearly threefold more often in patients enrolled in the intensive therapy regime and were characterized as requiring assistance of another person. This precluded the enrollment of children into the study. Severe hypoglycemic episodes occurred in 25% of the total number of reported cases of hypoglycemia and were manifested by coma or convulsions. Of the adult patients receiving intensive insulin therapy, 22% experienced at least five episodes of severe hypoglycemia vs. 4% of conventionally treated subjects. Life-threatening complications of hypoglycemia are not uncommon, limiting the availability of intensive insulin therapy as a means to prevent onset of DN.

Hypertension

High blood pressure is prevalent in families in which T1DN is present compared with T1D families without DN (43). Hypertension-associated microalbuminuria is a predictive indicator of overt nephropathy in T1D patients (71). While normalization of blood glucose levels has been linked to healing of microvascular lesions in the kidney, treatment of hypertension has resulted in improved renal outcome by preventing glomerular damage. Clinical studies have indicated a decline in the incidence of nephropathy in T1D patients (72–74). However, many T1D subjects only attain HbA1C levels of 8.5% well in excess of the recommended levels of blood glucose. Regression of microalbuminuria has been observed upon blood pressure control, and remission of overt nephropathy

has been observed in T1D patients treated for hypertension (5, 75).

There is an exponential impact from hypertension on increasing risk for renal disease (76). Maintaining a sustained reduction in blood pressure is the single most influential intervention for reducing progression of nephropathy in T1D as well as T2D patients. Studies of initially normotensive T2D subjects without renal disease who subsequently developed and were treated for hypertension indicated that patients with blood pressure less than 130/80 mm Hg rarely developed nephropathy. In contrast, diabetic patients with blood pressure in the range of 130/80 to 140/90 mm Hg exhibit a significant decline in GFR coincident with 30% of patients progressing to microalbuminuria within 12–15 yr (77). Improvements in blood pressure treatment and glycemic control along with decreased incidence of smoking lead to improved outcomes for T1D patients.

The kidney structures implicated in the pathogenesis of the disease

The glomerular filtration barrier in T1DN

A thorough understanding of the molecular properties of the glomerular filtration barrier (GFB) is crucial to comprehension of the pathology of proteinuria encountered in T1DN. Structurally, the GFB is composed of three layers that mediate the process of ultrafiltration of blood flowing through anastomosing capillary loops leading to the formation of the primary urine in the Bowman's capsule and finally into the tubular system (Fig. 1). The first layer is a highly fenestrated vascular endothelium that covers the wall of the capillaries. It has been suggested that a protein

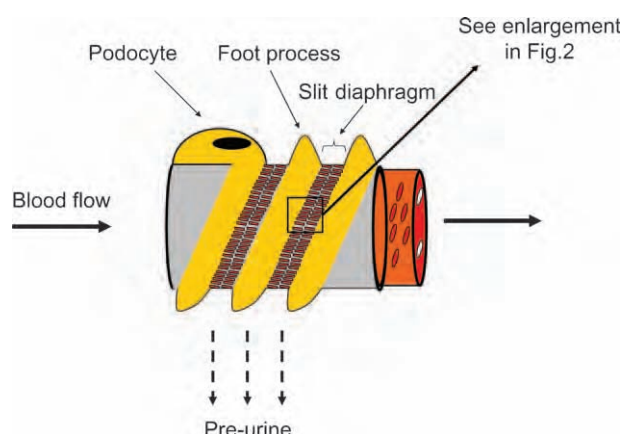


Fig. 1. The GFB. Ultrafiltration occurs when the blood flows through the glomerular capillaries. The GFB comprises the fenestrated endothelial cell layer (red) and the glomerular basement membrane (gray). The podocytes (yellow) loop to the capillaries with their pedicules or foot processes. A protein complex forming the slit diaphragm covers the space between the podocytes processes. GFB, glomerular filtration barrier.

filtration role of the endothelium may be critical to proper kidney function because of the barrier properties of glycocalyx coating of the endothelial cells and filling in of the intracellular space (78). The second layer is the GBM, forming the boundary between blood and urine primarily composed of an interconnecting network of type IV collagen (alpha-1 and -2 during fetal development and alpha-3, -4, and -5 in the adult) and laminin-1 (consisting of alpha-1/beta-1/gamma-1 chains in the fetus) and laminin-11 (consisting of alpha-5/beta-2/gamma-1 chains in the adult). The third layer is composed of highly specialized cells, the podocytes whose cytoplasm extends into interdigitating pedicles or foot processes. The area between the podocyte foot processes is the slit diaphragm composed of a number of cell surface proteins including nephrin, neph 1, and P-cadherin. Understanding GFB function has centered on the role of the slit diaphragm formed by these proteins, serving as the ultimate layer ensuring that large macromolecules such as serum albumin and gamma globulin remain in the bloodstream while allowing small molecules such as water, glucose, and ionic salts to pass through (79).

The genesis of albuminuria is consistent with generalized vascular dysfunction, alterations in extracellular matrix components, and impaired basement membrane organization resulting from hyperglycemia (80). Increasing consideration has been given to the GFB and its central role in the filtration of plasma proteins. High-molecular-weight tracer molecules have been used to investigate the molecular sieving properties of the GFB. Ferritin has an estimated Stokes radius (SR) of 61 Å and when injected into healthy rats failed to pass through the GBM (81). In puromycin aminonucleoside-induced nephrosis models, which induce glomerular injury evidenced by flattening of podocyte foot processes, ferritin is only partially retained (82). Smaller proteins have also been used to examine the selective permeability of the GBM. For example, horseradish peroxidase (SR = 30 Å) has been observed to pass through both the GBM and slit diaphragm, while myeloperoxidase (SR = 36 Å) and catalase (SR = 52 Å) are GBM permeable but are captured by the slit diaphragm prior to entering the urine, consistent with the hypothesis that for large proteins, GBM selectivity is the primary barrier separating the blood and urine space (79).

Genetic polymorphisms of extracellular matrix proteins as well as enzymes involved in their metabolism have been suggested as possible explanations for the variation in susceptibility to kidney disease observed in T1D patients (80, 83). Type IV collagens are a principal component of basement membranes (84). In the adult glomerulus, collagens encoded by the COL4A3, COL4A4, and COL4A5 loci replace the fetal collagens COL4A1 and COL4A2 (85). Absence of the adult forms of collagen has been associated with proteinuria

because of Alport syndrome, a genetically determined disease characterized by heavy proteinuria. In these patients, the pathology is sustained by an abnormal basement membrane because of defects and/or absence of adult type IV collagens (86, 87).

SNPs associated with fetal expressed collagen COL4A1 have also been linked with susceptibility to nephropathy. GBM abnormalities characterized by irregularities in the parietal epithelium lining Bowman's capsule have been observed in heterozygous mice containing a single nucleotide mutation in COL4A1, resulting in a Gly627Trp amino acid substitution in exon 26 (83) as well as mice harboring a G to A polymorphism in a COL4A1-encoded splice site resulting in loss of exon 40 from the mRNA transcript (88). Loss of COL4A1 exon 40 has been linked to nearly 100% prevalence of albuminuria in animals by the time they reach 2 yr of age (89). In humans, mutations affecting GBM structure have been linked with hereditary risk of nephropathy (89, 90). While deletion of COL4A1 is lethal, mice die by embryonic day 9.5 (83), and heterozygous individuals may survive to adulthood carrying increased risk of microvascular complications as a result of altered basement membrane structure occurring during early development and organogenesis.

The third layer and ultimate barrier for plasma protein ultrafiltration is the slit diaphragm of the podocytes

Podocytes, highly specialized epithelial cells, lie on the outer surface of GBM to which they affix by cell surface adhesion proteins such as the alpha-3 beta-1

integrin and dystroglycan (91, 92). The podocyte foot process (polypoid extraflections) cover the outer layer of the GBM. The intrapodocyte connections are typified by narrow spaces (30–40 nm) covered by a porous membrane known as the slit diaphragm (Fig. 2). The slit-diaphragm protein complex is an adherens-type junction and presents a dense zipper-like structure composed of the extracellular components of nephrin, neph 1, P-cadherin and FAT tumor suppressor homolog 1 (FAT 1) (93, 94). Podocin and CD2-associated protein (CD2AP) are localized in the intercellular compartment and interact with the extracellular components of the slit diaphragm anchoring the cytoplasm domain of nephrin to cholesterol-rich regions of the plasma membrane and to the actin filament structure of the podocyte cytoskeleton (79, 95). The protein zona occludens-1 is located at the neph 1 insertion site of the slit diaphragm interacting with the cytoskeleton as well as other components of the cell–cell junction. Recent findings have demonstrated the role of the slit-diaphragm adapter protein NCK (96). NCK binds the cytoplasmatic tail of nephrin and following a phosphorylation signal leads to cytoskeletal reorganization. This finding provides evidence that the central role of the cytoplasmatic region of the nephrin/NCK complex is to act in a signaling transduction capacity, transmitting antiapoptotic signals (via Akt, a serine–threonine kinase) (96), promoting remodeling of the cytoskeletal structure that drive formation of the actin-based foot processes of the podocyte.

The key role of the slit-diaphragm components in maintaining correct permeability function of the GFB is underscored by the results obtained from animal

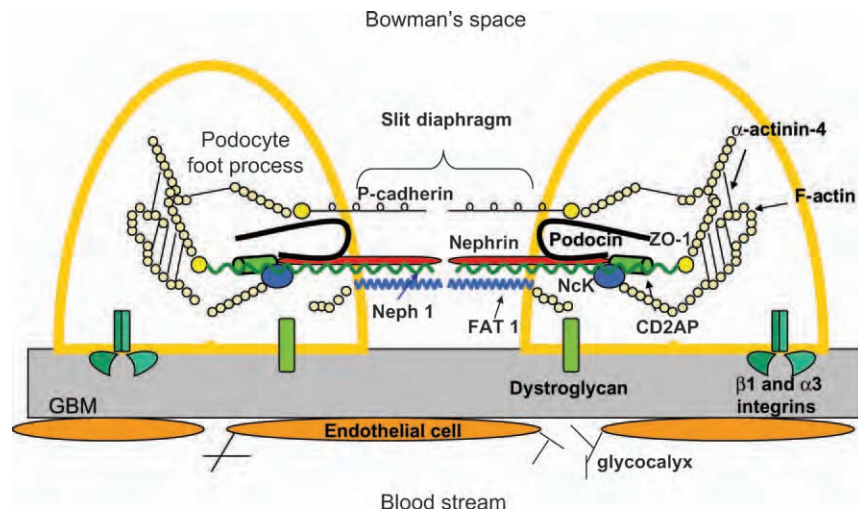


Fig. 2. Schematic view of the molecular anatomy of two podocyte foot processes (yellow) with the interposed slit-diaphragm complex. Interference with proteins that structurally sustain the slit diaphragm (e.g., CD2AP, nephrin, and podocin) can cause foot process effacement resulting in proteinuria. Filtrate from the bloodstream passes through the glycocalyx-filled fenestrae located between endothelial cells lining the GBM. The filtrate then flows through the GBM as well as the slit diaphragm and into the Bowman's space. The image is modified and adapted from Vincenti and Ghiggeri (151) and Johnstone and Holzman (152). CD2AP, CD2-associated protein; FAT 1, FAT tumor suppressor homolog 1; GBM, glomerular basement membrane, NCK, NCK adaptor protein 1; ZO-1, zona occludens-1.

models and human findings. Mutation in genes encoding nephrin, podocin, and α -actinin proteins leads to severe hereditary forms of nephrotic syndrome in humans (97, 98). Mice lacking CD2AP (99) develop nephrotic syndrome, and mutations in CD2AP were found in two human patients with focal segmental glomerulosclerosis. NCK-deficient animals fail in the formation of podocyte foot processes (96).

Progress in elucidating podocyte biology and signaling have shown that the complex of proteins composing the slit diaphragm is critical to maintaining podocyte architecture as well as supporting the overall function of the glomerular filter of the kidney. For T1D, as well as T2D, nephropathy, there are reports of a reduced number and density of the podocytes and an increase in foot process width (100–105). Steffes et al. (102) has reported loss of podocytes occurring early in T1D, while other authors detected the loss of podocytes continuing later in disease progression (104). The loss of podocytes from the glomerular space has been correlated with increased albumin excretion.

A loss of nephrin along with the onset of microalbuminuria occurs in early stages of DN in T1D patients (106). The loss of nephrin was detected even before the appearance of microalbuminuria, suggesting that damage to the slit diaphragm may occur early in disease pathogenesis. Other studies confirmed reduction of nephrin and other slit-diaphragm proteins in the glomeruli of patients with both T1D and T2D nephropathies (107–109). Koop et al. (108) reported on DN in six patients, observing statistically significant decrease in protein level of nephrin along with reduced expression of podocin and podocalyxin. Nephrin mRNA expression inversely correlated with increasing severity of proteinuria (108).

The tubular system

T1DN is often considered a glomerular disease; however, progression to end-stage organ failure also correlates with increased level of renal tubulointerstitial fibrosis (110, 111). Changes occurring in the renal tubular system have been implicated as a primary contributor to the process of renal cortex fibrosis observed in DN (112). Increased fibrosis correlates with macroalbuminuria, nephron tubular cell injury, induction of apoptosis, and hypertension (110, 111, 113–117).

Renal tubular system epithelial cells and interstitial tissue undergo changes during progression of T1DN. These include tubulointerstitial alterations, tubular hypertrophy, and basement membrane alterations that precede tubulointerstitial fibrosis. Tubular cell hypertrophy is an early feature of T1DN. Exposure of proximal tubular epithelial cells to hyperglycemia

occurs as a result of glycosuria as well as from high glucose concentration present in interstitial tissue. Cellular response to elevated glucose includes increased tubular basement membrane thickening as a result of increased synthesis of type IV collagen and fibronectin as well as altered matrix protein metabolism as a result of increased expression of metalloproteinase inhibitors tissue inhibitor of metalloproteinase (TIMP)-1 and TIMP-2 (114, 115, 118). Changes to the tubulointerstitium co-occur along with changes to the glomerulus. Poor filtration of the primary urine may lead to presentation of cytotoxic compounds to the nephron tubular cells. Combining the deleterious affects of glycosuria with exposure to cytokines may stimulate cellular responses leading to organ failure.

Primary filtration of urine occurs at the slit diaphragm of the GFB (45); however, glucose and sodium ions are freely filtered. Glucose is entirely reabsorbed in the proximal tubule by a sodium–glucose cotransport system. Recovery of greater than 99% of filtered sodium ion occurs within the nephron via the action of specialized epithelial cells lining the renal tubular system proximal tubule (responsible for 50% sodium absorption), thick ascending loop of Henle (30–40% sodium absorption), distal convoluted tubule (5% sodium absorption), and the collection duct (4% sodium absorption) (Fig. 3). Sodium reuptake by the distal convoluted tubule and collection duct account of a small percentage of total salt reabsorption but are the principal sites at which net salt balance is determined (119). A widely held model for explaining the role of the kidney in blood pressure

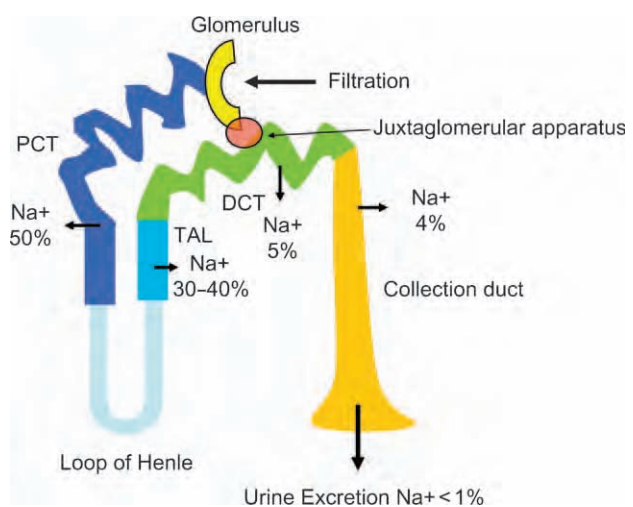


Fig. 3. A schematic view of sodium reabsorption along the nephron. Urine is processed via the PCT, TAL, and DCT. The juxtaglomerular apparatus comprises the macula densa cells, which represent specialized tubular cells at the end of the thick ascending limb, comprising cells from the extraglomerular mesangium, vascular smooth muscle cells, and renin-secreting cells in the media of the afferent glomerular arteriole. DCT, distal convoluted tubule; PCT, proximal convoluting tubule; TAL, thick ascending limb.

control is through its role balancing sodium excretion and recovery. Hypertension results from impaired blood pressure control and correlates with changes in the kidney that lead to impaired renal function, i.e., inability to maintain sodium ion homeostasis.

Increased kidney mass is an early feature of DN (120) with expansion of the proximal tubular cells accounting for most of the growth (121, 122). Along with tubular cell expansion there is increased sodium recovery. Vallon et al. (123) have suggested a model in which increased sodium recovery by the proximal convoluted tubule causes glomerular hyperfiltration, leading to nephropathy. The primary increase in proximal tubular reabsorption in early diabetes may be because of proximal tubular reabsorption through enhanced sodium–glucose cotransport. Studies on patients with T1DN have indicated increased sodium recovery occurring primarily within nephron tubular segments upstream from the macula densa in the distal convoluted tubule (124, 125) and have indicated that there is increased tubular recovery of sodium ions occurring in patients with early-stage T1D.

The juxtaglomerular apparatus comprises different structures in functional and structural link: cells of the extraglomerular mesangium, which fill the angle between the afferent and the efferent glomerular arteriole; vascular smooth muscle cells and renin-secreting cells in the media of the afferent glomerular arteriole; and the macula densa. The macula densa is an area of specialized cells lining the region of the distal convoluted tubule next to the glomerular vascular pole. These cells are sensitive to the ionic content and water volume of the fluid in the distal convoluting tubule. An increase or decrease in sodium, chloride, and potassium uptake elicits inverse changes in the single-nephron GFR by altering the vascular tone, predominantly of the afferent arteriole. The mechanism serves to establish an appropriate balance between GFR and tubular reabsorption upstream from the macula densa. As the proximal tubule grows, more of the glomerular filtrate sodium is reabsorbed and less reaches the macula densa at the end of Henle's loop causing GFR to increase through the normal physiologic actions.

The link between increased tubular sodium recovery and diabetic kidney disease is echoed in observations obtained from studies involving hyperfiltering T1D patients in which there is reported a positive correlation between GFR and sodium recovery in the proximal tubular region of the nephron (125). Examination of T1D patients have indicated that hyperfiltration by the nephron may continue even once blood glucose levels are controlled by intensive insulin therapy (126–128) and may continue to progress independent of glucose control as a result of persisting enlargement of the nephron tubular compartment.

Molecular pathways

Pathways leading to fibrogenesis

The interplay between glomerular hypertension and hyperglycemia may be linked to the pathological changes seen in T1DN. In non-diabetic individuals, glomeruli are protected from deleterious effects associated with essential hypertension by interacting autoregulatory mechanisms (129). Increased blood pressure is associated with increased preglomerular resistance thus isolating glomerular capillaries from potential damage. However, the ability to regulate glomerular blood flow is impaired when significant ablation of renal mass occurs, resulting in increased single-nephron GFR. Carmines et al. (130) demonstrated that regulatory mechanisms are damaged by hyperglycemia-induced inhibition of voltage-gated calcium channels. Endothelial cell injury as a result of hypertensive glomerular damage may be responsible for initiating glomerulosclerosis, with the process involving increased expression of transforming growth factor (TGF)-beta and extracellular matrix proteins (131). The accumulation of excess extracellular matrix within the glomerulus and the interstitium is associated, at least in part, with the profibrotic cytokine, TGF- β (132–134).

The observation that conditions characterized by a severe but relatively selective albuminuria, such as minimal change nephropathy, do not initiate interstitial fibrosis led to the study of the role of higher molecular weight ultrafiltrated proteins in DN. Ultrafiltrated growth factors, such as insulin-like growth factor 1 (IGF-1), hepatocyte growth factor (HGF), and TGF- β , may have a direct effect on the nephron tubular epithelial cells by inducing transcription of genes with profibrogenic effects, whereas other cytokines such as bone morphogenic protein 7 (BMP-7) act as inhibitors of these pathways (135) (Fig. 4). The importance of HGF/IGF-1 action is underscored by the demonstration of a direct effect of these hormones on renal hypertrophy, microalbuminuria, and glomerulosclerosis (136) and that increased excretion rate of both urinary IGF-1 and urinary HGF strongly correlate with microalbuminuria and kidney volume in T1D patients (137).

Pathophysiological mechanisms leading to sclerosis may be related to simultaneous exposure to prosclerotic cytokines in glomeruli and tubulointerstitium as well as tubulotoxicity caused by protein contents in filtrate overloading the proximal tubule's absorption ability. Proteinuria is proposed to be more than a highly reliable predictive factor having a causal role during disease progression (138). Ultrafiltrated proteins undergo endocytosis by the proximal tubular cells, resulting in a cytotoxic effect directly leading to tubular damage. The interaction of filtrated protein

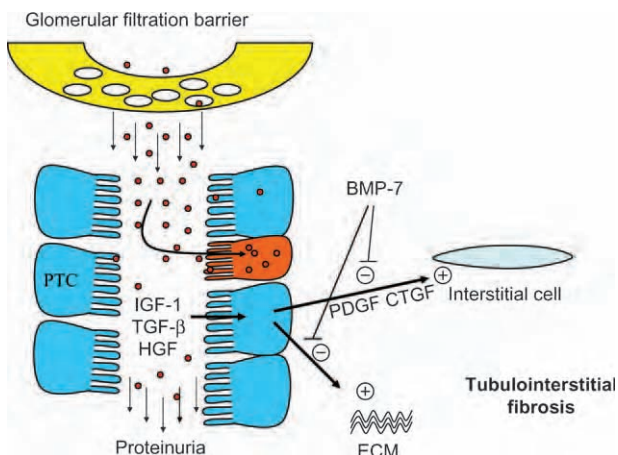


Fig. 4. Interstitial fibrogenesis. When glomerular proteinuria occurs, excess filtrated proteins undergo endocytosis by the PTC (in blue), resulting in cytotoxic effects and tubular damage (red PTC). Ultrafiltrated growth factor cytokines (IGF-1, TGF- β , and HGF) activate a number of genes, enabling PTC to directly contribute to interstitial fibrosis by producing ECM proteins. Tubular cell interaction with growth factor cytokines elicited production of other cytokine signals (PDGF and CTGF) able to induce ECM production by interstitial cells. Other signals such as BMP-7 act as inhibitors of these pathways. BMP-7, bone morphogenic protein 7; CTGF, connective tissue growth factor; ECM, extracellular matrix; HGF, hepatocyte growth factor; IGF-1, insulin-like growth factor 1; PDGF, platelet-derived growth factor; PTC, proximal tubular cells; TGF- β , tissue growth factor-beta.

with proximal tubular cells could be one of the initiating signals enabling a cascade of events leading to changes in extracellular matrix composition and eventually to interstitial fibrogenesis.

Candidate genes and their pathways

Studies of candidate genes for T1DN have focused on genes controlling the balance between extracellular matrix protein synthesis and degradation, glucose metabolism, as well as those whose products control the interaction between kidney function and blood pressure control. Genes influencing the activity of growth factors, protein kinase C activation, hormones regulating blood pressure, accumulation of advanced glycosylation end products, aldose reductase pathway flux, and altered glucose transport have each been extensively evaluated. The roles of hypertension candidate genes have also been studied, although most of the work has focused on the renin-angiotensin system (RAS).

Candidate gene studies have evaluated both functional (i.e., nonsynonymous codons) and allelic markers linked statistically for their influence on T1DN. However, this approach has as yet to convincingly identify risk factors when replicated in independent cohorts (139). The failure to replicate first-stage results from carefully controlled genetic studies possibly reflects the confounding influence of environmental

factors on statistical power to detect a true positive signal. Strategies for the selection of candidate genes are improved by consideration of linkage scans along with relevant biologic information about the implicated loci. For example, chromosome 3q has been identified in multiple linkage studies for T1DN (48, 140). This region of the genome has also been identified in studies of T2DN in Pima Indians (141) and in African-American families (142). Other chromosomal regions have also been identified by linkage analysis to T1DN, but chromosome 3q is strongly implicated in hypertension (48) and hypertension is frequently found to co-occur with T1DN. A number of candidate genes are contained within the region of chromosome 3q implicated in these studies (Tables 3 and 4). However, one of the possible candidates, the succinate receptor (SUCNR1), has been linked with carbohydrate catabolism and with control of blood pressure. He et al. (143) reported that the orphan G-protein-coupled receptor encoded by the SUCNR1 locus detected succinate, which is a metabolic intermediate produced by the tricarboxylic acid (TCA) cycle during respiration, and increased succinate levels were causal for increased blood pressure in mice. In diabetic patients, it is possible that local mismatch of energy supply and demand, altered metabolism of TCA-cycle intermediates, or injury may lead to mitochondrial dysfunction and the release of succinate into circulation. Succinate molecules activate receptors in the kidney, causing the release of renin and activation of the RAS. The RAS leads to an increase in blood pressure and altered local blood flow. In healthy individuals, this system might act to regulate local blood flow to match metabolic demands. However, in diabetic patients with impaired metabolic control, it might also result in hypertension or altered cellular function and may contribute to renin-mediated constriction of the renal artery (144).

Many other candidate genes have been examined during genetic evaluation of T1DN. For example, Ewens et al. (90) investigated 110 candidate genes by transmission/disequilibrium testing (TDT) (145) using 72 family trios of which the offspring experienced T1DN. Genes were chosen based on the results of previous studies associating various regions of the human genome to the phenotype of T1DN and have implicated proteins expressed within the GBM. Extracellular matrix proteins encoded by the loci COL4A1, LAMA4, and LAMC1 comprise important components of GBM forming the blood-urine barrier in the kidney. Genetic variants linked to different alleles of the COL4A1 locus have been studied by TDT statistical analysis supporting the hypothesis for genetic linkage of COL4A1 (p value = 0.0002) to the nephropathy phenotype along with additional linkage to the laminin-encoding loci, LAMA4 (p value, 0.016) and LAMC1 (p value, 0.026) (90).

Concluding remarks

The goal of reducing the incidence of T1D complications has been intensively investigated. T1DN is the principal etiology leading to ESRD. The molecular mechanism(s) underlying the disease involve an interplay between genes and gene-environmental exposures. Improved understanding of the disease pathogenesis will lead to better identification of those at risk and by doing so lead to improved treatment regimens.

The evidence for a dominant genetic role in determining susceptibility to kidney disease in T1D patients is primarily the result of epidemiological studies indicating that prevalence of DN increased during the first 15 yr after onset of T1D. After 20 yr duration of diabetes, the incidence of new cases of nephropathy among T1D patients plateaus and in fact may decrease (3, 19, 20). These observations have frequently been interpreted as indicating that there exists a subset of patients susceptible to develop kidney disease. Additional evidence for genetic risk has been obtained from family studies, showing the clustering of DN among T1D siblings (21–24). Siblings experiencing T1D have a significantly increased risk for DN when the T1D proband experiences the disease. Interpretation of the data generated from genetic analysis of T1DN is complicated by the possibility that signals are related to coincident diseases (e.g., hypertension) as well as environmental exposures such as smoking. In order to interpret these results, it is necessary to compare the results of genetic testing of control populations as well as replication of the results in independently recruited case cohorts.

Replication of genome-wide linkage and candidate gene studies for T1DN have been limited by lack of adequate sample size. Recruitment of large independent cohorts for T1DN genetic analysis is required to attain statistical power to detect true genetic signals. Several initiatives are ongoing to address this issue. The most recent of these studies is the genetics of kidneys in diabetes (GoKinD), which has provided a collection of DNA samples and relevant clinical information from greater than 3000 study participants (146). A genome-wide association study of the GoKinD cohort has recently been funded as part of the Genetic Association Information Network's collaborative effort to evaluate genes in complex diseases (http://www.fnih.org/GAIN/GAIN_home.shtml). The initial results of a 500 000 SNP genome-wide association scan based on the GoKinD cohort is due in the fall of 2007. Collection of additional cohorts is ongoing at a number of institutions investigating T1DN genetic risk. Careful collection practices centered on recording relevant health history of participants are essential for success. Knowledge of patient environmental exposures (e.g., history of hypertension, use of anti-hypertensive medications, and smoking) are

as essential as recording T1D history and will greatly aid in stratification of populations when comparing participants recruited at different centers.

Acknowledgements

This work was supported by grants U19-AI056374-01 Autoimmunity Centers of Excellence (S. R. and M. T.) and RO1DK24021 (M. T.) from the National Institutes of Health and ERMS #00035010 (S. R. and M. T.) from the Department of Defense.

References

1. PARVING HH. Diabetic nephropathy: prevention and treatment. *Kidney Int* 2001; 60: 2041–2055.
2. REMUZZI G, BENIGNI A, REMUZZI A. Mechanisms of progression and regression of renal lesions of chronic nephropathies and diabetes. *J Clin Invest* 2006; 116: 288–296.
3. PAMBIANCO G, COSTACOU T, ELLIS D, BECKER DJ, KLEIN R, ORCHARD TJ. The 30-year natural history of type 1 diabetes complications: the Pittsburgh Epidemiology of Diabetes Complications Study experience. *Diabetes* 2006; 55: 1463–1469.
4. HASSLACHER C, RITZ E, WAHL P, MICHAEL C. Similar risks of nephropathy in patients with type I or type II diabetes mellitus. *Nephrol Dial Transplant* 1989; 4: 859–863.
5. MOGENSEN CE. Microalbuminuria and hypertension with focus on type 1 and type 2 diabetes. *J Intern Med* 2003; 254: 45–66.
6. ORTH SR, STOCKMANN A, CONRADT C et al. Smoking as a risk factor for end-stage renal failure in men with primary renal disease. *Kidney Int* 1998; 54: 926–931.
7. CHATURVEDI N, FULLER JH, TASKINEN MR. Differing associations of lipid and lipoprotein disturbances with the macrovascular and microvascular complications of type 1 diabetes. *Diabetes Care* 2001; 24: 2071–2077.
8. HOVIND P, TARNOW L, ROSSING P et al. Progression of diabetic nephropathy: role of plasma homocysteine and plasminogen activator inhibitor-1. *Am J Kidney Dis* 2001; 38: 1376–1380.
9. GALL MA, BORCH-JOHNSEN K, HOUGAARD P, NIELSEN FS, PARVING HH. Albuminuria and poor glycemic control predict mortality in NIDDM. *Diabetes* 1995; 44: 1303–1309.
10. RITZ E, STEFANSKI A. Diabetic nephropathy in type II diabetes. *Am J Kidney Dis* 1996; 27: 167–194.
11. KIMMELSTIEL P, WILSON C. Intercapillary lesions in the glomeruli of the kidney. *Am J Pathol* 1936; 12: 82–97.
12. DRUMMOND K, MAUER M; International Diabetic Nephropathy Study Group. The early natural history of nephropathy in type 1 diabetes: II. Early renal structural changes in type 1 diabetes. *Diabetes* 2002; 51: 1580–1587.
13. FIORETTI P, MAUER M, BROCCO E et al. Patterns of renal injury in NIDDM patients with microalbuminuria. *Diabetologia* 1996; 39: 1569–1576.
14. SCHWARTZ MM, LEWIS EJ, LEONARD-MARTIN T, LEWIS JB, BATLLE D. Renal pathology patterns in type II diabetes mellitus: relationship with retinopathy. The Collaborative Study Group. *Nephrol Dial Transplant* 1998; 13: 2547–2552.
15. GAMBARA V, MECCA G, REMUZZI G, BERTANI T. Heterogeneous nature of renal lesions in type II diabetes. *J Am Soc Nephrol* 1993; 3: 1458–1466.

16. DCCT. THE DIABETES CONTROL AND COMPLICATIONS TRIAL RESEARCH GROUP. The effect of intensive treatment of diabetes on the development and progression of long-term complications in insulin-dependent diabetes mellitus. *N Engl J Med* 1993; 329: 977–986.

17. DCCT. THE DIABETES CONTROL AND COMPLICATIONS TRIAL RESEARCH GROUP. Effect of intensive therapy on the development and progression of diabetic nephropathy in the Diabetes Control and Complications Trial. *Kidney Int* 1995; 47: 1703–1720.

18. KROLEWSKI M, EGGLERS PW, WARRAM JH. Magnitude of end-stage renal disease in IDDM: a 35 year follow-up study. *Kidney Int* 1996; 50: 2041–2046.

19. KROLEWSKI AS, WARRAM JH, CHRISTLIEB AR, BUSICK EJ, KAHN CR. The changing natural history of nephropathy in type I diabetes. *Am J Med* 1985; 78: 785–794.

20. DIABETES RESEARCH WORKING GROUP (DRWG). Conquering diabetes: a strategic plan for the 21st century. NIH Publication No. 99–4398. 1999 (available from <http://www.niddk.nih.gov/federal/dwg/fr.pdf>). Accessed 6 June 2007.

21. SEAQUIST ER, GOETZ FC, RICH S, BARBOSA J. Familial clustering of diabetic kidney disease. Evidence for genetic susceptibility to diabetic nephropathy. *N Engl J Med* 1989; 320: 1161–1165.

22. BORCH-JOHNSEN K, NORGARD K, HOMMEL E et al. Is diabetic nephropathy an inherited complication? *Kidney Int* 1992; 41: 719–722.

23. QUINN M, ANGELICO MC, WARRAM JH, KROLEWSKI AS. Familial factors determine the development of diabetic nephropathy in patients with IDDM. *Diabetologia* 1996; 39: 940–945.

24. HARJUTSALO V, KATOH S, SARTI C, TAJIMA N, TUOMILEHTO J. Population-based assessment of familial clustering of diabetic nephropathy in type 1 diabetes. *Diabetes* 2004; 53: 2449–2454.

25. ROGUS JJ, WARRAM JH, KROLEWSKI AS. Genetic studies of late diabetic complications: the overlooked importance of diabetes duration before complication onset. *Diabetes* 2002; 51: 1655–1662.

26. TODD JA, BELL JI, MCDEVITT HO. HLA-DQ beta gene contributes to susceptibility and resistance to insulin-dependent diabetes mellitus. *Nature* 1987; 329: 599–604.

27. MOREL PA, DORMAN JS, TODD JA, MCDEVITT HO, TRUCCO M. Aspartic acid at position 57 of the HLA-DQ beta chain protects against type I diabetes: a family study. *Proc Natl Acad Sci U S A* 1988; 85: 8111–8115.

28. THOMSON G. HLA DR antigens and susceptibility to insulin-dependent diabetes mellitus. *Am J Hum Genet* 1984; 36: 1309–1317.

29. VAN DER AUWERA B, SCHUIT F, LYARUU I et al. Genetic susceptibility for insulin-dependent diabetes mellitus in Caucasians revisited: the importance of diabetes registries in disclosing interactions between HLA-DQ- and insulin gene-linked risk. *Belgian Diabetes Registry. J Clin Endocrinol Metab* 1995; 80: 2567–2573.

30. REWERS M, BUGAWAN TL, NORRIS JM et al. Newborn screening for HLA markers associated with IDDM: diabetes autoimmunity study in the young (DAISY). *Diabetologia* 1996; 39: 807–812.

31. RICH SS, CONCANNON P. Challenges and strategies for investigating the genetic complexity of common human diseases. *Diabetes* 2002; 51 (Suppl. 3): S288–S294.

32. RICH SS. Mapping genes in diabetes. Genetic epidemiological perspective. *Diabetes* 1990; 39: 1315–1319.

33. RONNINGEN KS, KEIDING N, GREEN A; EURODIAB ACE Study Group. Europe and Diabetes. Correlations between the incidence of childhood-onset type I diabetes in Europe and HLA genotypes. *Diabetologia* 2001; 44 (Suppl. 3): B51–B59.

34. CONCANNON P, ERLICH HA, JULIER C et al. Type 1 diabetes: evidence for susceptibility loci from four genome-wide linkage scans in 1,435 multiplex families. *Diabetes* 2005; 54: 2995–3001.

35. CONCANNON P, GOGOLIN-EWENS KJ, HINDS DA et al. A second-generation screen of the human genome for susceptibility to insulin-dependent diabetes mellitus. *Nat Genet* 1998; 19: 292–296.

36. ONENGUT-GUMUSCU S, CONCANNON P. The genetics of type 1 diabetes: lessons learned and future challenges. *J Autoimmun* 2005; 25 (Suppl.): 34–39.

37. FIORETTI P, STEFFES MW, BARBOSA J, RICH SS, MILLER ME, MAUER M. Is diabetic nephropathy inherited? Studies of glomerular structure in type 1 diabetic sibling pairs. *Diabetes* 1999; 48: 865–869.

38. MAUER SM, STEFFES MW, CONNETT J, NAJARIAN JS, SUTHERLAND DE, BARBOSA J. The development of lesions in the glomerular basement membrane and mesangium after transplantation of normal kidneys to diabetic patients. *Diabetes* 1983; 32: 948–952.

39. MAUER SM, GOETZ FC, MCHUGH LE et al. Long-term study of normal kidneys transplanted into patients with type I diabetes. *Diabetes* 1989; 38: 516–523.

40. THE MICROALBUMINURIA COLLABORATIVE STUDY GROUP (MCSG). Predictors of the development of microalbuminuria in patients with Type 1 diabetes mellitus: a seven-year prospective study. *The Microalbuminuria Collaborative Study Group. Diabet Med* 1999; 16: 918–925.

41. STERN M, SOWERS, TUCK ML. Pathophysiology of hypertension in diabetes. In: Le Roith D, Taylor SI, Olefsky JM, eds. *Diabetes Mellitus: A Fundamental and Clinical Text*, 3rd edn. Philadelphia, PA: Lippincott, Williams, and Wilkins, 2004: 1377–1400.

42. VIBERTI GC, KEEN H, WISEMAN MJ. Raised arterial pressure in parents of proteinuric insulin dependent diabetics. *Br Med J* 1987; 295: 515–517.

43. KROLEWSKI AS, CANESSA M, WARRAM JH et al. Predisposition to hypertension and susceptibility to renal disease in insulin-dependent diabetes mellitus. *N Engl J Med* 1988; 318: 140–145.

44. DEWAN AT, ARNETT DK, ATWOOD LD et al. A genome scan for renal function among hypertensives: the HyperGEN study. *Am J Hum Genet* 2001; 68: 136–144.

45. MULLINS LJ, BAILEY MA, MULLINS JJ. Hypertension, kidney, and transgenics: a fresh perspective. *Physiol Rev* 2006; 86: 709–746.

46. FREEDMAN BI, BECK SR, RICH SS et al. A genome-wide scan for urinary albumin excretion in hypertensive families. *Hypertension* 2003; 42: 291–296.

47. SHIMAZAKI A, KAWAMURA Y, KANAZAWA A et al. Genetic variations in the gene encoding ELMO1 are associated with susceptibility to diabetic nephropathy. *Diabetes* 2005; 54: 1171–1178.

48. OSTERHOLM AM, HE B, PITKANIEMI J et al. Genome-wide scan for type 1 diabetic nephropathy in the Finnish population reveals suggestive linkage to a single locus on chromosome 3q. *Kidney Int* 2007; 71: 140–145.

49. ALAVERAS AE, THOMAS SM, SAGRIOTIS A, VIBERTI GC. Promoters of progression of diabetic nephropathy: the relative roles of blood glucose and blood pressure control. *Nephrol Dial Transplant* 1997; 12 (Suppl. 2): 71–74.

50. SNIEDER H, SAWTELL PA, ROSS L, WALKER J, SPECTOR TD, LESLIE RD. HbA(1c) levels are genetically

determined even in type 1 diabetes: evidence from healthy and diabetic twins. *Diabetes* 2001; 50: 2858–2863.

51. HARVEY JN, ALLAGOA B. The long-term renal and retinal outcome of childhood-onset type 1 diabetes. *Diabet Med* 2004; 21: 26–31.
52. KOSTRABA JN, DORMAN JS, ORCHARD TJ et al. Contribution of diabetes duration before puberty to development of microvascular complications in IDDM subjects. *Diabetes Care* 1989; 12: 686–693.
53. SVENSSON M, NYSTROM L, SCHON S, DAHLQUIST G. Age at onset of childhood-onset type 1 diabetes and the development of end-stage renal disease: a nationwide population-based study. *Diabetes Care* 2006; 29: 538–542.
54. HAMILTON J, DANEMAN D. Deteriorating diabetes control during adolescence: physiological or psychosocial? *J Pediatr Endocrinol Metab* 2002; 15: 115–126.
55. POLONSKY WH, ANDERSON BJ, LOHRER PA, APONTE JE, JACOBSON AM, COLE CF. Insulin omission in women with IDDM. *Diabetes Care* 1994; 17: 1178–1185.
56. HINCHLIFFE SA, LYNCH MR, SARGENT PH, HOWARD CV, VAN VELZEN D. The effect of intrauterine growth retardation on the development of renal nephrons. *Br J Obstet Gynaecol* 1992; 99: 296–301.
57. LUYCKX VA, BRENNER BM. Low birth weight, nephron number, and kidney disease. *Kidney Int* 2005; 97 (Suppl.): S68–S77.
58. BRENNER BM, CHERTOW GM. Congenital oligonephropathy and the etiology of adult hypertension and progressive renal injury. *Am J Kidney Dis* 1994; 23: 171–175.
59. ROSSING P, TARNOW L, NIELSEN FS, HANSEN BV, BRENNER BM, PARVING HH. Low birth weight. A risk factor for development of diabetic nephropathy? *Diabetes* 1995; 44: 1405–1407.
60. NELSON RG, MORGENSEN H, BENNETT PH. Birth weight and renal disease in Pima Indians with type 2 diabetes mellitus. *Am J Epidemiol* 1998; 148: 650–656.
61. ESHOJ O, VAAG A, BORCH-JOHNSEN K, FELDT-RASMUSSEN B, BECK-NIELSEN H. Is low birth weight a risk factor for the development of diabetic nephropathy in patients with type 1 diabetes? A population-based case-control study. *J Intern Med* 2002; 252: 524–528.
62. FAGERUDD J, FORSBLOM C, PETTERSSON-FERNHOLM K et al. Low birth weight does not increase the risk of nephropathy in Finnish type 1 diabetic patients. *Nephrol Dial Transplant* 2006; 21: 2159–2165.
63. HUXLEY RR, SHIELL AW, LAW CM. The role of size at birth and postnatal catch-up growth in determining systolic blood pressure: a systematic review of the literature. *J Hypertens* 2000; 18: 815–831.
64. PARVING HH, ROSSING P, HOMMEL E, SMIDT UM. Angiotensin-converting enzyme inhibition in diabetic nephropathy: ten years' experience. *Am J Kidney Dis* 1995; 26: 99–107.
65. PARVING HH, OXENBOLL B, SVENDSEN PA, CHRISTIANSEN JS, ANDERSEN AR. Early detection of patients at risk of developing diabetic nephropathy. A longitudinal study of urinary albumin excretion. *Acta Endocrinol (Copenh)* 1982; 100: 550–555.
66. VIBERTI GC, HILL RD, JARRETT RJ, ARGYROPOULOS A, MAHMUD U, KEEN H. Microalbuminuria as a predictor of clinical nephropathy in insulin-dependent diabetes mellitus. *Lancet* 1982; 1: 1430–1432.
67. MATHIESSEN ER, OXENBOLL B, JOHANSEN K, SVENDSEN PA, DECKERT T. Incipient nephropathy in type 1 (insulin-dependent) diabetes. *Diabetologia* 1984; 26: 406–410.
68. MOGENSEN CE, CHRISTENSEN CK. Predicting diabetic nephropathy in insulin-dependent patients. *N Engl J Med* 1984; 311: 89–93.
69. MESSENT JW, ELLIOTT TG, HILL RD, JARRETT RJ, KEEN H, VIBERTI GC. Prognostic significance of microalbuminuria in insulin-dependent diabetes mellitus: a twenty-three year follow-up study. *Kidney Int* 1992; 41: 836–839.
70. WRITING TEAM FOR THE DIABETES CONTROL AND COMPLICATIONS TRIAL/EPIDEMIOLOGY OF DIABETES INTERVENTIONS AND COMPLICATIONS RESEARCH GROUP (EDIC). Effect of intensive therapy on the microvascular complications of type 1 diabetes mellitus. *JAMA* 2002; 287: 2563–2569.
71. MULEC H, BLOHME G, GRANDE B, BJORCK S. The effect of metabolic control on rate of decline in renal function in insulin-dependent diabetes mellitus with overt diabetic nephropathy. *Nephrol Dial Transplant* 1998; 13: 651–655.
72. BOJESTIG M, ARNQVIST HF, HERMANSSON G, KARLBERG B, LUDVIGSSON J. Declining incidence of nephropathy in insulin-dependent diabetes mellitus. *N Engl J Med* 1994; 330: 977–986.
73. HOVIND P, TARNOW L, ROSSING K et al. Decreasing incidence of severe diabetic microangiopathy in type 1 diabetes. *Diabetes Care* 2003; 26: 1258–1264.
74. FAGERUDD J, FORSBLOM C, PETTERSSON-FERNHOLM K, GROOP PH; Finndiane Study Group. Implementation of guidelines for the prevention of diabetic nephropathy. *Diabetes Care* 2004; 27: 803–804.
75. HOVIND P, ROSSING P, TARNOW L, TOFT H, PARVING J, PARVING HH. Remission of nephrotic-range albuminuria in type 1 diabetic patients. *Diabetes Care* 2001; 24: 1972–1977.
76. GIUNTI S, BARIT D, COOPER ME. Mechanisms of diabetic nephropathy: role of hypertension. *Hypertension* 2006; 48: 519–526.
77. RAVID M, SAVIN H, JUTRIN I, BENTAL T, KATZ B, LISHNER M. Long-term stabilizing effect of angiotensin-converting enzyme inhibition on plasma creatinine and on proteinuria in normotensive type II diabetic patients. *Ann Intern Med* 1993; 118: 577–581.
78. DEEN WM, LAZZARA MJ, MYERS BD. Structural determinants of glomerular permeability. *Am J Physiol Renal Physiol* 2001; 281: F579–F596.
79. PAVENSTADT H, KRIZ W, KRETZLER M. Cell biology of the glomerular podocyte. *Physiol Rev* 2003; 83: 253–307.
80. DECKERT T, FELDT-RASMUSSEN B, BORCH-JOHNSEN K, JENSEN T, KOFOED-ENEVOLDSEN A. Albuminuria reflects widespread vascular damage. The Steno hypothesis. *Diabetologia* 1989; 32: 219–226.
81. FARQUHAR MG, WISSIG SL, PALADE GE. Glomerular permeability. I. Ferritin transfer across the normal glomerular capillary wall. *J Exp Med* 1961; 113: 47–66.
82. FARQUHAR MG, PALADE GE. Glomerular permeability. II. Ferritin transfer across the glomerular capillary wall in nephrotic rats. *J Exp Med* 1961; 114: 699–716.
83. VAN AGTMAEL T, SCHLOTZER-SCHREHARDT U, MCKIE L et al. Dominant mutations of Col4a1 result in basement membrane defects which lead to anterior segment dysgenesis and glomerulopathy. *Hum Mol Genet* 2005; 14: 3161–3168.
84. KALLURI R. Basement membranes: structure, assembly and role in tumour angiogenesis. *Nat Rev Cancer* 2003; 3: 422–433.
85. MINER JH, SANES JR. Collagen IV alpha 3, alpha 4, and alpha 5 chains in rodent basal laminae: sequence, distribution, association with laminins, and developmental switches. *J Cell Biol* 1994; 127: 879–891.
86. HUDSON BG, REEDERS ST, TRYGGVASON K. Type IV collagen: structure, gene organization, and role in human diseases. Molecular basis of Goodpasture and

Alport syndromes and diffuse leiomyomatosis. *J Biol Chem* 1993; 268: 26033–26036.

87. MINER JH, SANES JR. Molecular and functional defects in kidneys of mice lacking collagen alpha 3(IV): implications for alport syndrome. *J Cell Biol* 1996; 135: 1403–1413.

88. GOULD DB, PHALAN FC, BREEDVELD GJ et al. Mutations in *Col4a1* cause perinatal cerebral hemorrhage and porencephaly. *Science* 2005; 308: 1167–1171.

89. GOULD DB, PHALAN FC, VAN MIL SE et al. Role of *COL4A1* in small-vessel disease and hemorrhagic stroke. *N Engl J Med* 2006; 354: 1489–1496.

90. EWENS KG, GEORGE RA, SHARMA K, ZIYADEH FN, SPIELMAN RS. Assessment of 115 candidate genes for diabetic nephropathy by transmission/disequilibrium test. *Diabetes* 2005; 54: 3305–3318.

91. KOJIMA K, KERJASCHKI D. Is podocyte shape controlled by the dystroglycan complex? *Nephrol Dial Transplant* 2002; 17 (Suppl. 9): 23–24.

92. TSILIBARY EC. Microvascular basement membranes in diabetes mellitus. *J Pathol* 2003; 200: 537–546.

93. RUOTSALAINEN V, LJUNGBERG P, WARTIOVAARA J et al. Nephrin is specifically located at the slit diaphragm of glomerular podocytes. *Proc Natl Acad Sci U S A* 1999; 96: 7962–7967.

94. REISER J, KRIZ W, KRETLER M, MUNDEL P. The glomerular slit diaphragm is a modified adherens junction. *J Am Soc Nephrol* 2000; 11: 1–8.

95. SALEEM MA, NI L, WITHERDEN I et al. Co-localization of nephrin, podocin, and the actin cytoskeleton: evidence for a role in podocyte foot process formation. *Am J Pathol* 2002; 161: 1459–1466.

96. JONES N, BLASUTIG IM, EREMINA V et al. Nck adaptor proteins link nephrin to the actin cytoskeleton of kidney podocytes. *Nature* 2006; 440: 818–823.

97. KOS CH, LE TC, SINHA S et al. Mice deficient in alpha-actinin-4 have severe glomerular disease. *J Clin Invest* 2003; 111: 1683–1690.

98. ROSELLI S, HEIDET L, SICH M et al. Early glomerular filtration defect and severe renal disease in podocin-deficient mice. *Mol Cell Biol* 2004; 24: 550–560.

99. SHIH NY, LI J, KARPITSKII V et al. Congenital nephrotic syndrome in mice lacking CD2-associated protein. *Science* 1999; 286: 312–315.

100. BERG UB, TORBJORNSDOTTER TB, JAREMKO G, THALME B. Kidney morphological changes in relation to long-term renal function and metabolic control in adolescents with IDDM. *Diabetologia* 1998; 41: 1047–1056.

101. MEYER TW, BENNETT PH, NELSON RG. Podocyte number predicts long-term urinary albumin excretion in Pima Indians with type II diabetes and microalbuminuria. *Diabetologia* 1999; 42: 1341–1344.

102. STEFFES MW, SCHMIDT D, MCCREARY R, BASGEN JM; International Diabetic Nephropathy Study Group. Glomerular cell number in normal subjects and in type 1 diabetic patients. *Kidney Int* 2001; 59: 2104–2113.

103. PAGTALUNAN ME, MILLER PL, JUMPING-EAGLE S et al. Podocyte loss and progressive glomerular injury in type II diabetes. *J Clin Invest* 1997; 99: 342–348.

104. WHITE KE, BILOUS RW, MARSHALL SM et al. Podocyte number in normotensive type 1 diabetic patients with albuminuria. *Diabetes* 2002; 51: 3083–3089.

105. DALLA VESTRA M, MASIERO A, ROTHER AM, SALLER A, CREPALDI G, FIORETTI P. Is podocyte injury relevant in diabetic nephropathy? Studies in patients with type 2 diabetes. *Diabetes* 2003; 52: 1031–1035.

106. PATARI A, FORSBLOM C, HAVANA M, TAIPALE H, GROOP PH, HOLTHOFER H. Nephritis in diabetic nephropathy of type 1 diabetes. *Diabetes* 2003; 52: 2969–2974.

107. DOUBLIER S, SALVIDIO G, LUPIA E et al. Nephrin expression is reduced in human diabetic nephropathy: evidence for a distinct role for glycated albumin and angiotensin II. *Diabetes* 2003; 52: 1023–1030.

108. KOOP K, EIKMANS M, BAELE HJ et al. Expression of podocyte-associated molecules in acquired human kidney diseases. *J Am Soc Nephrol* 2003; 14: 2063–2071.

109. BENIGNI A, GAGLIARDINI E, TOMASONI S et al. Selective impairment of gene expression and assembly of nephrin in human diabetic nephropathy. *Kidney Int* 2004; 65: 2193–2200.

110. MAUER SM, STEFFES MW, ELLIS EN, SUTHERLAND DE, BROWN DM, GOETZ FC. Structural-functional relationships in diabetic nephropathy. *J Clin Invest* 1984; 74: 1143–1155.

111. BOHLE A, WEHRMANN M, BOGENSCHUTZ O, BATZ C, MULLER CA, MULLER GA. The pathogenesis of chronic renal failure in diabetic nephropathy. Investigation of 488 cases of diabetic glomerulosclerosis. *Pathol Res Pract* 1991; 187: 251–259.

112. PHILLIPS AO. The role of renal proximal tubular cells in diabetic nephropathy. *Curr Diab Rep* 2003; 3: 491–496.

113. PHILLIPS AO, STEADMAN R, MORRISEY K, MARTIN J, EYNSTONE L, WILLIAMS JD. Exposure of human renal proximal tubular cells to glucose leads to accumulation of type IV collagen and fibronectin by decreased degradation. *Kidney Int* 1997; 52: 973–984.

114. MORRISEY K, STEADMAN R, WILLIAMS JD, PHILLIPS AO. Renal proximal tubular cell fibronectin accumulation in response to glucose is polyol pathway dependent. *Kidney Int* 1999; 55: 160–167.

115. PHILLIPS AO, MORRISEY K, STEADMAN R, WILLIAMS JD. Decreased degradation of collagen and fibronectin following exposure of proximal cells to glucose. *Exp Nephrol* 1999; 7: 449–462.

116. JANSSEN U, RILEY SG, VASSILIADOU A, FLOEGE J, PHILLIPS AO. Hypertension superimposed on type II diabetes in Goto Kakizaki rats induces progressive nephropathy. *Kidney Int* 2003; 63: 2162–2170.

117. ERKAN E, GARCIA CD, PATTERSON LT et al. Induction of renal tubular cell apoptosis in focal segmental glomerulosclerosis: roles of proteinuria and Fas-dependent pathways. *J Am Soc Nephrol* 2005; 16: 398–407.

118. FUMO P, KUNCIO GS, ZIYADEH FN. PKC and high glucose stimulate collagen alpha 1 (IV) transcriptional activity in a reporter mesangial cell line. *Am J Physiol* 1994; 267: F632–F638.

119. LIFTON RP, GHARAVI AG, GELLER DS. Molecular mechanisms of human hypertension. *Cell* 2001; 104: 545–556.

120. RASCH R, NORGAARD JO. Renal enlargement: comparative autoradiographic studies of 3H-thymidine uptake in diabetic and uninephrectomized rats. *Diabetologia* 1983; 25: 280–287.

121. SEYER-HANSEN K, HANSEN J, GUNDERSEN HJ. Renal hypertrophy in experimental diabetes. A morphometric study. *Diabetologia* 1980; 18: 501–505.

122. RASCH R, DORUP J. Quantitative morphology of the rat kidney during diabetes mellitus and insulin treatment. *Diabetologia* 1997; 40: 802–809.

123. VALLON V, BLANTZ RC, THOMSON S. Glomerular hyperfiltration and the salt paradox in early type 1 diabetes mellitus: a tubulo-centric view. *J Am Soc Nephrol* 2003; 14: 530–537.

124. BROCHNER-MORTENSEN J, STOCKEL M, SORENSEN PJ, NIELSEN AH, DITZEL J. Proximal glomerulo-tubular balance in patients with type 1 (insulin-dependent) diabetes mellitus. *Diabetologia* 1984; 27: 189–192.

125. HANNEDOUCHE TP, DELGADO AG, GNIONSAHE DA, BOITARD C, LACOUR B, GRUNFELD JP. Renal hemodynamics and segmental tubular reabsorption in early type 1 diabetes. *Kidney Int* 1990; 37: 1126–1133.

126. WISEMAN MJ, SAUNDERS AJ, KEEN H, VIBERTI G. Effect of blood glucose control on increased glomerular filtration rate and kidney size in insulin-dependent diabetes. *N Engl J Med* 1985; 312: 617–621.

127. CHRISTENSEN CK, CHRISTIANSEN JS, CHRISTENSEN T, HERMANSEN K, MOGENSEN CE. The effect of six months continuous subcutaneous insulin infusion on kidney function and size in insulin-dependent diabetics. *Diabet Med* 1986; 3: 29–32.

128. TUTTLE KR, BRUTON JL, PERUSEK MC, LANCASTER JL, KOPP DT, DEFRONZO RA. Effect of strict glycemic control on renal hemodynamic response to amino acids and renal enlargement in insulin-dependent diabetes mellitus. *N Engl J Med* 1991; 324: 1626–1632.

129. KEVEN K, EKMEKCI Y. Opposing mechanisms in tubuloglomerular feedback. *Am J Kidney Dis* 2004; 44: 574.

130. CARMINES PK, OHISHI K, IKENAGA H. Functional impairment of renal afferent arteriolar voltage-gated calcium channels in rats with diabetes mellitus. *J Clin Invest* 1996; 98: 2564–2571.

131. LEE LK, MEYER TW, POLLOCK AS, LOVETT DH. Endothelial cell injury initiates glomerular sclerosis in the rat remnant kidney. *J Clin Invest* 1995; 96: 953–964.

132. STEFFES MW, BILOUS RW, SUTHERLAND DE, MAUER SM. Cell and matrix components of the glomerular mesangium in type I diabetes. *Diabetes* 1992; 41: 679–684.

133. LANE PH, STEFFES MW, FIORETTI P, MAUER SM. Renal interstitial expansion in insulin-dependent diabetes mellitus. *Kidney Int* 1993; 43: 661–667.

134. ZIYADEH FN, SHARMA K, ERICKSEN M, WOLF G. Stimulation of collagen gene expression and protein synthesis in murine mesangial cells by high glucose is mediated by autocrine activation of transforming growth factor-beta. *J Clin Invest* 1994; 93: 536–542.

135. WANG S, HIRSCHBERG R. BMP7 antagonizes TGF-beta-dependent fibrogenesis in mesangial cells. *Am J Physiol Renal Physiol* 2003; 284: F1006–F1013.

136. BLANKESTIJN PJ, DERKX FH, BIRKENHAGER JC et al. Glomerular hyperfiltration in insulin-dependent diabetes mellitus is correlated with enhanced growth hormone secretion. *J Clin Endocrinol Metab* 1993; 77: 498–502.

137. CUMMINGS EA, SOCHETT EB, DEKKER MG, LAWSON ML, DANEMAN D. Contribution of growth hormone and IGF-I to early diabetic nephropathy in type 1 diabetes. *Diabetes* 1998; 47: 1341–1346.

138. ZOJA C, MORIGI M, REMUZZI G. Proteinuria and phenotypic change of proximal tubular cells. *J Am Soc Nephrol* 2003; 14: S36–S41.

139. RICH SS. Genetics of diabetes and its complications. *J Am Soc Nephrol* 2006; 17: 353–360.

140. MOCZULSKI DK, ROGUS JJ, ANTONELLIS A, WARRAM JH, KROLEWSKI AS. Major susceptibility locus for nephropathy in type 1 diabetes on chromosome 3q: results of novel discordant sib-pair analysis. *Diabetes* 1998; 47: 1164–1169.

141. IMPERATORE G, HANSON RL, PETTITT DJ, KOBES S, BENNETT PH, KNOWLER WC. Sib-pair linkage analysis for susceptibility genes for microvascular complications among Pima Indians with type 2 diabetes. *Pima Diabetes Genes Group. Diabetes* 1998; 47: 821–830.

142. BOWDEN DW, COLICINGO CJ, LANGEFELD CD et al. A genome scan for diabetic nephropathy in African Americans. *Kidney Int* 2004; 66: 1517–1526.

143. HE W, MIAO FJ, LIN DC et al. Citric acid cycle intermediates as ligands for orphan G-protein-coupled receptors. *Nature* 2004; 429: 188–193.

144. HEBERT SC. Physiology: orphan detectors of metabolism. *Nature* 2004; 429: 143–145.

145. EWENS WJ, SPIELMAN RS. The transmission/disequilibrium test: history, subdivision, and admixture. *Am J Hum Genet* 1995; 57: 455–464.

146. MUELLER PW, ROGUS JJ, CLEARY PA et al. Genetics of Kidneys in Diabetes (GoKinD) Study: a genetics collection available for identifying genetic susceptibility factors for diabetic nephropathy in type 1 diabetes. *J Am Soc Nephrol* 2006; 17: 1782–1790.

147. MOTZO C, CONTU D, CORDELL HJ et al. Heterogeneity in the magnitude of the insulin gene effect on HLA risk in type 1 diabetes. *Diabetes* 2004; 53: 3286–3291.

148. COWLEY AW Jr. The genetic dissection of essential hypertension. *Nat Rev Genet* 2006; 7: 829–840.

149. HAMET P, MERLO E, SEDA O et al. Quantitative founder-effect analysis of French Canadian families identifies specific loci contributing to metabolic phenotypes of hypertension. *Am J Hum Genet* 2005; 76: 815–832.

150. JEUNEMAITRE X, GIMENEZ-ROQUEPLO A-P, DISSE-NODEME S, CORVOL P. Molecular basis of human hypertension. In: Rimoin DL, Connor JM, Pyeritz RE, Korf BR, eds. *Emery and Rimoin's Principles and Practice of Medical Genetics*, 5th edn. Philadelphia, PA: Churchill Livingstone, 2007: 1283–1300.

151. VINCENTI F, GHIGGERI GM. New insights into the pathogenesis and the therapy of recurrent focal glomerulosclerosis. *Am J Transplant* 2005; 5: 1179–1185.

152. JOHNSTONE DB, HOLZMAN LB. Clinical impact of research on the podocyte slit diaphragm. *Nat Clin Pract Nephrol* 2006; 2: 271–282.

On the Use of General Control Samples for Genome-wide Association Studies: Genetic Matching Highlights Causal Variants

Diana Luca,^{1,7} Steven Ringquist,^{2,7} Lambertus Klei,³ Ann B. Lee,¹ Christian Gieger,^{4,5} H.-Erich Wichmann,^{4,5} Stefan Schreiber,⁶ Michael Krawczak,⁶ Ying Lu,² Alexis Styche,² Bernie Devlin,³ Kathryn Roeder,^{1,7,*} and Massimo Trucco^{2,7}

Resources being amassed for genome-wide association (GWA) studies include “control databases” genotyped with a large-scale SNP array. How to use these databases effectively is an open question. We develop a method to match, by genetic ancestry, controls to affected individuals (cases). The impact of this method, especially for heterogeneous human populations, is to reduce the false-positive rate, inflate other spuriously small p values, and have little impact on the p values associated with true positive loci. Thus, it highlights true positives by downplaying false positives. We perform a GWA by matching Americans with type 1 diabetes (T1D) to controls from Germany. Despite the complex study design, these analyses identify numerous loci known to confer risk for T1D.

Introduction

Systematic GWA studies are critically dependent on the availability of very large and well-characterized control populations. With a different degree of structure in modern populations, ideally, multiple, diverse, and large control populations will be used. As platforms for GWA become standardized, numerous sources of pregenotyped control individuals are becoming available. Typically, many more controls are available than cases, and we believe these controls can be advantageous for discovering risk loci and for controlling the false-positive rate. For example, the data analyzed here include 416 Americans of European descent diagnosed with T1D (MIM 222100) and a control database of 2159 individuals from different regions of Germany.

Ancestry matching based on nongenetic variables¹ and SNP genotypes² for genetic-association studies has been proposed previously. Our approach, which we call genetic matching or GEM, goes further in that we show how to systematically obtain favorable matching by using a panel of genetic markers and how to determine outlying individuals as well as individuals that cannot be successfully matched to others in the available registry. By simulations, we will contrast matching to a commonly used method for controlling the confounding of ancestry, namely the use of eigenvector analysis³ via Eigenstrat⁴ to identify predictors of ancestry; for the real data, we contrast matching to both Eigenstrat and identification of common ancestry, such as European American.

We propose matching on the basis of genetic similarities derived from eigenvector decomposition (EVD), making our initial analyses similar to that taken in Eigenstrat.⁴ The best known form of matching is matched pairs (pMatch); however, assuming the criterion for matching are sufficient to remove the effects of unmeasured confounding, an alternative to matched pairs known as full matching (fMatch) is optimal.⁵ Consider a scenario in which three cases (a, b, and c) and three controls (x, y, and z) fall into two distinct ancestral clusters (a, x, and y) and (b, c, and z). Matching pairs creates three strata, (a and x), (c and z), and (b and y), but the pair (b and y) does not define a homogeneous strata. Alternatively, fMatch minimizes the total distance between individuals within strata with the constraint being that each stratum includes a single case and one or more controls, or vice versa, i.e., clusters (a, x, and y) and (b, c, and z). Of the two, fMatch is optimal because case and control samples are unlikely to have identical distributions of ancestry, and in this situation, forcing each case to match a unique control leads to suboptimal matches. (pMatch can be very useful, however, in designing follow-up studies that require preselection of case and control samples.)

In large association studies, the sample typically includes some individuals with widely varying ancestry. EVD is highly sensitive to outlying observations. A few points lying far from the majority of the data can determine multiple principal axes of the representation. Indeed, outliers can obscure the discovery of axes that potentially separate the data into distinct types. For this reason, individuals

¹Department of Statistics, Carnegie Mellon University; Pittsburgh, PA 15213, USA; ²Division of Immunogenetics, Department of Pediatrics, Children's Hospital, Pittsburgh, PA 15213, USA; ³Department of Psychiatry, University of Pittsburgh School of Medicine, Pittsburgh, PA 15213, USA; ⁴GSF National Research Center for Environment and Health, Institute of Epidemiology, Neuherberg 85764, Germany; ⁵Ludwig-Maximilians-University Munich, IBE, Chair of Epidemiology, Munich 85764, Germany; ⁶Institute of Clinical Molecular Biology and PopGen biobank, Christian Albrechts University, Kiel 24105, Germany

⁷These authors contributed equally to this work.

*Correspondence: roeder@stat.cmu.edu

DOI 10.1016/j.ajhg.2007.11.003. ©2008 by The American Society of Human Genetics. All rights reserved.

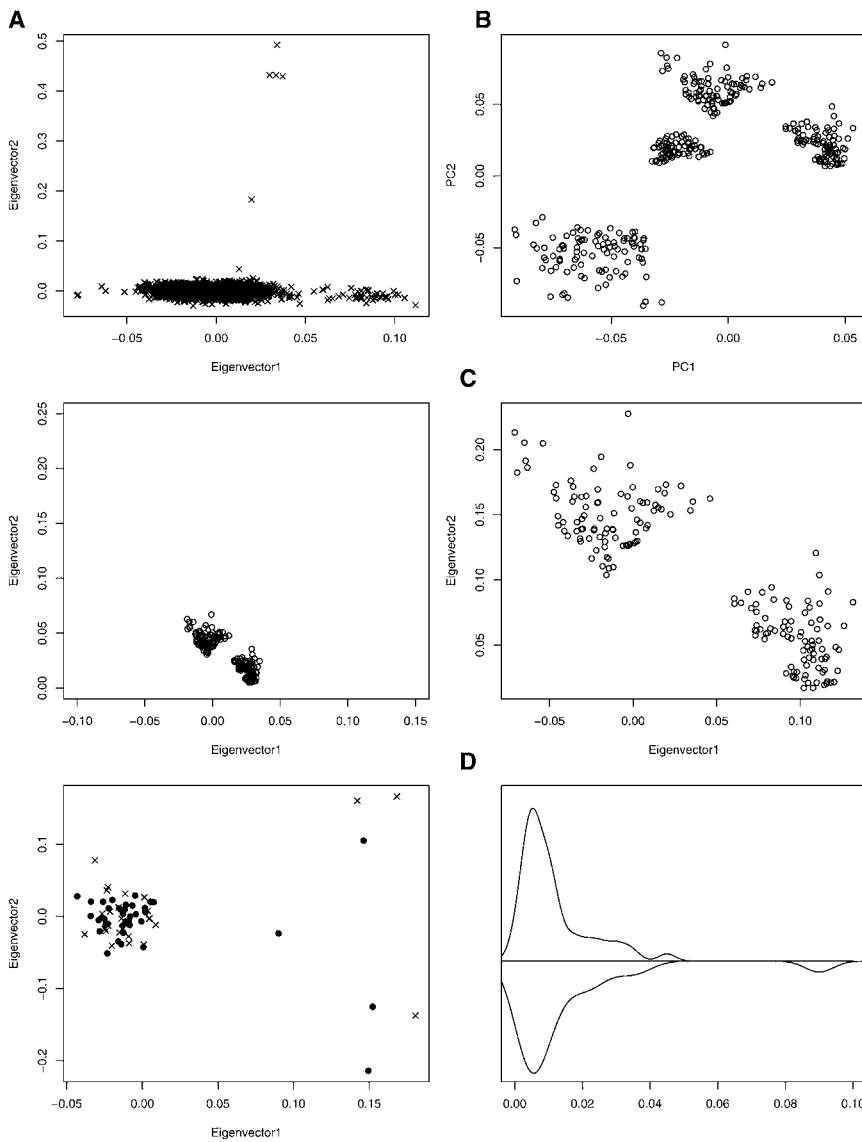


Figure 1. Flowchart for Genetic-Matching Algorithm Illustrated with Portions of the T1D Data

Distances between individuals are determined by the major axes of variation in the EVD representation. Outlier removal, illustrated by (A), is critical for revealing the subtle variability between individuals of similar ancestry. After major outliers are removed, clustering is used for discovery of homogeneous clusters; four distinct clusters are displayed here (B), plotted as principal component axes. Two of these clusters are displayed before ([C], left) and after ([C], right) rescaling of axes. Some observations are not outliers, but they are unmatchable ([D], left); for example, the isolated case in the center of the plot. Rescaled distances are compared to distances expected in homogeneous samples ([D], right) to identify cases and controls that can not be successfully matched. Association analysis is performed on matched strata so that the effects of population structure could be removed (not shown).

D dimensional map describing the “ancestry” of each individual, i.e., the mapping of the i th subject in each dimension is determined by the i th element in the d th eigenvector. The d th eigenvalue determines the importance of the d th dimension in the new representation of the data. Individuals of similar ancestry map to similar values in the eigenvectors associated with large eigenvalues (Figure 1). Eigenvectors associated with small eigenvalues have little or no genetic interpretation.

For a homogeneous population, the largest eigenvalues provides the basis for a significance test for population structure (see Patterson⁶ and Appendix). Applying this test with significance level $\alpha = 0.01$, we determine the number of dimensions D to be used in the eigenvector representation. The EVD determines the distance between individuals on the basis of the top D eigenvectors, serving as coordinates or dimensions, and eigenvalues serving as weights to exaggerate differences in dimensions of greater importance (see Appendix).

If the data have many outliers, D will be relatively large, and the principal eigenvectors will be poorly estimated.⁷ Outliers (Figure 1A) can be removed with visual diagnostics or the criterion from Eigenstrat,⁴ namely, remove any individuals with ancestry coefficients greater than 6 SDs in at least one of the D eigenvector axes. After removing outliers, the EVD should be recomputed. If the estimated dimension, D , is still greater than two or three, we suggest finding the distance between nearest pairs of controls and cases. A subject with ancestry that does not lend itself to matching will appear as an outlier via this criterion and should be removed (see the T1D example).

To determine how to match and which individuals are unmatchable, we rely on the distribution of distances between individuals

having highly unusual measures on any of the major eigenvectors are removed.⁴ Likewise, with matching it is necessary to determine which strata span an unusual distance leading to “unmatchable individuals.” If the controls are more numerous than the cases, they typically span a larger range of ancestries than cases, and it should be possible to find one or more controls similar to each case. Conversely, some cases may have to be removed to account for the effects of structure. In this work, we formalize the notions of outlying and unmatchable individuals and propose a method to discover the key axes that describe the population structure.

Material and Methods

A Sketch of the Matching Procedure Employed by GEM and Displayed in Figure 1

The illustration (Figure 1) shows the steps involved in matching genotyped cases and controls. To begin, create an L SNPs and N individuals matrix of scaled allele counts from which the EVD is computed (see Appendix). The top D eigenvectors form a

in a homogeneous population. For a homogeneous sample, the distribution of distances will depend on sample size N and the number of loci L . By using simulations, we can find the distribution of distances for a homogeneous population. These simulations also yield the distribution of eigenvalues for a homogeneous sample of size N .

Real populations are heterogeneous but can be modeled as mixtures of relatively homogeneous subpopulations (Figure 1B). We wish to represent these subpopulations so that the between-subject distances within a homogeneous subpopulation are comparable to expectation if the entire sample were homogeneous. To do so, we need to model the underlying population substructure and adjust real data so that they are scaled properly (Figure 1C); otherwise, the between subpopulation variance will cause distances between individuals to be poorly calibrated (Figure 1C). We do this via a two-stage algorithm involving clustering and scaling. In stage one, we cluster individuals that appear to have common ancestry. This is done iteratively, by addition of clusters and then testing for structure (see [Appendix](#) for testing) until each cluster is homogeneous. We use Ward's algorithm^{8,9} to form hierarchical groups of mutually exclusive subsets based on the first D axes of the EVD. We need a stopping rule for choosing K , the number of clusters. Start with $K = 2$ and apply the test for population structure on each of the clusters ($\alpha = 0.001$). Homogeneous clusters, as judged by the significance test, are set aside, and Ward's algorithm is applied only to the remaining data. Repeat this process, increasing K until all the clusters are homogeneous or consisting of too few observations (~20). Finally, we rescale interindividual distances as described in the [Appendix](#) so that they are comparable to distances found in a homogeneous population. At this rescaling step, unmatchable individuals are uncovered and removed (Figure 1D).

After outliers and unmatchable individuals are removed from the sample, recalculate the EVD and determine D . Reverting back to unscaled eigenvectors, find the distance between cases and controls on the basis of the Euclidean distance with D dimensions as described in the [Appendix](#). Match strata with either full match or pair match. Software implementing matching algorithms is widely available (e.g., we use the optmatch function in the statistical package R). Then, the data can be analyzed for disease and SNP association by conditional logistic regression. Other covariates can be entered into the model at this point.

T1D Analyses

Purified samples of genomic DNA were obtained from the Genetics of Kidneys in Diabetes (GoKinD) study¹⁰ and from T1D patients recruited at the Children's Hospital of Pittsburgh (CHP) and University of Pittsburgh Medical Center. The study employed a human gene-chip microarray (Affymetrix, Santa Clara, CA) for evaluation of genetic variants with DNA samples from T1D (case) participants with genetic typing data obtained from the KORA¹¹ and PopGen¹² "control" cohorts.¹³ Genotyping results were obtained with the same Affymetrix 500K SNP typing array; however, assays for case and control cohorts were performed independently. Case participants ($n = 416$) were recruited in the U.S., with self-declared European ancestry and T1D; control participants ($n = 2159$) were citizens of Germany recruited independent of phenotype (Table 1). Recruitment of participants at CHP was governed by the human subjects protocol approved by the University of Pittsburgh Institutional Review Board (IRB #011052: New Advanced Technology to Improve Prediction of Type 1 Diabetes). CHP patients ($n = 28$) consented to providing 10 ml blood obtained by vein puncture as well as a brief medical history relating to onset of T1D. The GoKinD

Table 1. Characteristics of Case and Control Participants

Demographic Characteristics	Case Participants		Control Participants	
	CHP	GoKinD	KORA	POPGEN
Number of singletons	28	394	1644	500
Nominal European American (%)	100%	100%	—	—
German residents (%)	—	—	100%	100%
Male gender (%)	50%	46.7%	49.5%	51.8%
History of Diabetes				
Type 1 diabetes (%)	100%	100%	—	—
Mean age at T1D	12.7 ± 7.9	12.2 ± 7.1	—	—
Diagnosis (yr)				

cohort ($n = 394$) was recruited independently from the CHP cohort by collaborative efforts of the Juvenile Diabetes Research Foundation, National Institutes of Health, and U.S. Center of Disease Control.¹⁰ Material from the GoKinD cohort was provided as solutions of DNA, purified from lymphoblastoid cell lines or from whole blood. DNA solutions were provided as 50 μ l aliquots containing ~100 ng/ μ l DNA per aliquot dissolved in 20 mM NaCl and 1 mM EDTA (pH 7.5). DNA from the CHP samples were obtained from whole blood with methods described in Ringquist,¹⁴ and genotyping was performed by Affymetrix Services Laboratory (Affymetrix) with GeneChip 500K arrays. All of the genotype data from GoKinD samples generated by this project will be submitted to an accessible database, such as dbGaP or T1Dbase (see [Web Resources](#)).

All T1D samples had a sufficient completion rate (>95%) for inclusion, as did almost all KORA and PopGen samples. Initially, genotypes for all three samples were called with the BRLMM algorithm.¹⁵ By using three criteria for genotype QC per SNP—greater than 90% genotype calls, test statistic for Hardy-Weinberg yields p value > 0.005, and minor allele frequency ≥ 0.05 —we removed ~140,000 SNPs and retained 360,000 for the T1D sample, similar to other studies. When we contrasted the T1D samples to the control samples, we noted SNPs with very different allele frequencies that were not in or near known T1D loci. Inspection of the allele frequencies showed that the control allele frequencies were remarkably similar to HapMap frequencies (see [Web Resources](#)), but the corresponding genotype clusters for the T1D samples had undesirable features.

We tried various ways to improve the genotype calls. First, we looked for substantial differences between the calls by using the two algorithms employed by Affymetrix, namely DM and BRLMM. Although some discrepancies were noted, we did not see a material improvement in the data by eliminating this small set of loci. Next, because we had the Affymetrix "cel" files for the PopGen control sample, we called all of these genotypes for PopGen and T1D together by using both the DM and BRLMM algorithms. Again, this process eliminated some problematic loci, but the results were not compelling. Finally, we tried the new Bayesian calling algorithm, CHIAMO.¹⁶ This algorithm led to a marked improvement for the genotype calls, as determined by inspection of the genotype clusters. For our data, we found that analyzing the PopGen and T1D data together (batch) yielded slightly better results than analyzing the two data sets as complementary strata, so these were the data we reported. Because we had greater confidence in the BRLMM calls for chromosome X, we reported those calls for X-linked SNPs. Because the KORA sample came to us only with

genotypes called by the BRLMM algorithm, we used those genotypes for that data set.

Preliminary quality control consisted of a six-step process that reduced the number of cases to 415, controls to 2112, and SNPs to 284,216. Step 1: Removed a case who was a clear outlier. Step 2: Removed 32 controls who had greater than 5% missing genotypes. Step 3: Removed 90,732 SNPs with >5% noncall rate in at least one of the three samples. Step 4: Removed 105,658 SNPs with minor allele frequencies less than 0.05 in either control sample. Step 5: Removed 1972 SNPs with $F_{ST} > 0.02$ (estimated for the two German control samples). Step 6: Removed 18,427 SNPs that violated Hardy-Weinberg equilibrium ($p < 0.005$) in either of the control samples.

Results

Simulations

We compare three approaches to correct for the effects of structure: Eigenstrat and GEM with fMatch and pMatch. Although we compare their size (i.e., rate of false positives) and power, these approaches are not direct competitors. The GEM methods are designed to limit analysis to strata that are chosen a priori, whereas Eigenstrat aims to remove the effects of structure in the analysis stage.

Allele frequencies for the subpopulations were generated with the “Balding-Nichols” model¹⁷ (see [Appendix](#)), with allele frequencies varying uniformly between 0.05 and 0.5. To correct for structure, L reference SNPs were generated. Of these SNPs, 99% had a minor amount of variability across subpopulations ($F_{ST} = 0.01$), and 1% had substantial differentiation ($F_{ST} = 0.1$). Null or causal candidate SNPs of three levels of F_{ST} were generated: Model (1) strongly differentiated SNPs, $F_{ST} = 0.1$; Model (2) moderately differentiated SNPs with $F_{ST} = 0.03$; and Model (3), modestly differentiated SNPs with $F_{ST} = 0.01$.

Ten panels of independent reference SNPs, with L ranging from 96 to 100,000, were generated. For each of these panels, we simulated 1000 independent causal SNPs and 1000 independent null candidate SNPs. We repeated this analysis for models (1), (2) and (3) and for six choices of L . Causal SNPs with relative risk $R = 2$ were generated with the approach described in Price⁴ for power calculations.

Our first battery of simulations is based on SNPs sampled from two subpopulations, with 200 individuals per subpopulation. Case status was assigned to 80 and 20 of the individuals from subpopulations 1 and 2, respectively. The remaining individuals were assigned control status. For the matched-pairs analysis, we paired each case to the closest control until we obtained 100 matched pairs. For the other two methods of analyses, we analyzed all 400 individuals. Each method readily detects population substructure and achieves the desired type I error rate as L increases ([Table 2](#)). pMatch and fMatch successfully remove the effect of structure with a smaller panel of reference SNPs than Eigenstrat does ([Figure 2A](#)). Indeed, when a large panel of reference SNPs is available, the GEM pro-

cedures are overly conservative; consequently, Eigenstrat is slightly more powerful than both matching procedures ([Table 2](#)) under these conditions. For SNPs with less information about population membership than present in our simulated reference panels, greater numbers of SNPs would be required to remove the effects of structure.⁴

Our second battery of simulations is based on nine subpopulations distributed along a gradient, designed to simulate a cline such as the north to south cline observed in western Europe. The 100 cases are distributed with 2, 4, 6, 7, 9, 12, 15, 20, and 25 individuals in populations 1–9, respectively. The 300 controls are distributed randomly across the nine subpopulations. Results from this simulation are qualitatively similar to those shown in [Figure 2A](#) ([Table 2](#)). The first two batteries of simulations illustrate that when the case and control samples are drawn from the same subpopulations, but with different frequencies, the effects of substructure can be removed with any of the three methods described. Even the effects of highly differentiated SNPs can be removed provided the reference panel is sufficiently informative.

Our third battery of simulations is also based on a nine population gradient; however, the cases and controls are apportioned in a manner that simulates the complexity of human populations and GWA designs. As in the previous simulation, we simulate nine populations and draw 300 controls randomly. In contrast, all 50 of the cases are drawn from populations 6–9. Because of the nature of this third battery, namely the presence of unmatchable observations, we analyze the data in two ways: Unmatchable observations are removed as described previously; or unmatchable observations are retained. In choosing only a single control for each case, pMatch includes only 50 of the controls in the study regardless of the treatment of outliers. Provided the reference panel is sufficiently informative, many of these controls will be derived from populations 6–9. Eigenstrat, on the other hand, uses all of the data, as will fMatch when unmatchable observations are retained. For fMatch, this means that cases drawn from population 6 will tend to have many controls in their strata sampled from populations 1–5. The remaining cases will tend to have only one or two controls in their strata. By grouping the outlying observations, fMatch attempts to minimize the effect of unmatchable observations. Eigenstrat must account for controls sampled from populations 1–5 with regression techniques, which are well known to suffer adverse consequences when they are extrapolating beyond the range of the data.

When unmatchable observations are retained, pMatch corrects for the effects of substructure with fewer reference SNPs than the other two methods ([Table 3](#) and [Figure 2B](#)). Indeed, Eigenstrat fails to remove the effects of population substructure. By comparing pMatch and fMatch, we see that the latter has greater power. This makes sense because fMatch is using more of the data ([Table 3](#)).

On the basis of the clustering and rescaling process, most of the controls from populations 1–5 are unmatchable, and

Table 2. Size and Power of Tests at Level 0.05

Statistic	Design	No. of Markers	Eigenstrat with F_{ST}			pMatch with F_{ST}			fMatch with F_{ST}				
			0.01	0.03	0.1	0.01	0.03	0.1	0.01	0.03	0.1		
Size													
Two Populations													
Gradient	96	.069	.106	.211	.062	.100	.202	.065	.101	.206			
	386	.055	.061	.085	.044	.045	.051	.047	.049	.054			
	1536	.052	.054	.055	.046	.045	.045	.047	.047	.046			
	6144	.053	.052	.051	.044	.045	.045	.047	.047	.046			
	12000	.053	.052	.052	.044	.044	.045	.047	.045	.047			
	24000	.053	.050	.051	.043	.042	.041	.046	.046	.045			
Power													
Two Populations													
Gradient	96	.783	.710	.683	.693	.635	.620	.754	.685	.659			
	386	.767	.701	.682	.682	.632	.621	.735	.673	.653			
	1536	.766	.702	.677	.683	.635	.622	.736	.674	.653			
	6144	.765	.694	.676	.684	.630	.623	.735	.671	.653			
	12000	.765	.697	.676	.684	.633	.624	.735	.673	.653			
	24000	.763	.696	.677	.684	.632	.624	.734	.671	.653			
Gradient	96	.939	.917	.833	.886	.872	.804	.922	.900	.814			
	386	.924	.891	.796	.877	.857	.782	.902	.869	.775			
	1536	.917	.876	.774	.876	.850	.775	.894	.856	.754			
	6144	.913	.874	.768	.873	.849	.773	.892	.853	.747			
	12000	.915	.873	.771	.874	.849	.774	.891	.850	.749			
	24000	.912	.874	.768	.873	.849	.771	.892	.852	.747			

Columns depict the results as F_{ST} varies (0.01, 0.03, and 0.1) in the candidate markers. Results are shown for two scenarios: a two-population mixture and a nine-population gradient. For the size, the expected number of p values smaller than 0.05 is 50.

such a result is desirable because cases were only drawn from populations 6–9. In this instance, the size of the matched analyses is now closer to the nominal level even when L is small, as expected. Interestingly, there is the considerable enhancement in power for fMatch and pMatch when unmatchable individuals are removed, as recommended by our methods, as opposed to when they are forced to be retained (Table 3). This occurs because removal of the outliers leads to improved performance of the EVD and hence superior choices of matches in the analysis. In addition, for fMatch the removal of controls from populations 1–5 leads to a more homogeneous sample that tends to increase power.

Eigenstrat defines outliers without specific reference to cases and controls; thus, none of the observations are unmatchable observations. Nevertheless, if the regression approach is applied after removal of those observations declared unmatchable by the fMatch procedure, the type I error is successfully controlled, and the power is slightly greater than it is for fMatch (Table 3). This hybrid approach to analysis has some potential for further development.

GWA of Type 1 Diabetes Data with fMatch

We analyzed 416 cases of T1D,¹⁸ derived from the GoKinD¹⁰ cohort ($n = 394$) and T1D patients recruited from the Children's Hospital of Pittsburgh ($n = 28$). Samples were genotyped with the Affymetrix 500K GeneChip. All identified their ancestors as European. The mean age of onset for T1D was 12.2 and 12.7 years of age for the GoKinD and Pittsburgh cohorts, respectively. Controls genotyped by the same chip were obtained from the PopGen and KORA repositories, which consist of 500 individuals from north Germany (PopGen) and 1644 individuals from southern Germany (KORA).^{11–13,19} The four cohorts were recruited independently of one another. The relevant characteristics of these cohorts are summarized in Table 1.

Stringent quality control reduced the number of SNPs to 284,216 and the number of controls to 2112 (samples were removed if the rate of missing genotypes exceeded 5%). To reconstruct ancestry, we chose 23,552 independent or “tag” SNPs by using the H-clust algorithm²⁰ with an r^2 cut-off value of 0.04. Both case and control individuals exhibit complex population heterogeneity. For example, individuals were included in the PopGen and KORA registry on

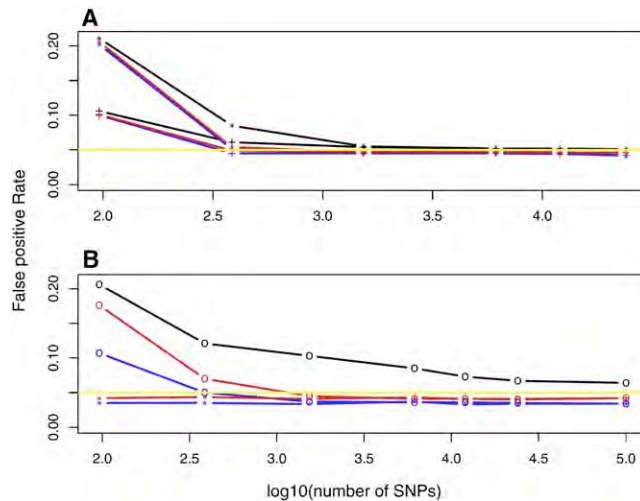


Figure 2. False-Positive Rate versus Log of the Number of Markers Available for Estimating Structure

Results are for Eigenstrat (black), pMatch (blue), and fMatch (red). The desired nominal rate of 0.05 is plotted as a yellow line. In (A), a sample derived from two simulated populations is shown. Results are displayed for markers with two levels of differentiation $F_{ST} = 0.1$ (*) and 0.03 (+). The former exhibits a higher rate of errors than the latter for small numbers of markers. In (B), a sample derived from a gradient of simulated populations is shown. Results are displayed for the full sample (plotting character "o") and with unmatchable individuals removed (plotting character "*"; this applies to the matching methods only).

the basis of residence rather than known German ancestry. We removed one case individual who had very different ancestry from the other 415. For 415 cases and 2112 controls, $D = 22$ dimensions were required to explain the significant axes of genetic variation. Many of these axes exhibited extreme outliers (Figure 1A). After removing 53 controls, only three important axes of variation remained. On the basis of the first two eigenvectors, a cluster of cases that differs in ancestry from the control sample was clearly evident (Figure 3A). To identify unmatchable individuals more completely, we computed the distance between each case and the nearest control and vice versa on the basis of three axes of the EVD map. The resulting distribution of distances indicated that 21 cases could not be matched to a control with similar ancestry (Figure 4). By repeating this process of finding the significant eigenvalues and the corresponding minimum distances between cases and controls in the corresponding axes, we subsequently removed an additional one case and 15 controls. After excluding these outliers, only two significant eigenvalues remain when a significance level of 0.01 was used.

Next, with cluster analysis to identify homogeneous strata, 2136 individuals were clustered into 26 strata, each with 20 or more elements and no significant structure within cluster ($p > 0.001$). The remaining 301 individuals were clustered into 24 small clusters. On the basis of these strata, the data were rescaled and the distance between cases and matched controls was determined. Those that

Table 3. Size and Power of the Tests before and after Removing Outliers, with Eigenstrat, pMatch, and fMatch

Statistic No. of Markers	Outliers Present					
	Eigenstrat with F_{ST}			pMatch with F_{ST}		
	.01	.03	.1	.01	.03	.1
Size						
96	.064	.097	.206	.044	.056	.107
386	.057	.068	.121	.038	.040	.050
1536	.056	.062	.103	.037	.037	.043
6144	.056	.061	.085	.037	.037	.035
12000	.058	.058	.073	.037	.036	.041
24000	.057	.058	.067	.037	.037	.035
100000	.055	.057	.064	.037	.037	.034
Power						
96	.804	.753	.650	.590	.579	.511
386	.784	.731	.630	.583	.566	.489
1536	.771	.716	.615	.581	.567	.482
6144	.762	.711	.604	.583	.566	.485
12000	.751	.704	.595	.582	.564	.485
24000	.746	.699	.593	.584	.565	.484
100000	.748	.694	.592	.588	.565	.484
Outliers Removed						
Size						
96	.061	.090	.195	.037	.036	.035
386	.057	.060	.095	.036	.036	.035
1536	.054	.053	.057	.035	.038	.033
6144	.054	.053	.056	.040	.037	.037
12000	.052	.053	.054	.038	.035	.033
24000	.052	.052	.053	.036	.039	.034
100000	.052	.052	.053	.037	.035	.034
Power						
96	.906	.931	.927	.706	.713	.656
386	.873	.885	.870	.698	.713	.656
1536	.856	.857	.834	.700	.716	.660
6144	.849	.850	.829	.703	.716	.666
12000	.843	.843	.818	.703	.713	.663
24000	.840	.840	.817	.701	.715	.667
100000	.835	.834	.813	.700	.719	.669

Columns depict the results as F_{ST} varies (.01, .03, and .1) in the candidate markers. The simulated data are a gradient with nine subpopulations; controls are drawn from 1–9 and cases are only from 6–9.

were considered unmatchable individuals on the basis of the simulation results were removed (see Appendix). With this process, an additional 20 cases and 48 controls are removed from the dataset for fMatch. The resulting distance between the remaining cases and controls in fMatch is consistent with expectations for cases and controls matched within homogeneous strata (data not shown). In the reduced fMatch sample, two principal axes separate the German control samples by region and define a space, spanned by both cases and controls, that facilitates matching (Figure 3B). These dimensions presumably map onto genetic gradients on the European continent; e.g., the horizontal axis is likely to be related to a north-south gradient

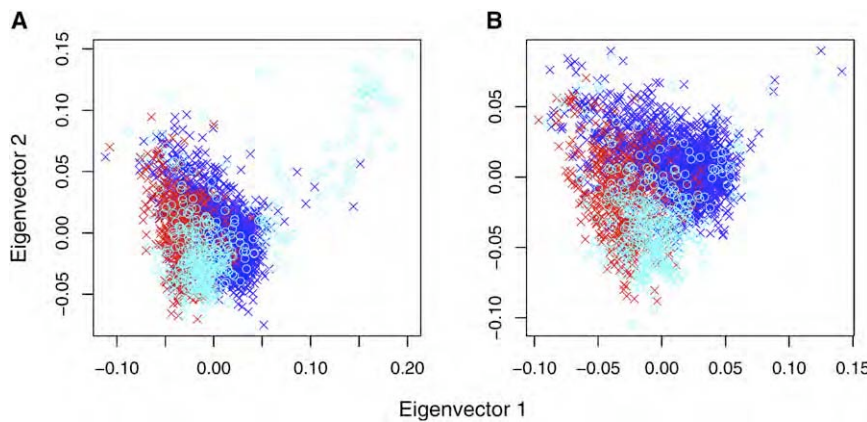


Figure 3. Plots of the First Two Eigenvector Axes for T1D Data before and after Removing the Unmatchable Individuals after Clustering and Rescaling of the Data

Each case (light blue) has a matched control (dark blue = South Germany, red = North Germany) in a close neighborhood after removal of unmatchable individuals; compare before (A) with after (B).

because it tends to separate the German samples by north (PopGen)¹² and south (KORA)¹¹ origin.^{21,22} In the pMatch sample, one additional axis is needed to explain important variation (data not shown).

After final removal of outliers and unmatchable individuals for fMatch, cases and controls were stratified on the basis of their genetic ancestry into 298 strata. Most of the strata (159) contain a single case matched to several controls. A single case matched to a single control occurred in 111 strata. A minority of strata (28) contain a single control matched to multiple cases. For example, in the most extreme strata, a single case was matched to 71 controls and a single control was matched to 13 cases. When a single case is matched to a large number of controls (or vice versa), the information gain from the strata is essentially equivalent to that obtained from a single case matched to a moderate number of individuals. Nevertheless, conditional logistic regression is valid regardless of the lack of

balance in the strata. In all, 373 cases were contrasted with 1996 controls by conditional logistic regression (Figure 5, top panel). The results highlight the HLA region, which contains numerous SNPs achieving GWA significance. Variation in the HLA region is well known to account for a large fraction of the risk for T1D.^{23–26} No

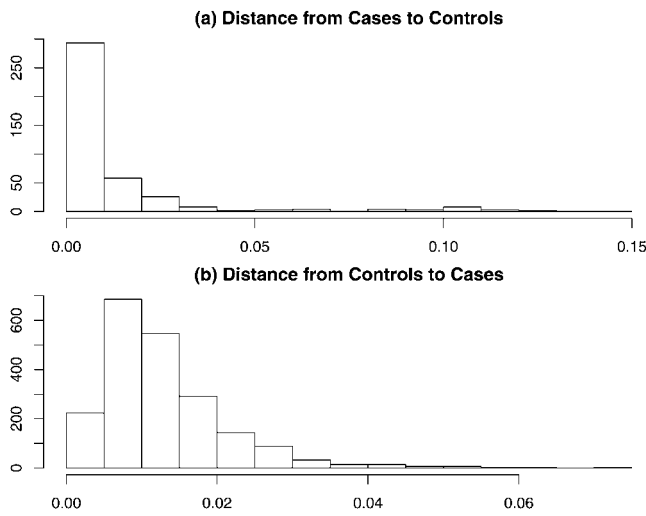


Figure 4. The Distance between Each Case and the Nearest Control and Vice Versa Based on Three Principal Components Are Computed

The distributions differ, and we eliminate 34 cases with distances to the nearest control greater than 0.075. (A) shows the histogram of distances between each case and the nearest control. (B) shows the histogram of distances between each control and the nearest case.

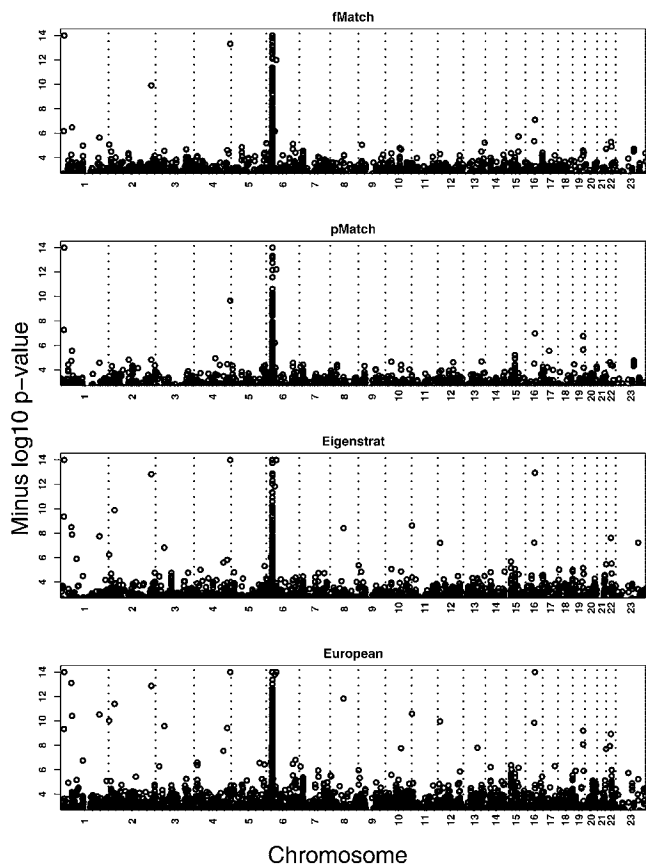


Figure 5. Transformed p Values after Conditional Logit Regression Was Performed on the Data Stratified with fMatch
 Transformed p values (negative of the log, base 10). Results from conditional logistic regression on the data stratified with fMatch (top panel) and pmatch (second panel) are shown. Results obtained with Eigenstrat are shown in the third panel. Results obtained when removing observations with very divergent ancestries (inferred with the Eigenstrat rule for outliers) from the bulk of the sample, which was European, are shown in the bottom panel.

other location in the genome contains SNPs with test statistics meeting reasonable criteria for GWA significance ($\leq 10^{-7}$) after ensuring quality genotype calls by visual inspection of the genotype clusters (see [Figures S1 and S2](#) available online for examples). It should be noted, however, that visual inspection of genotype clusters is essential to interpret this Affymetrix “first-generation” genotype data, a feature other GWA studies with this genotyping platform also report.²⁷

Results from fMatch agree with our expectations. Other GWA studies have established that all genetic variation thus far uncovered, aside from variation in the HLA region, account for a modest portion of the risk for T1D.^{28,29} For detecting loci of modest effect with good power, either sample sizes must be substantial (i.e., thousands of cases and controls genotyped) or a staged study design must be employed. The staged design typically sets a significance level between 0.01 and 0.001 in stage 1, then genotypes all loci meeting this significance level (and quality-control criteria) in a second, larger sample.^{30,31} Treating our study as stage 1 with a significance level of 0.007,³⁰ results from fMatch would include SNPs for genotyping in stage 2 from six out of ten loci now believed to confer risk to T1D.²⁹ Of the remaining four loci, only one had more than a few SNPs in the region.

Aside from the HLA region, SNPs in or near *PTPN22* (MIM 600716), *IL2RA* (CD25 [MIM 147730]), and *CTLA4* ([MIM 123890]; window = gene location \pm 40 Kb) showed enough signal to be passed to stage 2. The smallest p value for each gene was 0.000706 (rs2488457), 0.000995 (rs10905669), and 0.000336 (rs231726). The smallest p values for SNPs close to “risk SNPs” rs2292239 and rs12708716 were 0.00667 (rs2292239) and 0.00539 (rs11647011) for window = SNP location \pm 50 Kb. Could it be that the signals in these regions occurred by chance? To answer this question, we performed a simulation experiment. We randomly select from the genome ten intervals that correspond to the same size as the original ten windows (for the HLA region, we assumed a window of 3 Mb). Then, we count the number of intervals in which one or more SNPs have $p < 0.007$ and would thus be genotyped in stage 2. We perform this random selection 10^6 times, counting how many times six or more intervals would have SNPs genotyped in Stage 2. By this experiment, we determined that our results would rarely occur by chance, roughly one in ten thousand times.

A few other observations from these analyses are worth noting. Within the HLA region, Todd²⁹ cites rs3129934 as the replicated SNP; our independent data and analyses yield a p value for association of 7.2×10^{-10} with this SNP; for the replicated SNP identified in *CTLA4*, rs3087243, our data and analyses yield a p value for association of 0.013, and, as noted above, the replicated SNP rs2292239 produced a p value of 0.00667 from our data. Although the HLA region needs no more support, our results provide further evidence for replication in *CTLA4* and at rs2292239. For genotype cluster plots for the cited SNPs, see [Figure S1](#). In

addition, for all of the loci cited above, we have compared our data to that reported by the Wellcome Trust Case Control Consortium.²⁷ For these loci, the allele in excess in cases is the same for both data sets (data not shown).

Four loci did not pass stage 1 criteria. None of these SNPs reported by Todd et al.²⁹ as risk loci were on our Affymetrix genotyping array. Of these four risk SNPs, only rs1893217 in 18p11 was covered well in terms of genotyped SNPs in substantial linkage disequilibrium (LD) with it. This SNP is in almost complete LD with rs2542151 according to HapMap; it passed our QC, but it shows no evidence for association in our data ($p = 0.51$). For the proinsulin precursor gene, *INS* (MIM 176730), only two SNPs on the array pass QC and fall in the region, but HapMap contains no information about their LD with the reported risk SNP, rs689, and they show no association ($p > 0.35$). For the gene encoding interferon-induced helicase C domain-containing protein 1, *IFIH1* (MIM 606951), the reported risk allele shows modest LD with a SNP we genotyped, namely rs7608315, which shows no association ($p = 0.38$). Finally, for the 12q24 region, rs3184504 is identified as the risk SNP. One SNP in this region passed QC for our data, and it is modestly associated with risk for T1D ($p = 0.046$).

The vast majority of the SNPs from this or any relevant GWA are independent of risk for T1D. Many SNPs from the HLA regions of chromosome 6 are associated, however. After eliminating HLA SNPs, ~5% of the association tests are expected to have p values < 0.05 . Of the 284,216 tests, 7.0% were significant at $\alpha = 0.05$ for fMatch. A moderate excess of false positives occurs for any reasonable choice of α . Given the success of the GEM method in the simulations, in terms of controlling the false-positive rate, we wondered whether the source of additional false positives could be poor-quality genotype calls. Indeed, by assessing genotype clusters for all SNPs producing p values $\leq 10^{-4}$, we find a rate of poor calls of 60%–67% ([Figure S2](#)). The rate of poor-quality genotype calls increases as the p value decreases. Predominantly, the problematic calls occur for the T1D sample. On the basis of our estimated rate of poor-quality genotype calls, we believe the excess false-positive rate is attributable to data-quality issues, not the method.

We also analyzed GWA data by using pMatch and Eigenstrat and by ignoring population substructure after discarding outliers with the Eigenstrat rule (see [Figure 5](#)). As expected, pMatch shows the lowest rates of positive findings, whereas ignoring structure yields the most. Like fMatch, it appears the excess of false positives for pMatch is due to poor-quality genotype calls. The same is predominantly true for Eigenstrat, but we note that an ample number of SNPs producing small p values are not attributable to poor quality, and this problem is amplified by ignoring structure. At significance level 0.0001, after visual inspection of genotypes fMatch has half the false-positive rate of Eigenstrat.

To further validate GEM, we tried a null experiment. We randomly labeled half of the KORA data as cases and half as controls and repeated the matching analysis. Removal of 72 outliers reduced the number of significant eigenvalues

required to explain the variation from 24 to 2. After this simplification, only 12 unmatchable individuals remained. All three methods of analysis (Eigenstrat, Pmatch, and fMatch) produced type I error rates that were on target.

Discussion

Our GWA analyses of T1D are meant to accomplish two goals. First, they illustrate the utility of ancestry matching in the face of a very difficult problem, that being when cases are sampled in a region quite different from the region of the controls. In our case, the T1D sample comes from any American of nominal European ancestry, whereas the controls were recruited among residents of Germany. Such constellations can also arise even if cases and controls are sampled from the same geographical region. We would expect the example to be especially salient for American samples. Second, we wished to use the results to evaluate reported T1D risk loci and, in later analyses, discover new loci. The results show that genetic or ancestry matching can be an important ingredient in the toolbox of researchers who are performing GWA analyses. Moreover, our results do lend support for previous GWA findings for T1D.^{28,29}

We do not yet know whether our analyses have identified any new risk loci for T1D. Although it seems unlikely given the modest sample of cases, a substantial number of controls have been analyzed. Moreover, for a rare disease like T1D, using unscreened instead of screened controls has almost no impact on power.³² We plan various kinds of stage 2 analyses to assess the association signals from our GWA results. In addition, by agreement the data generated by our project will be reported back to the GoKinD database, and GoKinD will make the data available to qualified investigators. Thus, these data will shortly be available to the research community, and we will be pleased to share detailed results upon request.

We have described how to use genetic matching to enhance a case-control study. We note, however, that these methods can also be used for the analysis of quantitative traits. Once homogeneous clusters are identified, they can be entered into a model as block effects, and the quantitative trait can be analyzed with standard statistical tools, such as analysis of variance.

Theory, simulations, and real-data analyses suggest that genetic matching is useful and powerful for GWA, especially when the samples of cases and controls cannot be guaranteed to be drawn from the same population. It can diminish the false-positive rate, sometimes substantially, and have only modest impact on power. Among others,^{33–36} methods similar to Eigenstrat⁴ also limit the impact of population structure, but for challenging designs, they cannot be expected to completely control the false-positive rate. Perhaps the gold standard for GWA studies should be to evaluate the data with both regression methods such as Eigenstrat and epidemiological methods such as fMatch. When the results of these methods agree,

researchers have greater assurance of validity; it is when the results diverge that we should be wary.

Appendix

EVD of Allele Counts

Using allele counts for SNPs $l = 1, \dots, L$, and individuals $i = 1, \dots, N$, create an $N \times L$ matrix X . For p_l , the l th allele frequency, center allele counts in column l by subtracting $2p_l$ and scale by dividing by $(2p_l(1 - p_l))^{1/2}$. Find the EVD of $XX^t = U\lambda U^t$. In the D dimensional space defined by the top D eigenvectors, the “ancestry” value for the i th subject is determined by the i th row of the eigenvectors u_{i1}, \dots, u_{iD} . The d th eigenvalue, λ_d , determines the scaling of distances in the d th dimension. These coordinates are used for matching.

Model for Population Stratification

The mean of allele frequencies from a set of populations is assumed to be the allele frequency of an ancestral population. Individual populations have each diverged from the ancestral population over time, with fixation index F_{ST} , a measure of population differentiation. Within a subpopulation j , suppose that allele counts are independent and identically distributed and that allele a is drawn with probability p_j . If X is counting allele a , then $X \sim \text{Binomial}(2p_j)$. Let P be the random variable that varies across subpopulations, with p_j as the realized value in subpopulation j : $P \sim \text{Beta}(\alpha_1, \alpha_2)$, $\alpha_1 + \alpha_2 = 1/F_{ST} - 1$. Assume that we have the minor allele frequencies of an ancestral population $p.loci$ (in our simulations $p.loci$ is uniform between .05 and .5) at L loci. From the ancestral population J , subpopulations have been formed. By knowing F_{ST} , for each marker l we can define $\alpha_{1,l} = p.loci_l \times (1/F_{ST} - 1)$ and $\alpha_{2,l} = (1 - p.loci_l) \times (1/F_{ST} - 1)$ and generate the alleles as described above. When used in simulation studies, this is often called the Balding-Nichols model.¹⁷ For simulation of a cline (or a gradient), it is enough to order p_{jl} so that $p_{11} \leq \dots \leq p_{jl}$ for each l .

Hypothesis Test for Population Structure

A formal significance test for population structure is based on a theoretical result for the eigenvalue distribution of a null sample covariance matrix.^{6,37} For a homogeneous population, the largest eigenvalue, properly normed, approximately follows the Tracy-Widom distribution³⁷ $W_d = (\lambda_d - \mu_{NL})/\sigma_{NL}$ with centering and scaling parameters that depend on both N and L , $\mu_{NL} = ((L - 1)^{1/2} + N^{1/2})^2$ and $\sigma_{NL} = ((L - 1)^{1/2} + N^{1/2})(1/((L - 1)^{1/2}) + 1/N^{1/2})^{1/3}$. We can test the null hypothesis of population homogeneity against an alternative hypothesis of population heterogeneity. The sample covariance matrix S follows a $(N - 1) \times (N - 1)$ Wishart distribution. The test for population structure will be applied iteratively (i.e., the leading eigenvalue, then the second and so on). If we find the first d eigenvalues $\lambda_1, \dots, \lambda_d$ to be significant, we test λ_{d+1} as

though S were an $(N - d - 1) \times (N - d - 1)$ Wishart matrix. If an eigenvalue is not significant, the smaller eigenvalues will not be significant either.

Removing Unmatchable Individuals

EVD determines the distance between individuals on the basis of the top D eigenvectors and eigenvalues. To stabilize the distance metric, we use the normed eigenvalues, W_d , plus a constant a , chosen to ensure the weights are positive. The distance between individuals i and i' is calculated as $g(i, i') = \left\{ \sum_{d=1}^D (W_d + a)(u_{id} - u_{i'd})^2 \right\}^{1/2}$.

To rescale the distances, let $S_k \subset \{1, 2, \dots, N\}$ be the indices of individuals in the k 'th cluster. Let r_k be the number of individuals in the k 'th cluster. For scaling subject $i \in S_k$, we use the eigenvector values (u_{i1}, \dots, u_{iD}) but not the eigenvalues. Assume that the eigenvector representation of each individual consists of an ancestry signal plus random noise: $u_{id} = \mu_{id} + \varepsilon_{id}$.

For homogeneous data, because all individuals came from a common source, the ancestry signal is 0 and the representation consists simply of random noise $u_{id} = \varepsilon_{id}$. Our target is to identify approximately homogeneous subpopulations that have little or no diversity for ancestry. If the clustering is successful, the signal of each individual in subset S_k can be approximated by $\bar{u}_{dk} = \sum_{i \in S_k} u_{id} / r_k$, and the noise can be approximated by $u_{id} - \bar{u}_{dk}$. But notice that EVD automatically scales the eigenvectors so that $\sum_i u_{id}^2 = 1$ and $\bar{u}_d = 0$. A traditional sum of squares decomposition leads to

$$1 = \sum_i u_{id}^2 = \sum_k \sum_{i \in S_k} (u_{id} - \bar{u}_{dk})^2 + \sum_k r_k \bar{u}_{dk}^2,$$

i.e., the total sum of squares (SSTotal) equals the sum of squares attributable to random variation or error (SSError) plus the sum of squares attributable to ancestry differences (SSModel). Unit scaling of SSTotal causes the distances between individuals from heterogeneous populations to be uncomparable to distances in homogeneous populations. For example, if the sample derives from two highly differentiated populations so that SSError = 0.01 and SSModel = 0.99, then the expected distance between two individuals with common ancestry is $\sim 0.01/n$. Alternatively, if the populations have identical ancestry, then the expected distance between two individuals is $\sim 1/n$. For comparing to a homogeneous scaling, we wish to rescale the random noise so that SSError is 1. It follows that the data will be rescaled equivalently to homogeneous data if we set $c_d^2 = \sum_k \sum_{i \in S_k} (u_{id} - \bar{u}_{dk})^2$ and rescale the data such that $u_{id}^* = u_{id} / c_d$.

In practice, \bar{u}_{dk} provides a good estimate of the signal only when the cluster size is sufficiently large, say greater than 10. Hence, to compute c_d^2 , include only those clusters S_k including 10 or more elements in the sum and then multiply by $n / \sum_k (r_k - 1)$ to account for the missing clusters. Notice that we scale differently for each of the d dimensions to stretch and shrink accordingly to get the proper scaling of the data.

In the final step, find the distances between individuals with the u_{id}^* instead of u_{id} and use the expected value of normed eigenvalues W_1, \dots, W_D obtained from the simulation, instead of the actual eigenvalues. Match rescaled data with fMatch or pMatch and measure the distances between cases and controls. Any individuals with distances in this metric exceeding the 99.9th quartile of the null distribution of distances are declared unmatchable.

Supplemental Data

Two figures are available at <http://www.ajhg.org/>.

Acknowledgments

The Genetics of Kidneys in Diabetes (GoKinD) Study sample collection is supported by the Juvenile Diabetes Research Foundation in collaboration with the Joslin Diabetes Center and George Washington University and by the United States Centers for Disease Control and Prevention. This work was funded by the National Institutes of Health grant MH057881 awarded to B.D. and K.R. and by the Department of Defense (grant W81XWH-07-1-0619) awarded to M.T. The MONICA/KORA Augsburg studies were financed by the GSF-National Research Center for Environment and Health, Neuherberg, Germany, and supported by grants from the German Federal Ministry of Education and Research (BMBF). Part of this work was financed by the German National Genome Research Network (NGFN). The genotypes reported in this publication were generated independently from any other initiatives supported by other organizations.

Received: October 1, 2007

Revised: November 16, 2007

Accepted: November 20, 2007

Published online: January 24, 2008

Web Resources

The URLs for data presented herein are as follows:

CHIAMO, <http://www.stats.ox.ac.uk/%7Emarchini/software/gwas/chiamo.html>
 dbGaP, <http://www.ncbi.nlm.nih.gov/sites/entrez?db=gap>
 GEM, <http://wpicr.wpic.pitt.edu/WPICCompGen/>
 GoKinD, <http://www.jdrf.org/gokind>
 HapMap Frequencies, <http://www.hapmap.org/>
 Online Mendelian Inheritance in Man (OMIM), <http://www.ncbi.nlm.nih.gov/Omim>
 Optmatch, <http://cran.r-project.org/doc/packages/T1Dbase>, <http://t1dbase.org/>

References

1. Lee, W.-C. (2004). Case-control association studies with matching and genomic controlling. *Genet. Epidemiol.* 27, 1–13.
2. Hinds, D.A., Stokowski, R.P., Patil, N., Konvicka, K., Kershenbich, D., Cox, D.R., and Ballinger, D.G. (2004). Matching strategies for genetic association studies in structured populations. *Am. J. Hum. Genet.* 74, 317–325.

3. Zhang, S., Zhu, X., and Zhao, H. (2003). On a semiparametric test to detect associations between quantitative traits and candidate genes using unrelated individuals. *Genet. Epidemiol.* **24**, 44–56.
4. Price, A.L., Patterson, N.J., Plenge, R.M., Weinblatt, M.E., Shadick, N.A., and Reich, D. (2006). Principal components analysis corrects for stratification in genome-wide association studies. *Nat. Genet.* **38**, 904–909.
5. Rosenbaum, P.R. (1995). *Observational Studies* (New York: Springer-Verlag).
6. Patterson, N., Price, A.L., and Reich, D. (2006). Population structure and eigenanalysis. *PLoS Genet.* **2** 10.1371/journal.pgen.0020190.
7. Jolliffe, I.T. (2002). *Principal Component Analysis* (New York: Springer).
8. Venables, W.N., and Ripley, B.D. (2002). *Modern Applied Statistics with S*, Fourth Edition (New York: Springer).
9. Everitt, B.S. (1993). *Cluster Analysis* (London: Edward Arnold).
10. Mueller, P.W., Rogus, J.J., Cleary, P.A., Zhao, Y., Smiles, A.M., Steffes, M.W., Bucksa, J., Gibson, T.B., Cordovado, S.K., Krolewski, A.S., et al. (2006). Genetics of Kidneys in Diabetes collection available for identifying genetic susceptibility factors for diabetic nephropathy in type 1 diabetes. *J. Am. Soc. Nephrol.* **17**, 1782–1790.
11. Wichmann, H.E., Gieger, C., Illig, T., and MONICA/KORA Study Group. (2006). KORA-gen-resource for population genetics, controls and a broad spectrum of disease phenotypes. *Gesundheitswesen* **67** (Suppl 1), S26–S30.
12. Krawczak, M., Nikolaus, S., von Eberstein, H., Croucher, P.J., El Mokhtari, N.E., and Schreiber, S. (2006). PopGen: Population-based recruitment of patients and controls for the analysis of complex genotype-phenotype relationships. *Community Genet.* **9**, 55–61.
13. Steffens, M., Lamina, C., Illig, T., Bettecken, T., Vogler, R., Entz, P., Suk, E.K., Toliat, M.R., Klopp, N., Caliebe, A., et al. (2006). SNP-based analysis of genetic substructure in the German population. *Hum. Hered.* **62**, 20–29.
14. Ringquist, S., Styche, A., Rudert, W.A., and Trucco, M. (2007). Pyrosequencing-based strategies for improved allele typing of human leukocyte antigen loci. *Methods Mol. Biol.* **373**, 115–134.
15. Rabbee, N., and Speed, T.P. (2006). A genotype calling algorithm for affymetrix SNP arrays. *Bioinformatics* **22**, 7–12.
16. Marchini, J., Howie, B., Myers, S., McVean, G., and Donnelly, P. (2007). A new multipoint method for genome-wide association studies via imputation of genotypes. *Nat. Genet.* **39**, 906–913.
17. Balding, D.J., and Nichols, R.A. (1995). A method for quantifying differentiation between populations at multi-allelic loci and its implications for investigating identity and paternity. *Genetica* **96**, 3–12.
18. Pasquali, L., Fan, Y., Trucco, M., and Ringquist, S. (2006). Rehabilitation of adaptive immunity and regeneration of beta cells. *Trends Biotechnol.* **24**, 516–522.
19. Lowel, H., Doring, A., Schneider, A., Heier, M., Thorand, B., and Meisinger, C. (2005). The MONICA Augsburg surveys—basis for prospective cohort studies. *Gesundheitswesen* **67** (Suppl 1), S13–S18.
20. Rinaldo, A., Bacanu, S.-A., Devlin, B., Sonpar, V., Wasserman, L., and Roeder, K. (2005). Characterization of multilocus linkage disequilibrium. *Genet. Epidemiol.* **28**, 193–206.
21. Cavalli-Sforza, L.L., Menozzi, P., and Piazza, A. (1994). *The History and Geography of Human Genes* (Princeton, NJ: Princeton University Press).
22. Rosenberg, N.A., Mahajan, S., Ramachandran, S., Zhao, C., Pritchard, J.K., and Feldman, M.W. (2005). Clines, clusters and effect of study design on the inference of human population structure. *PLoS Genetics* **1**, e70.
23. Todd, J.A., Bell, J.I., and McDevitt, H.O. (1987). HLA-DQ beta gene contributes to susceptibility and resistance to insulin-dependent diabetes mellitus. *Nature* **329**, 599–604.
24. Morel, P.A., Dorman, J.S., Todd, J.A., McDevitt, H.O., and Trucco, M. (1988). Aspartic acid at position 57 of the HLA-DQ beta chain protects against type I diabetes: A family study. *Proc. Natl. Acad. Sci. USA* **85**, 8111–8115.
25. Dorman, J.S., LaPorte, R.E., Stone, R.A., and Trucco, M. (1990). Worldwide differences in the incidence of type I diabetes are associated with amino acid variation at position 57 of the HLA-DQ beta chain. *Proc. Natl. Acad. Sci. USA* **87**, 7370–7374.
26. Hyttinen, V., Kaprio, J., Kinnunen, L., Koskenvuo, M., and Tuomilehto, J. (2003). Genetic liability of type 1 diabetes and the onset age among 22,650 young Finnish twin pairs: A nationwide follow-up study. *Diabetes* **52**, 1052–1055.
27. Wellcome Trust Case Control Consortium (2007). Genome-wide association study of 14,000 cases of seven common diseases and 3,000 shared controls. *Nature* **447**, 661–678.
28. Hakonarson, H., Grant, S.F., Bradfield, J.P., Marchand, L., Kim, C.E., Glessner, J.T., Grabs, R., Casalunovo, T., Taback, S.P., Frackelton, E.C., et al. (2007). A genome-wide association study identifies KIAA0350 as a type 1 diabetes gene. *Nature* **448**, 591–594.
29. Todd, J.A., Walker, N.M., Cooper, J.D., Smyth, D.J., Downes, K., Plagnol, V., Bailey, R., Nejentsev, S., Field, S.F., and Payne, F. (2007). Robust associations of four new chromosome regions from genome-wide analyses of type 1 diabetes. *Nat. Genet.* **39**, 857–864.
30. Wang, H., Thomas, D.C., Pe'er, I., and Stram, D.O. (2006). Optimal two-stage genotyping designs for genome-wide association scans. *Genet. Epidemiol.* **30**, 356–368.
31. Skol, A.D., Scott, L.J., Abecasis, G.R., and Boehnke, M. (2007). Optimal designs for two-stage genome-wide association studies. *Genet. Epidemiol.* **31**, 776–788.
32. Bacanu, S.A., Devlin, B., and Roeder, K. (2000). The power of genomic control. *Am. J. Hum. Genet.* **66**, 1933–1944.
33. Devlin, B., and Roeder, K. (1999). Genomic control for association studies. *Biometrics* **55**, 997–1004.
34. Pritchard, J., Stephens, M., and Donnelly, P. (2000). Inference of population structure using multilocus genotype data. *Genetics* **155**, 945–959.
35. Devlin, B., Bacanu, S.A., and Roeder, K. (2004). Genomic control to the extreme. *Nat. Genet.* **36**, 1129–1130.
36. Epstein, M.P., Allen, A.S., and Satten, G.A. (2007). A simple and improved correction for population stratification in case-control studies. *Am. J. Hum. Genet.* **80**, 921–930.
37. Johnstone, I. (2001). On the distribution of the largest eigenvalue in principal components analysis. *Annals of Statistics* **29**, 295–327.